

Aus der II. Medizinische Klinik  
der Medizinischen Fakultät Mannheim  
(Direktor: Prof. Dr. med. Matthias Ebert)

SOX9 in the development and chemotherapy of cholangiocarcinoma  
(CCA)

Inauguraldissertation  
zur Erlangung des Doctor scientiarum humanarum (Dr. sc. hum.)  
der  
Medizinischen Fakultät Mannheim  
der Ruprecht-Karls-Universität  
zu  
Heidelberg

vorgelegt von  
Xiaodong Yuan

aus  
Anhui, China  
2017

Dekan: Prof. Dr. med. Sergij Goerd  
Referent: Prof. Dr. rer. nat. Steven Dooley

Für meine lieben Eltern

# CONTENTS

Page

LIST OF ABRREVIATIONS.....	1
----------------------------	---

1 INTRODUCTION .....	4
----------------------	---

1.1 Sex-determining region Y-box containing gene 9 (SOX9) .....	4
---	---

1.2 General functions of SOX9 in physiological and disease states .....	4
---	---

1.3 SOX9 in the liver.....	5
----------------------------	---

1.3.1 Expression of SOX9 in embryonic and adult liver .....	5
---	---

1.3.2 Function of SOX9 in liver development.....	5
--	---

1.3.3 SOX9 in liver homeostasis and regeneration.....	6
---	---

1.3.4 SOX9 in chronic liver disease .....	7
---	---

1.3.5 SOX9 in liver cancer .....	8
----------------------------------	---

1.4 Cholangiocarcinoma.....	8
-----------------------------	---

1.4.1 Epidemiology .....	9
--------------------------	---

1.4.2 Classification .....	9
----------------------------	---

1.4.3 Risk factors.....	10
-------------------------	----

1.4.4 Cellular origins.....	11
-----------------------------	----

1.4.5 Molecular pathogenesis.....	12
-----------------------------------	----

1.4.6 Treatment .....	16
-----------------------	----

1.5 Aims of this study .....	18
------------------------------	----

2 MATERIALS AND METHODS .....	19
-------------------------------	----

2.1 Materials.....	19
--------------------	----

2.1.1 Patients and liver tissues .....	19
--	----

2.1.2 Chemicals and reagents .....	20
------------------------------------	----

2.1.3 Antibodies.....	21
-----------------------	----

2.1.4 Buffer preparation .....	23
--------------------------------	----

2.1.5 Cell culture material .....	25
-----------------------------------	----

2.1.6 Instruments and Software.....	25
-------------------------------------	----

2.2 Methods.....	26
------------------	----

2.2.1	Immunohistochemical staining.....	26
2.2.2	Immunohistochemistry evaluation.....	28
2.2.3	Cell lines .....	29
2.2.4	Cell culture and treatment.....	29
2.2.5	RNA interference (RNAi) of SOX9 .....	30
2.2.6	Whole cell protein extraction.....	30
2.2.7	Cell Subcellular fractionation .....	31
2.2.8	Protein concentration determination .....	31
2.2.9	Immunoblotting .....	31
2.2.10	MTT assay.....	32
2.2.11	Cell cycle analysis .....	32
2.2.12	Transwell migration assay .....	32
2.2.13	Caspase 3 assay .....	33
2.2.14	Tumor sphere formation assay .....	33
2.2.15	RNA isolation and RNA concentration determination .....	33
2.2.16	Quantitative real-time reverse transcription polymerase chain reaction	35
2.2.17	Microarray analyses and Gene set enrichment analysis (GSEA) ...	35
2.2.18	Statistical analyses .....	36
<b>3</b>	<b>RESULTS.....</b>	<b>37</b>
3.1	Clinical significance of SOX9.....	37
3.1.1	SOX9 expression in chronic liver disease.....	37
3.1.2	SOX9 expression in iCCA.....	38
3.1.3	CCA patients with high SOX9 expression have poor clinical outcome 40	
3.1.4	Integrated analysis of CCA patients gene expression signatures .....	46
3.2	Investigating SOX9 function in CCA tumorigenesis and chemotherapy <i>in vitro</i> 50	
3.2.1	SOX9 is highly expressed in CCA cell lines.....	50
3.2.2	Comparative microarray analysis of parental and SOX9 depleted CC- SW-1 cells .....	50
3.2.3	Depleting SOX9 suppresses CCA cell survival.....	53
3.2.4	SOX9 is required for cell migration .....	56
3.2.5	SOX9 is required for CCA cell stemness .....	58
3.2.6	SOX9 inhibition sensitizes CCA cells to gemcitabine .....	60

3.2.7	SOX9 is downstream of EGFR/ERK1/2 signaling.....	63
4	DISCUSSION .....	66
4.1	SOX9 is a prognostic marker for iCCA .....	66
4.2	SOX9 determines the response of CCA cells to chemotherapy .....	66
4.3	SOX9 as oncogene in CCA .....	68
4.3.1	Survival .....	68
4.3.2	Migration .....	69
4.3.3	Cancer stem cell features .....	70
4.4	Regulation of SOX9 expression.....	71
5	SUMMARY .....	72
6	REFERENCES .....	74
7	LISTS OF FIGURES AND TABLES.....	83
7.1	List of figures .....	83
7.2	List of tables .....	85
8	CURRICULUM VITAE .....	86
9	ACKNOWLEDGEMENT .....	88

## LIST OF ABRREVIATIONS

°C	grad Celsius
μ	Micro ( $10^{-6}$ )
AAV	Adeno-associated virus
APS	Ammoniumpersulfate
BSA	Bovine serum albumin
BECs	Biliary epithelial cells
CCA	Cholangiocarcinoma
CD	Campomelic dysplasia
CLCs	Cholangiolocellular carcinomas
CSC	Cancer stem cells
CXCR4	C-X-C chemokine receptor type 4
dCCA	Distal cholangiocarcinoma
DRs	Ductular reactions
DMEM	Dulbecco's modified eagle medium
DMSO	Dimethylsulfoxide
eCCA	Extrahepatic cholangiocarcinoma
ECM	Extracellular matrix
EDTA	Ethylene diaminetetraacetic acid
EGF	Epidermal growth factor
EGFR	Epidermal growth factor receptor
EMT	Epithelial-to-mesenchymal transition
EpCAM	Epithelial cell adhesion molecule
ERK1/2	Extracellular signal-regulated kinase1/2
FBS	Fetal bovine serum
FDR	False discover rate
FGFR2	Fibroblast growth factor receptor-2
GAPDH	Glyceraldehyde 3-phosphate dehydrogenase
GEO	Gene Expression Omnibus
GSEA	Gene set enrichment analysis
HBV	Hepatitis B virus
HCC	Hepatocellular carcinoma

HCl	Hydrogen chloride
HCV	Hepatitis C virus
HGF	Hepatocyte growth factor
Hh	Hedgehog
HNF4 $\alpha$	Hepatocyte nuclear factor 4 $\alpha$
HPCs	Hepatic progenitor cells
HRP	Horseradish peroxidase
HSCs	Hepatic stellate cells
IBD	Inflammatory bowel disease
iCCA	Intrahepatic cholangiocarcinoma
IDH	Isocitrate dehydrogenesis
iNOS	Inducible nitric oxide synthase
KEGG	Kyoto Encyclopedia of Genes and Genomes
kg	kilo gram
m	Milli ( $10^{-3}$ )
M	molar (mol/l)
MRP4	Multidrug resistance-associated protein 4
MTT	3-(4,5-Dimethylthiazol-2-yl)-2,5-Diphenyltetrazolium Bromide
NCAM	Neural cell adhesion molecule
NSCLS	Non-small cell lung cancer
OPN	Osteopontin
PAGE	Polyacrylamide-Gel-electrophoresis
PBS	Phosphate buffered saline
PBG	Peribiliary gland
pCCA	Perihilar cholangiocarcinoma
PDAC	Pancreatic ductal adenocarcinoma
PDC	Primitive ductal structure
PDGF	Platelet-derived growth factor
PI	Propidium Iodide
PVDF	Polyvinylidene fluoride
PSC	Primary sclerosing cholangitis
Rmp	Revolutions per minute
SCD	Symmetrical cell division
SDS	Sodium dodecyl sulfate



## LIST OF ABRREVIATIONS

---

SOX9	Sex-determining region Y-box containing gene 9
TBS	Tris buffered saline
TBS-T	Tris buffered saline with Tween20
TEMED	N,N,N',N'-Tetramethylethylenediamine
TGF- $\beta$	Transforming growth factor $\beta$
Tris	Tris(hydroxymethyl)-aminoethane
WPC	Weeks post-conception

## 1 INTRODUCTION

### 1.1 Sex-determining region Y-box containing gene 9 (SOX9)

SOX9 was first identified as a critical gene associated with Campomelic dysplasia (CD), a human haploinsufficiency disorder characterized by skeletal malformations, male-to-female sex reversal in XY males and neonatal lethality [1]. SOX9 belongs to SOX transcription factor family and possesses a high-mobility-group (HMG) DNA binding domain which exhibits a high degree of homology with that of the mammalian testis-determining factor, SRY [2].

### 1.2 General functions of SOX9 in physiological and disease states

During embryonic development, SOX9 is widely expressed in chondrocytes, testes, heart, lung, pancreas, bile duct, hair follicles, retina, and the central nervous system (CNS) [3-8]. The functions of SOX9 involve the regulation of cell proliferation, differentiation, extracellular matrix (ECM) deposition, and epithelial-to-mesenchymal transition (EMT) [8, 9].

In adult, SOX9 is expressed in local stem/progenitor cells of various organs with high turnover in physiological state [10-13]. SOX9 positive cells have the capability of differentiation into multiple mature organ cells, either in the physiological state or the regenerative state after injury, particularly in intestine, pancreas and hair follicles [10, 11]. In some setting, SOX9 is required for the maintenance of progenitor cells in undifferentiated status [9, 14].

In fibrosis-associated disease, SOX9 regulates ECM deposition by activating genes encoding extracellular matrix components [15-19]. In addition, elevated SOX9 expression has been reported in a wide range of human cancers, including non-small cell lung cancer (NSCLS), pancreatic ductal adenocarcinoma (PDAC) and melanoma [20-25]. The role of SOX9 in carcinogenesis is unclear. High levels of SOX9 expression in cancers are linked to the malignant characters, progression, and poor prognosis of cancer. SOX9 exhibits pro-oncogenic properties, including promoting cell proliferation, inhibiting senescence and collaboration with other oncogenes in neoplastic transformation [26]. On the other hand, SOX9 displays as a tumor suppressor by inhibiting tumor cell growth and facilitating chemotherapy [26].

### 1.3 SOX9 in the liver

#### 1.3.1 Expression of SOX9 in embryonic and adult liver

Most knowledge on the biological functions of SOX9 in liver development is obtained from studying animal embryonic development. In mice, SOX9 is the most specific and earliest marker of biliary tree during liver development [27]. At E10.5, SOX9 expression is detected in the endodermal cells lining the liver diverticulum; however it is undetectable in the hepatoblasts invading the septum transversum [27]. At E11.5, SOX9 emerges in hepatoblasts near the portal vein [27]. At E13.5, the SOX9 positive cells form a single-layered ductal plate around the portal vein, which gives rise to cholangiocytes, the ductules, and the canals of Herings and periportal hepatocytes [27, 28]. At E15.5, SOX9 is expressed on the portal side of primitive ductal structure (PDC). From E18.5, SOX9 localizes in all biliary cells until birth [27]. After birth, SOX9 expression persists in small bile ducts but regresses from large bile ducts [27].

In human, SOX9 exhibits a similar expression pattern as in mice. During normal human liver embryonic development, SOX9 positive cells are detected near portal vein at 8 weeks post-conception (WPC). At 18 WPC, SOX9 expression is detected in the ductal plate encircling the portal vein. In adult, SOX9 expresses in bile ducts but not in hepatocytes [29]. SOX9 expression in embryonic and adult liver in mouse and human is presented in Table 1.

#### 1.3.2 Function of SOX9 in liver development

SOX9 plays a critical role in controlling the timing of intrahepatic bile duct morphogenesis in liver development. Liver-specific inactivation of SOX9 leads to a delay in the resolution of the asymmetric primary ductal structures in mice [27]. In addition, SOX9 functions in cooperation with SOX4, another member of SOX family, in the process of bile duct development [30]. During mice bile duct development, SOX4 displays similar expression profiles in the PDC and developing bile duct as SOX9. Liver-specific inactivation of SOX4 leads to delayed bile differentiation and morphogenesis, while double mutation in SOX9 and SOX4 completely blocks biliary development and results in dilated and truncated hilar ducts, cholestasis, liver fibrosis and ductular reactions (DRs) [30]. In normal human fetal livers, accumulating studies have demonstrated that SOX9 expression is detectable in PDS with asymmetrical

expression, suggesting a similar bile duct morphogenesis process as in mice [27, 31, 32].

Table 1. SOX9 expression in embryonic and adult liver

Mouse		Human	
Embryonic day	SOX9 expression	weeks postconception (WPC)	SOX9 expression
<b>E10.5</b>	Endodermal cells lining the liver diverticulum, undetectable in hepatoblasts		
<b>E11.5</b>	Hepatoblasts near portal vein	<b>8 WPC</b>	Hepatoblasts near portal vein
<b>E13.5</b>	Single-layered ductal plate around the portal vein	<b>18 WPC</b>	Ductal plate encircling the portal vein
<b>E15.5</b>	Portal side of primitive ductal structure (PDC)		
<b>E18.5 to birth</b>	Biliary cells		
<b>After birth</b>	Small ducts	<b>Adult</b>	Bile ducts

### 1.3.3 SOX9 in liver homeostasis and regeneration

In normal adult liver, SOX9 expression is observed in the periportal small intrahepatic ducts and peribiliary glands lining the large bile ducts [33]. In acute or chronic liver disease, SOX9 expression is detected in DRs which contain putative progenitors capable of producing cholangiocytes and hepatocytes[34]. Increasing evidence shows that a subpopulation of SOX9 positive cells in liver express stem cell markers, such as Epithelial cell adhesion molecule (EpCAM), neural cell adhesion molecule (NCAM), CD133, C-X-C chemokine receptor type 4 (CXCR4) [33, 35]. Thus, these SOX9 positive cells are thought as hepatic progenitor cells (HPCs) and are able to differentiate into hepatocytes and cholangiocytes. This notion is supported by several experimental evidences. Cardinale et al. showed that SOX9 positive cells isolated

from the peribiliary glands of adult human extrahepatic biliary system give rise to functional hepatocytes and cholangiocytes *in vitro* and in immunocompromised mice [35]. With the SOX9<sup>IRES-CreERT2</sup> knock-in mice, Furuyama et al. illustrated that the adult HPCs locate in the SOX9-expressing progenitor cell zones and these SOX9 positive cells physiologically supply the hepatocytes and intrahepatic biliary cells [11]. Dorrell C and colleagues conducted lineage tracing study using SOX9<sup>CreERT2</sup> transgenic mice and revealed that SOX9-expressing cells contribute to both hepatocytes and bile duct cell lineages in normal and injured livers [36]. However, the notion that SOX9 positive HPCs contribute to hepatocytes is not supported by other experiments. Tarlow et al. used the same strain of SOX9<sup>CreERT2</sup> transgenic mice for lineage tracing as Dorrell's. In contrast to Dorrell's strategy, they adopted a lower dosage of tamoxifen to drive specific Cre expression. They found that hepatic progenitors of SOX9 positive ductal origin did not significantly contribute to hepatocyte replacement in different liver injury models [37]. The conflicting results from different studies may be attributed to two reasons. Firstly, in the SOX9<sup>IRES-CreERT2</sup> knockin mice, inserting IRES-CreERT2 into 3'UTR of the SOX9 gene may lead to endogenous SOX9 expression in the liver [11]. Secondly, although the SOX9<sup>CreERT2</sup> transgenic mice maintain the intact genomic SOX9 locus, high dosage of tamoxifen may induce ectopic expression of SOX9 in the hepatocytes [28, 37]. In contrary to previous reported stem/progenitor-cell-based lineage tracing models, two groups performed hepatocyte-specific lineage tracing studies using adeno-associated virus (AAV) to drive hepatocyte-specific Cre expression instead of tamoxifen. The results showed that liver homeostasis and regeneration are mediated by self-duplication of preexisting hepatocytes, rather than differentiation from HPCs in classic toxin-induced liver injury models [38, 39]. However, Lu and colleagues demonstrated that SOX9 positive HPCs contribute to liver regeneration when hepatocytes proliferation is impaired [40]. These results indicate that SOX9 positive HPCs may provide a backup system for injury states in which the proliferative capabilities of hepatocytes are impaired [39, 40].

#### 1.3.4 SOX9 in chronic liver disease

In chronic liver disease, hepatic stellate cells (HSCs) are primary cell type responsible for extracellular matrix (ECM) deposition [41]. In response to liver injury, HSCs are activated by transforming growth factor  $\beta$ 1 (TGF $\beta$ 1) and platelet-derived growth factor (PDGF). Subsequently, activated HSCs secrete ECM that defines

fibrosis in the liver parenchyma [41]. Hanley et al. reported that activating HSCs under influence of TGF- $\beta$ 1 produce ectopic expression of SOX9, which leads to significant production of type I collagen [42]. In addition, SOX9 is responsible for the expression of Osteopontin (OPN), which is an important component of ECM and has been described as a biomarker for liver fibrosis [18]. As in the developmental and adult liver, SOX9 and OPN were coexpressed in biliary ducts. Increased expressions of both SOX9 and OPN colocalize to fibrotic region, particularly in activated HSCs. *In vitro*, SOX9 and OPN are coexpressed in activated human and rat HSCs, while abrogation of SOX9 expression results in decreased OPN expression [18]. Moreover, it has been reported that SOX9 is a downstream target of Hedgehog (Hh) signaling, which plays a crucial role in promoting EMT and the evolution of biliary fibrosis during chronic cholestasis [43].

### 1.3.5 SOX9 in liver cancer

Elevated SOX9 expression is detected in hepatocellular carcinoma (HCC) and cholangiocarcinoma (CCA) [44, 45]. In HCC, SOX9 expression is increased in tumor tissue and is positively related to tumor cell differentiation, venous invasion, advanced tumor stage and shorter overall survival [44, 46]. Functionally, SOX9 confers stemness properties to HCC cells through Frizzled-7 mediated Wnt/ $\beta$ -catenin pathway [46]. In addition, Liu et al. reported that SOX9 is highly expressed in liver cancer stem cells (CSC) and required for maintaining the proliferation, self-renewal, and tumorigenicity of the liver CSCs [47]. SOX9 acts as a downstream regulator of Notch signaling through inhibition of Numb, an antagonist of Notch, thereby directing symmetrical cell division (SCD) and promoting tumorigenicity in liver CSCs [47]. In CCA, Matsushima et al. found that SOX9 expression decreases from the normal biliary epithelium to the biliary intraepithelial neoplasia in a stepwise pattern: SOX9 expression in intrahepatic cholangiocarcinoma (iCCA) is lower than that in normal biliary epithelium [45]. However, elevated SOX9 expression in iCCA is associated with the biliary infiltration and poor clinical outcome [45]. Their results implied that SOX9 may be involved in a multi-step carcinogenesis of iCCA.

### 1.4 Cholangiocarcinoma

CCA is a heterogeneous carcinoma originating from bile duct system with cholangiocyte differentiation features [48].

### 1.4.1 Epidemiology

CCA is the second most common primary epithelial malignancy of liver following hepatocellular carcinoma [49]. CCA accounts for approximately 3% of all gastrointestinal cancers and 10% to 25% of primary hepatobiliary malignancies [50]. Advanced CCA has poor prognosis with a median survival of less than 24 months [51]. The incidence and mortality of CCA is increasing worldwide [52]. Figure 1 presents the worldwide incidence of CCA from 1971 to 2009. Notably, the worldwide incidence of CCA varies greatly due to variations in geographic region and risk factors.

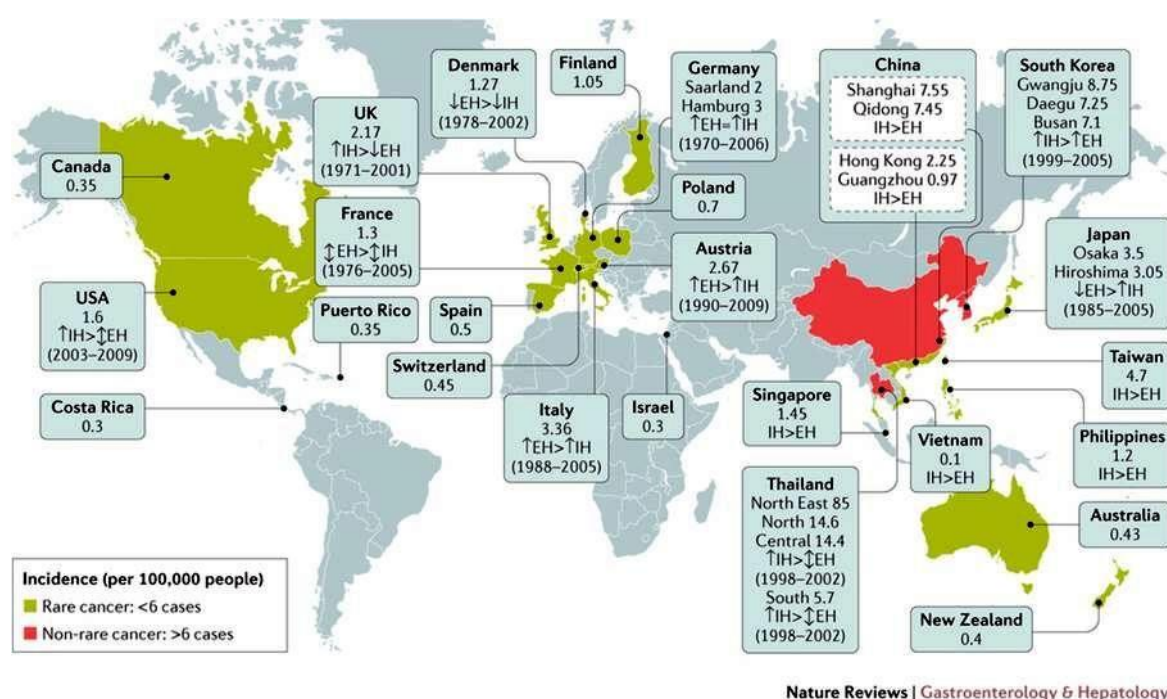


Figure 1. Worldwide incidence of cholangiocarcinoma [52]. Data were collected from 1971 to 2009. Diagnoses of cholangiocarcinoma were made according to international classification of disease (ICD) codes. The trends of incidence were indicated as ↑, increasing; ↔, stable; or ↓, decreasing. The incidences for extrahepatic (eCCA or EH) and intrahepatic (iCCA or IH) cholangiocarcinoma were counted and the more incident type was indicated.

### 1.4.2 Classification

Anatomically, CCA is classified into intrahepatic (iCCA or ICC) and extrahepatic cholangiocarcinoma (eCCA) depending on the location of the tumor [53]. In detail, iCCA is defined as a cholangiocarcinoma locating proximally to the second degree bile ducts while eCCA confines to the area between the second degree bile ducts and ampulla of Vater. Moreover, the eCCA can be further divided into perihilar cholangiocarcinoma (pCCA) and distal cholangiocarcinoma (dCCA) with the

insertion of cystic duct as the separation point. pCCA localizes to the insertion of the cystic duct into the common bile duct, whereas dCCA confines to the area between the origin of the cystic duct and ampulla of Vater.

Based on histological diversity, iCCA is categorized into two groups: pure muc-ICC and mixed-ICC (mucin-producing adenocarcinoma with hepatocytic differentiation areas and/or ductular areas) [54]. Muc-ICCs have similar clinicopathological, immunohistochemical, and gene expression profiles as hilar CCA. These tumors have a similar profile as cylindrical, taller, mucin-producing cholangiocytes that line hilar and intrahepatic large bile ducts [54]. However, mixed-ICC show similar clinicopathological, immunohistochemical, and gene expression profiles as cholangiolocellular carcinomas (CLCs) that comprise histopathological features of both hepatocellular carcinoma and cholangiocarcinoma and thus, are thought to originate from HPCs [54]. The proposed histological classification of CCA provides a new sight for understanding the biological features of CCA and may serve as a more accurate, reliable and simple approach for the diagnosis and treatment of the cancer.

### 1.4.3 Risk factors

Risk factors that lead to the multistep development of CCA are not well known. To date, most CCA cases lack a recognized risk factor. Moreover, most cases appear to develop in what is believed to be otherwise healthy livers. Approximately only 10% of cases resulted from a chronic inflammatory process of the bile ducts that might induce progressive changes in the biliary epithelium that culminate in cancer. Nevertheless, several well-established risk factors associated with the development of CCA have been reported, including parasitic infections, primary sclerosing cholangitis (PSC), biliary-duct cysts, hepatolithiasis, and thorotrast [55]. In addition, there are less-established or potential risk factors for CCA, including hepatitis C virus (HCV), hepatitis B virus (HBV), inflammatory bowel disease (IBD), cirrhosis, diabetes, obesity, alcohol, smoking, and host genetic polymorphisms [55]. Table 2 and 3 present these recognized and potential risk factors of CCA.



Table 2. Established risk factors and corresponding geographic distribution for cholangiocarcinoma [55]

Established risk factors	Geographic distribution
<b>Hepatobiliary flukes</b>	
<i>Opisthorchis viverrini</i> ( <i>O. viverrini</i> ) and <i>Clonorchis sinensis</i> ( <i>C. sinensis</i> )	Southeast and Northeast Asia
<b>Biliary-Tract Disorders:</b>	
Bile-duct cysts	Prevalence is higher in Asian than Western countries
Primary Sclerosing Cholangitis (PSC)	Most common known risk factor of CCA in Western countries
Hepatolithiasis	Established risk factor for ICC in Asian countries
<b>Toxins:</b>	
Thorotrast	Eastern and Western countries

Table 3. Possible risk factors for cholangiocarcinoma [55]

<b>Possible Risk Factors</b>
Inflammatory Bowel Disease (IBD)
Choledocholithiasis and Cholangitis
Chronic Viral Hepatitis and Cirrhosis:
Hepatitis C virus (HCV)
Hepatitis B virus (HBV)
Cirrhosis regardless of etiology
Diabetes and Obesity
Alcohol Drinking
Smoking
Genetic Polymorphisms

#### 1.4.4 Cellular origins

For decades, the cell origin of CCA has been the object of extensive investigation. There is no doubt that mature cholangiocytes have the requisite to be targets of

transformation because of their self-renewal and longevity, which would allow the sequential accumulation of genetic or epigenetic mutations required for oncogenesis [56, 57]. However, several histopathologic and gene expression profiling studies have documented a group of CCA with the histopathological features of both hepatocellular carcinoma and cholangiocarcinoma, indicating a cell origin of CCA from HPCs localized in the canal of Hering [58-61]. Moreover, it has been proposed that the mucin-CCAs are derived from the PBGs, which are stem cell niches of the intrahepatic and extrahepatic biliary tree [62-64]. Thus, the cells lining the bile ducts, biliary epithelial cells (BECs), PBGs and HPCs can give rises to CCA. In addition, experimental studies even demonstrate that differentiated/mature hepatocytes can convert into biliary lineage cells through the activation of Notch signaling and have the potential to give rise to iCCA [65, 66]. Figure 2 shows the potential cells source of iCCA.

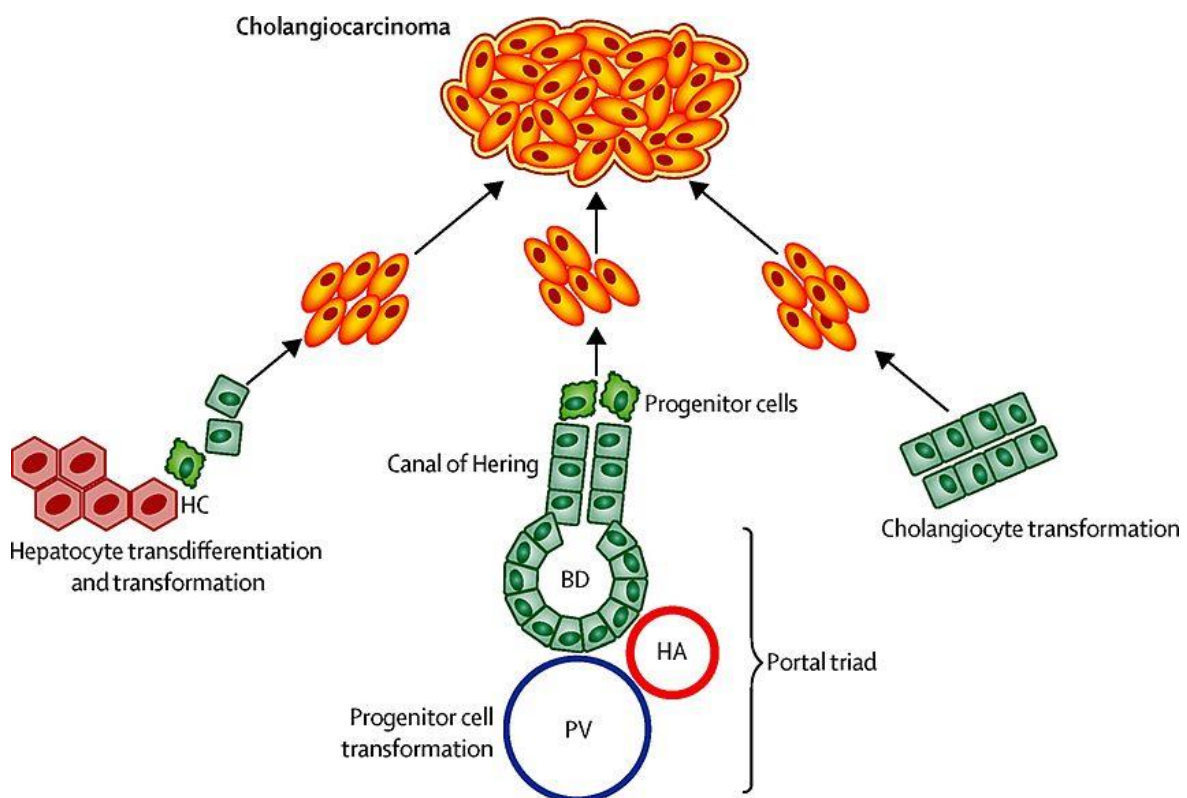


Figure 2. Potential cells of origin in intrahepatic cholangiocarcinoma (iCCA) [53].

#### 1.4.5 Molecular pathogenesis

CCA is a cancer with genomic heterogeneity, which is not only related to the diverse anatomical location of the tumor but also to various risk factors and associated pathologies [52]. To date, the most prevalent genetic alterations identified in CCA

include DNA repair, the WNT-CTNNB1 pathway, tyrosine kinase signaling, protein tyrosine phosphatase, epigenetic and chromatin remodeling factors and deregulated Notch signaling, a critical component in cholangiocyte differentiation and biliary duct development [52].

In the epigenetic landscape, isocitrate dehydrogenases 1 and 2 (IDH1 and IDH2) are frequently mutated in CCA [67, 68]. Mutation in IDH1 reshapes the genomic landscape and results in an altered differentiation state of cells [69]. In addition, IDH1 mutation causes the deregulation of hepatocyte nuclear factor 4 $\alpha$  (HNF4 $\alpha$ ), consequently blocks hepatocyte differentiation and promotes the development of bile duct cancer [70].

Fibroblast growth factor receptor 2 (FGFR2) gene fusions with multiple partners have been described in patients with CCA [71-75]. To date, seven FGFR2 fusion gene products have been identified in CCA, including FGFR2-BICC1, FGFR2-KIAA1589, FGFR2-TACC3, FGFR2-AHCYL1, FGFR2-MGEA5, FGFR2-KCTD1 and FGFR2-TXLNA29 [52]. FGFR gene fusions facilitate oligomerization and FGFR kinase activation, which results in cell morphology alteration and increased cell proliferation [52, 74].

Several growth factor tyrosine kinases are involved in the carcinogenesis and progression of CCAs, including the ERBB family of receptor tyrosine kinases, such as the epidermal growth factor (EGF) receptor EGFR, and the hepatocyte growth factor (HGF) receptor HGFR, also known as c-Met. Immunohistochemistry studies showed EGFR overexpression in human CCA samples [76, 77]. Moreover, mutations and amplifications in the EGFR gene occur in 15% and 5% CCAs, respectively [78, 79]. In addition to EGFR, overexpression of c-Met is also associated with poor prognosis of CCA patients [80]. Both EGF/EGFR and HGF/c-Met pathways are implicated in the metastatic potential of CCA. Immunohistochemistry staining showed that cytoplasmic localization of E-cadherin is associated with EGFR overexpression. *In vitro* study further confirmed that EGF/EGFR axis triggers EMT of CCA cells [81]. Besides, stimulation of c-Met by HGF induces invasiveness and motility of CCA cells through activating AKT and ERK pathways [82]. These findings demonstrate the critical role of growth factors pathway in the progression of CCA.

CCA often arises in the context of biliary inflammation [50]. Whole-transcriptome analyses reveal two subclasses of iCCA with distinct molecular signatures: (1) iCCA with predominant activation of inflammatory pathways and overexpression of different cytokines, (2) iCCA of a proliferation class with feature of predominant activation of oncogenes [83]. One of the key cytokines, which is constitutively secreted by CCA cells, is IL-6 [84]. *In vivo*, elevated IL-6 expression is detected in the serum and tumor stroma of CCA patients [85, 86]. *In vitro*, IL-6 promotes cholangiocyte growth *via* the activation of the MAPK pathway and modulates the survival of CCA cells through the induction of anti-apoptotic proteins such as myeloid leukemia cell differentiation protein Mcl-1 (MCL1) [87]. In addition to IL-6, CCA cells also overexpress TGF- $\beta$  and TGF- $\beta$  receptor II [88, 89]. TGF- $\beta$  contributes to the invasion and migration of CCA *via* induction of EMT of CCA cells [90]. The continuous production of inflammatory cytokines might induce the expression of inducible nitric oxide synthase (iNOS) and oxidative and nitrosative stress in cholangiocytes [91]. Oxidative and nitrosative stress further induce DNA damage by producing oxidative DNA lesions and inhibit DNA repair enzymes, thereby promoting carcinogenesis (Figure 3) [91, 92].

Notch, Wnt/  $\beta$ -catenin, and Hh signaling pathways are involved in iCCA pathogenesis. Notch signaling pathway is required for modulating cell fate decisions throughout the development of invertebrate and vertebrate species [93]. In mammals, the canonical Notch signaling pathway has four Notch receptors (Notch 1, 2, 3 and 4) and five ligands belonging to the Jagged (Jagged1, 2) and Delta-like (Delta-like, Dll1, 3, and 4) family [94]. During liver embryonic development, the Notch signaling is critical for cholangiocyte differentiation and biliary duct morphogenesis [95]. In post-natal liver homeostasis and liver disease, Notch pathway is implicated in HPCs mediated liver repair and in reparative morphogenesis of the biliary tree [96]. In liver cancer, upregulated expression of Notch1 and Notch2 are reported in 82.2% and 56.1% of human CCAs, respectively [97]. In mice, the combined activation of Notch and AKT leads to hepatocytes-derived iCCA [65, 66]. Inhibition of Notch and its ligand Jagged 1 almost eliminate mouse CCA development driven by transfection of activated AKT and Ras oncogenes [98]. *In vitro*, activation of Notch signaling is implicated in the induction of EMT and the migration of CCA cells [99]. Like Notch, the Wnt/ $\beta$ -catenin signaling pathway is upregulated in patients with cholangiocarcinoma [100]. The activation of Wnt pathway is often associated with overexpression of the ligands WNT7B and WNT10A along with several Wnt pathway target genes in human CCAs

[100]. An animal experiment that recapitulates the multi-stage progression of human CCA showed upregulated WNT7B and WNT10A during the course of CCA development [100]. The results indicated that the activation of canonical Wnt pathway may contribute to cholangiocarcinogenesis. In addition to Notch and Wnt signalings, the Hh ligand Sonic hedgehog protein is also overexpressed in human CCAs. *In vitro*, inhibition of its receptor Smoothed by cyclopamine inhibits proliferation and invasion of CCA cells [101]. Moreover, activation of Hh pathway by myofibroblast-derived PDGF-BB protected CCA cells from TRAIL-induced apoptosis, indicating a preventive role of Hh signaling pathway in CCA [102].

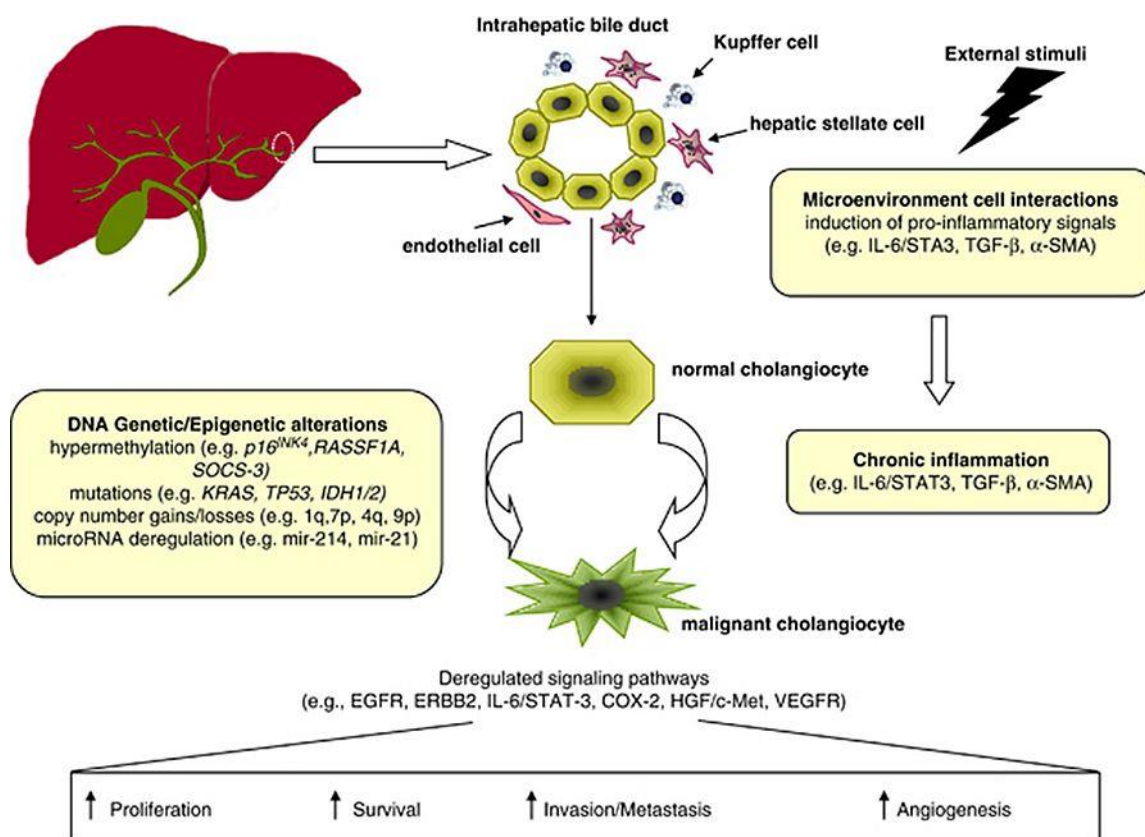


Figure 3. Summary of key molecular alterations involved in iCCA carcinogenesis [103].

Table 4. Molecular pathogenesis of CCA [52]

---

Gene or molecule	Type of alteration
<b>Genetic and epigenetic factors</b>	
TP53	Loss-of-function mutations
KRAS	Activating mutations in hotspots located at codon 12
IL-6/STAT3, SOCS-3	Overexpression of IL-6 due to epigenetic silencing of SOCS-3 in 27 % of CCA
IDH1/IDH2	Activating mutation in 10–23% of CCA
<b>Deregulated cell signaling pathways</b>	
EGFR and ERBB2	Overexpression of the receptors occurs in 10–32 % of iCCA
HGF/MET	Overexpression of MET occurs in 12–58 % of iCCA
VEGF	Overexpression in 50 % of iCCA
KRAS/MAPK	Activation
Interleukin-6 (IL-6)/STAT	Overexpression and activation
Notch	Upregulation of NOTCH1 and NOTCH2
WNT/beta-Catenin	Upregulated
Hedgehog	Activation

---

#### 1.4.6 Treatment

CCA is a devastating malignancy with limited treatment options. At present, surgical resection and liver transplantation represent the potentially curative treatment modalities for the all three types of CCA (intrahepatic, perihilar, and distal cholangiocarcinoma) [104]. However, the median survivals for R0-resected intrahepatic, perihilar, and distal CCAs were 80, 30, and 25 months, respectively, while the 5-year survivals were 63%, 30%, and 27%, respectively [105]. Moreover, curative liver transplantation is an option for selected patients with perihilar cholangiocarcinoma, while iCCA is considered as a contraindication for liver transplantation [53, 104]. For patients who are not suitable for surgical resection or liver transplantation, the prognosis is even more dismal with a life expectancy around 1 year [106]. Currently, the practice standard for advanced CCA is systemic

chemotherapy with gemcitabine and cisplatin, which demonstrated a median overall survival around 11.7 months [107]. No molecular targeted therapy so far has been proven effective for CCA [104]. During the last decade, the application of next-generation sequencing and other new technologies has made it feasible to discover more potential targetable molecular alterations in CCA. Currently, clinical trials with targetable molecular alterations in CCA are undergoing. BGJ398, a selective FGFR inhibitor, has shown efficacy in blocking the neoplastic transformation and growth of cell lines expressing FGFR2 fusion *in vitro* [108]. At present, clinical efficacy of BGJ398 is being investigated in a phase II multicenter single-arm study in advanced CCA patient with FGFR2 alterations (ClinicalTrials.gov number. NCT02150967). Promising preliminary data have also been reported that treatment with ponatinib, a multikinase inhibitor, leads to reduction of tumor size in 2 iCCA patients of FGFR2–TACC3 and FGFR2–MGEA5 gene fusions [71]. Furthermore, AG-120 and AG-221, inhibitor of IDH1 and IDH2, are currently being investigated in phase I (ClinicalTrials.gov number.NCT02073994) and phase I/II (ClinicalTrials.gov number.NCT02273739) clinical trials, respectively [109]. Since that the current existing stratification system based on the location and extent of the tumor in the biliary tree is not predictive for resectability or survival of CCA patients [110], establishing a novel patient stratification system based on molecular biomarkers is essential for the development of more personalized therapeutic approaches for the treatment of CCA patients [109].

### 1.5 Aims of this study

On the basis of the aforementioned state of art, I learned that SOX9 is a critical transcription factor for liver embryogenesis, homeostasis, regeneration and HCC development. However, the oncogenic role of SOX9 has not been investigated in CCA. As CCA is a devastating malignancy with limited treatment options, elucidation of its underlying mechanisms and identification of new molecular markers for the tumorigenesis and progression of CCA is necessary for improving diagnosis and prognosis of this cancer type. Considering that (1) SOX9 positive HPCs are required for liver homeostasis and regeneration, (2) chronic injury increases the risk of forming liver cancer, (3) HPCs are a potential cellular origin of CCA, I hypothesized that SOX9 might contribute to the tumorigenesis of CCA. Thus, the aims of this study are (i) to investigate the oncogenic role of SOX9 in cholangiocarcinoma and (ii) to evaluate the therapeutic potential of targeting SOX9 as a treatment of CCA.



## 2 MATERIALS AND METHODS

### 2.1 Materials

#### 2.1.1 Patients and liver tissues

Resected liver tissues were obtained from two cohorts: one cohort from Germany contains 28 iCCA patients and 5 eCCA; and the other cohort from France contains 41 iCCA patients. In addition, 21 liver tissues from patients without liver cancer were enrolled as control. Basic characteristics of the enrolled iCCA patients are shown in Table 5. The study protocol fulfilled national laws and regulations and was approved by the local Ethics Committee.

Table 5. Clinicopathological features of the validating set iCCA

Clinicopathological Features	NO. of patients	Value
Age (year mean $\pm$ SD)	69	63.0 $\pm$ 9.6
Gender (male:female)	69	48:21
Vascular invasion	10 (63)	15.9%
Satellite nodules	20 (63)	31.7%
Cirrhosis	22 (66)	33.3%
AJCC classification	67	
I	23	34.33%
II	18	26.87%
III	10	14.93%
IV	16	23.88%
Follow up (month mean $\pm$ SD)	60	28.4 $\pm$ 26.6
Range	60	0-110.5
Death	30	50%

### 2.1.2 Chemicals and reagents

Table 6. Chemicals and reagents

<b>Chemicals and reagents</b>	<b>Cat. No.</b>	<b>Company</b>
AC-DEVD-AFC (substrate)	13401	AAT Bioquest (USA)
Acetic acid	338826	Sigma-Aldrich (USA)
Albumin standard (BSA)	12659	Merck (Germany)
Ammonium persulfate (APS)	A3678	Sigma-Aldrich (USA)
BIT 9500	09500	Stem cell (Canada)
3,3'-diaminobenzidine (DAB)	D-5905	Sigma-Aldrich (USA)
DMEM	BE12-709F	Lonza (Germany)
DMEM/F12	12634-010	Life Technology (Canada)
Dimethyl sulfoxide (DMSO)	41639	Sigma-Aldrich (USA)
DRQ5 dye	4084	Cell Signaling Technology (USA)
Peroxidase Blocking Reagent	S2003	Dako (Denmark)
Dulbecco's Phosphate Buffered Saline	D8537	Sigma Aldrich (Germany)
EDTA	324503	Calbiochem (Germany)
Epidermal growth factor (EGF)	354001	BD Biosciences (USA)
Erlotinib	5083S	Cell Signaling Technology (USA)
Ethanol 100%	K928.4	Carl Roth (Germany)
Fetal Bovine Serum (FBS)	10270-098	Invitrogen (Germany)
Formaldehyde	F1635	Sigma-Aldrich (USA)
L-glutamine	BE17-605E	Lonza (Germany)
Hematoxylin	HX69715174	Carl Roth (Germany)
Hydrogen peroxide (H <sub>2</sub> O <sub>2</sub> )	H1009	Sigma-Aldrich (USA)
Laemmli-buffer	161-0737	BioRad (USA)
Insulin	HI0210	Lilly (Germany)
Malinol mounting medium	3C-242	Waldeck (Germany)
2-β-Mercaptoethanol	516732	Sigma-Aldrich (Germany)
Mounting medium	S3023	Dako
Methanol	8388	Carl Roth (Germany)
MTT reagent	M5655	Sigma Aldrich (Germany)

Penicillin/streptomycin	A2210	Biochrom KG
Phosphatase Inhibitor Cocktail 2	P5726	Sigma-Aldrich (Germany)
Protease Inhibitor Cocktail Tablets	S8820	Sigma-Aldrich (Germany)
Propidium Iodide (PI)	P-1470	Sigma-Aldrich (Germany)
RPMI1640	31870	Thermo Fisher Scientific (USA)
RNase A	19101	Qiagen (Germany)
Sodium dodecyl sulfate (SDS)	L3771	Sigma-Aldrich (Germany)
Supersignal Ultra	34095	Thermo Fisher Scientific (USA)
TEMED	T9821	Sigma-Aldrich (Germany)
TGF- $\beta$ 1	100-21	Peprtech
TRIS	4855	Carl Roth (Germany)
Triton® X-100	T-9284	Sigma-Aldrich (Germany)
Trypsin/EDTA 10x	T4174	Sigma-Aldrich (Germany)
Tween® 20	9127.2	Carl Roth (Germany)

### 2.1.3 Antibodies

Table 7. Primary antibodies used for immunoblotting

<b>Antibody</b>	<b>Company</b>	<b>Cat. No.</b>	<b>Predict molecular weight</b>
SOX9	Sigma Aldrich	HPA001758	70kDa
Cytokeratin 19	Santa Cruz Biotechnology	sc-6278	40kDa
EpCAM	Abcam	ab32392	39kDa
p21 <sup>WAF1/Cip1</sup>	Sigma Aldrich	P1484	21kDa
p27 Kip1	Cell Signaling Technology	#2552	27kDa
p16 INK4A	Cell Signaling Technology	#4824	16kDa
p53	Cell Signaling Technology	9282S	53kDa
pERK1/2	Santa Cruz Biotechnology	sc-7383	42/44kDa
ERK 1/2	Santa Cruz Biotechnology	sc-135900	42/44kDa

MRP4	Abcam	ab15598	230kDa
pChk1(Ser345)	Cell Signaling Technology	2341T	56kDa
Chk1	Cell Signaling Technology	#2360	56kDa
pChk2(Thr68)	Cell Signaling Technology	#2661	62kDa
pEGFR	Cell Signaling Technology	#2234	175kDa
Bcl-xL	Cell Signaling Technology	2764	30kDa
Bcl-2	Cell Signaling Technology	2870	26kDa
Cyclin D1	Cell Signaling Technology	#2978	36kDa
E-Cadherin	Cell Signaling Technology	3195S	135kDa
$\beta$ -catenin	Sigma	C7207	92kDa
Vimentin	Abcam	ab20346	54kDa
N-cadherin	Abcam	ab12221	130kDa
Alpha-Tubulin	Abcam	ab4074	55kDa
GAPDH	Santa Cruz Biotechnology	sc25778	37kDa

Table 8. Primary antibodies used for immunohistochemistry

<b>Antibody</b>	<b>Species</b>	<b>Company</b>	<b>Cat. No.</b>	<b>Dilution</b>
SOX9	rabbit	Sigma Aldrich	HPA001758	1:100
Cytokeratin 19	mouse	Santa Cruz Biotechnology	sc-6278	1:100

Table 9. Primary antibodies used for immunofluorescence

<b>Antibody</b>	<b>Species</b>	<b>Company</b>	<b>Cat. No.</b>	<b>Dilution</b>
$\beta$ -catenin	mouse	Merck/Millipore	05-665	1:100
E-Cadherin	rabbit	Cell Signaling Technology	3195s	1:100

Table 10. Secondary antibodies

<b>Antibody</b>	<b>Source</b>	<b>Dilution in WB</b>	<b>Dilution in IHC</b>	<b>Dilution in IF</b>
Goat anti rabbit IgG HRP	Santa Cruz	1:10000	-----	-----
Goat anti mouse IgG HRP	Santa Cruz	1:10000	-----	-----
Goat anti rabbit IgG HRP	DAKO	-----	1:200	-----
Goat anti mouse IgG HRP	DAKO	-----	1:200	-----
Goat-anti-rabbit Rhodamine	Merck/Millipore	-----	-----	1:200
Goat-anti-mouse FITC	Merck/Millipore	-----	-----	1:200

#### 2.1.4 Buffer preparation

Table 11. Buffer

<b>Chemicals</b>	<b>Ingredient</b>
APS (for WB)	1g APS add to 10ml ddH <sub>2</sub> O
Ladder (for WB)	950 µl Laemmli buffer 50 µl β-mercapto ethanol
RIPA buffer, stock	50 mM Tris-HCl pH 7.2-7.6 150 mM NaCl 2 mM EDTA 0.1 % SDS 0.5 % Sodium-Desoxycholate 1% Nonidet P-40 10% v/v Glycerol
Lysis buffer, ready to use (for WB)	90 µl RIPA buffer 1 µl Phosphatase Inhibitor 15 µl Protease Inhibitor
NL buffer	50mM Tris HCl pH 8.0 150mM NaCl, 1% NP-40 0.5% sodium deoxycholate 0.1% SDS

	1% glycerol
Lysis buffer (for caspase 3 activity)	50 mM HEPES 100 mM NaCl 0.1% CHAPS 1 mM DTT 0.1 mM EDTA pH 7.4
Reaction Buffer	50 mM HEPES 100 mM NaCl 0.1% CHAPS 10 mM DTT 0.1 mM EDTA 10% (w/v) glycerol pH 7.4
0.3% PBST	PBS, 1× 0.3 % Tween20
1% BSA	20mg BSA 20ml 0.3% PBST
TBS, 10×	24.23g 0.2M Tris PH7.5, 58.44g 1M NaCl, add to 1L ddH <sub>2</sub> O adjust pH value to 8.0
TG, 10×	30.27 g 0.2M Tris, 144g Glycine, add to 1L ddH <sub>2</sub> O Adjust pH value to 8.3
Transfer buffer 1×	100ml TG 10×, 200ml methanol, add to 1L ddH <sub>2</sub> O
Running buffer 1×	100ml TG 10x 10ml 10%SDS Add to 1L ddH <sub>2</sub> O
TBST	100ml TBS 10x 10ml 10%Tween 20 Add to 1L ddH <sub>2</sub> O
SF buffer	250mM Sucrose

---

	20mM HEPES pH7.4
	1.5mM MgCl <sub>2</sub>
	10mM KCl
	1mM EDTA
	1mM EGTA

---

### 2.1.5 Cell culture material

Table 12. Cell culture materials

<b>Material</b>	<b>Company</b>
Cell culture flasks 25 cm <sup>2</sup> / 75 cm <sup>2</sup> / 175 cm <sup>2</sup>	Greiner Bio-one(Germany)
Cell scraper	Falcon (Germany)
Conical centrifuge tubes 15 ml / 50 ml	Falcon (Germany)
Cell culture plate 96 well (white)	Greiner Bio-one (Germany)
Cell culture plate 96 well (flat bottom)	Greiner Bio-one(Germany)
Cell culture plate 24 well	Greiner Bio-one(Germany)
Cell culture plate 12 well	Greiner Bio-one(Germany)
Cell culture plate 12 well (non-adherent)	Greiner Bio-one(Germany)
Cell culture plate 6 well	Greiner Bio-one(Germany)
0.5 or 1.5 ml tube	Eppendorf, Germany
Eppendorf epT.I.P.S	Eppendorf, Germany
Inserts with 8 µm pore size	Falcon (Germany)
Microscope slide	Carl Roth (Germany)
PCR-Tubes™ 0.2 ml	Life Technology (Germany)
Petri dishes	Falcon (Germany)
Flow cytometry tubes	Falcon (Germany)
Sterile pipette	Greiner Bio-one(Germany)

---

### 2.1.6 Instruments and Software

Table 13. Instruments and Software

<b>Instruments or softwares</b>	<b>Company</b>
BD FACS Canto II	BD Becton Dickinson (Germany)
Centrifugation	Eppendorf (Germany)

---

TCS SP2 Confocal microscope	Leica (Germany)
FlowJo software 10.1	Tree Star (USA)
GraphPad Prism 5.0	GraphPad Software, Inc (USA)
Immunofluorescence optical microscopy	Olympus (Germany)
Incubator for Cell culture	Heraeus GmbH (Germany)
Infinite M200	Tecan
Inverted microscopy	Zeiss (Germany)
Image J	National institute of Health
Light microscope	Leica (Germany)
Microwave oven	Sharp (USA)
pH-Meter 538 Multical	WTW (Germany)
Real-time PCR	Biosystems
Weight balance	Sartorius (Germany)
Western-Blot imaging system Chemismart 5100	PEQLAB (Germany)

---

## 2.2 Methods

### 2.2.1 Immunohistochemical staining

#### Protocol for immunohistochemistry

Tissue type: formalin-fixed, paraffin-embedded specimens

Note: Do not allow slides to dry at any time during this procedure.

Day1

#### Step1: Deparaffinization and rehydration

- (1) Incubate sections in 3 times xylene for 5 minutes each time
- (2) Incubate sections in 1 time washes of 100% ethanol for 10 minutes
- (3) Incubate sections in 1 time washes of 100% ethanol for 5 minutes
- (4) Incubate sections in 1 time washes of 96% ethanol for 5 minutes
- (5) Wash sections 2 times in PBS for 5 minutes each time

#### Step2: Antigen Unmasking

Heat-induced epitope retrieval using a microwave with 1mM EDTA (Disodium salt) solution, pH8.4

Total 10 min: 10 to15 seconds boiling

45 to 50 seconds waiting

Cool slides on bench to room temperature.



**Step3: Blocking**

- (1) Wash sections in PBS 3x times for 10 minutes each time.
- (2) Blocking: incubate sections in DAKO Blocking Peroxide for 30 minutes. Alternatively, wash the sections for 1 time with PBS, and then incubate sections in 0.3 %H<sub>2</sub>O<sub>2</sub> for 15 minutes.

**Step4: Staining primary antibody**

- (1) Wash sections in PBS twice for 10 minutes each.
- (2) Dilute the primary antibody to the indicated concentration (Table 8) and adds the diluted antibody to the sections.
- (3) Incubate sections overnight at 4°C.

**Day 2****Step5: Staining secondary antibody**

- (1) Remove primary antibody and wash sections in PBS 3 times for 10 minutes each time.
- (2) Add corresponding secondary antibody diluted to the indicated concentration (Table 10) in PBS to each section and incubate for 45 minutes at room temperature.
- (3) Remove secondary antibody and rinse sections 3 times with PBS for 10min.

**Step6: Staining to detect horse radish peroxidase (HRP)**

- (1) Prepare DAB solution: add 10mg DAB in 15ml 50mM Tris (hydroxymethyl)-aminomethane solution (pH 7.6), and then filter the clumps.
- (2) Add 12µl H<sub>2</sub>O<sub>2</sub> to the DAB solution to active DAB, and then add the activated DAB to each section and monitor staining under a microscope.

Note: Let the sections develop 10 minutes but do not exceed 10 minutes and immerse slides in ddH<sub>2</sub>O.

- (3) Counterstain sections in hematoxylin for 10 to 30 seconds.
- (4) Wash sections using tap water for 10 minutes.

**Step7: Dehydrate sections**

- (1) Incubate sections in 95% ethanol 2 times for 10 seconds each time.
- (2) Repeat in 100% ethanol, incubating sections two times for 10 seconds each time.
- (3) Repeat in xylene, incubating sections two times for 10 seconds each time.
- (4) Mounted the sections with malinol mounting medium.

**Step8: Record the staining results using Leica upright research microscope**

## 2.2.2 Immunohistochemistry evaluation

Immunostaining results for SOX9 were scored semi-quantitatively based on the intensity score and proportion score of positively stained tumor cell nuclei. In detail, the intensity score of SOX9 nuclear staining was defined as four grades: 0, negative; 1, weak with color yellow; 2, middle with color brown; 3, strong with color black. The number of SOX9 positive cell nuclei was defined as 6 grades: 0, no positive cells; 1, positive cells:  $\leq 1\%$ ; 2,  $1\% < \text{positive cells} \leq 10\%$ ; 3,  $11\% < \text{positive cells} \leq 33\%$ ; 4,  $34\% < \text{positive cells} \leq 66\%$ ; 5,  $66\% < \text{positive cells}$ . The final immune staining scores were calculated as number intensity by multiplying the intensity score and proportion score. The samples with final scores over 10 were identified as high SOX9 expression, and the others were identified as low SOX9 expression. The representative pictures of SOX9 staining and for semi-quantitative scoring system are presented in Figure 4. CK19 expression was categorized into high expression and low expression according to the immunoreactivity (Figure5).

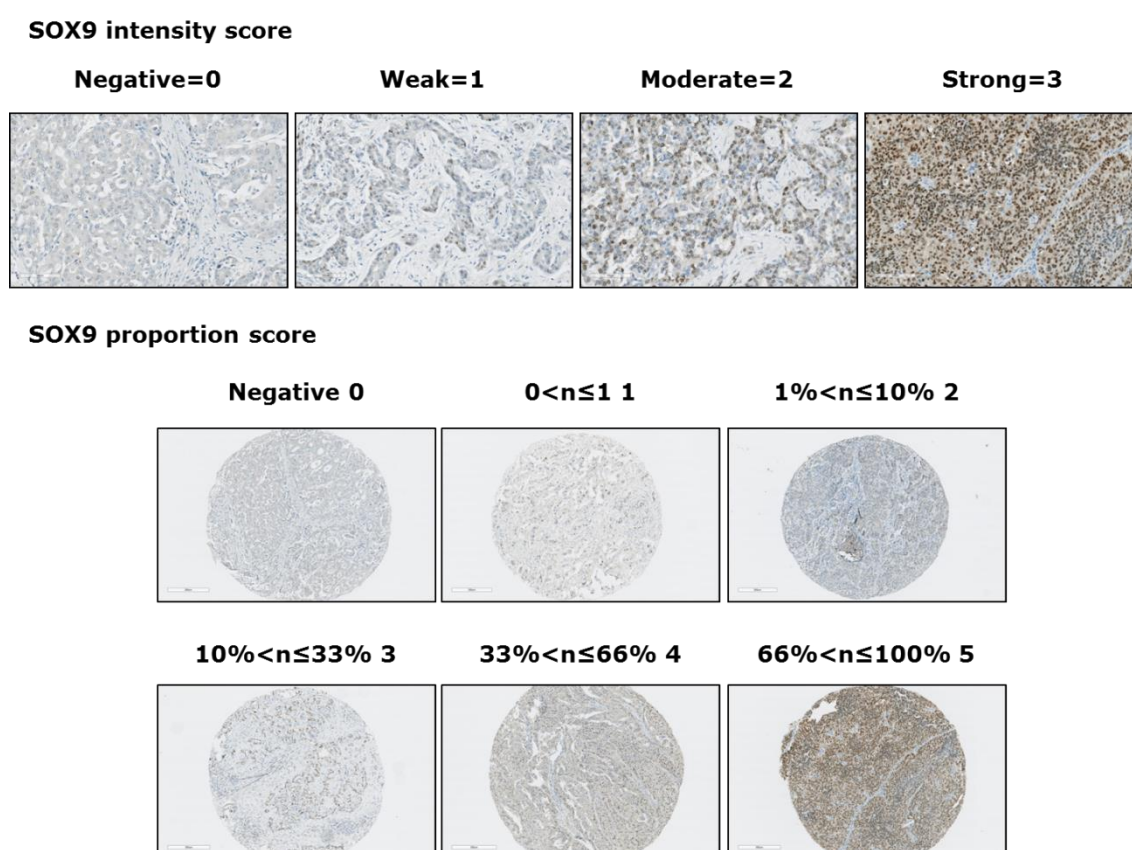


Figure 4. A semi-quantitative scoring system for evaluation of SOX9 expression in intrahepatic cholangiocarcinoma. Representative images show the intensity and proportion scores of the positively stained tumor cell nuclei for the evaluation of SOX9 expression in iCCA.

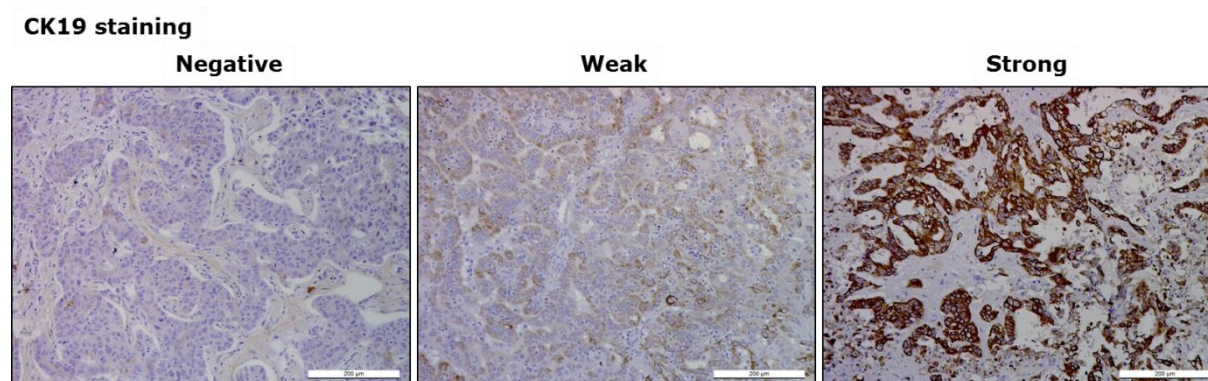


Figure 5. CK19 expression in iCCA (Immunohistochemistry staining).

### 2.2.3 Cell lines

Cell lines used in this study are presented in Table 14.

Table 14. Cell lines and cell culture medium used in the study

	Cell lines	Culture medium	reference
iCCA	CC-SW-1	DMEM, 10% FCS, 5ml P/S*, 10ml L-Glutamine	[111]
	HuCCT-1	RPMI 1640 Medium with 10% FBS, 5ml P/S, 10ml L-Glutamine	[112]
	HCCC-9810	RPMI 1640 Medium with 10% FBS, 5ml P/S, 10ml L-Glutamine	
eCCA	TFK-1	RPMI 1640 Medium with 10% FBS, 5ml P/S, 10ml L-Glutamine	[113]
	EGI-1	DMEM, 10% FCS, 5ml P/S, 10ml L-Glutamine	
NBEC*	MMNK-1	DMEM, 10% FCS, 5ml P/S, 10ml L-Glutamine	[114]
mHPCs*	BMOL	William E, 10%FCS, 5ml P/S, 10ml L-Glutamine, 30ng/ml IGF-2, 50ng/ml EGF, 10µg/ml	[115]

\*: NBEC: normal biliary epithelial cells, mHPCs: mouse HPCs, P/S: penicillin/streptomycin

### 2.2.4 Cell culture and treatment

All the cell lines were cultured in a humidified incubator at 37° and 5% CO<sub>2</sub> atmosphere. For transient transfection of siRNA, cells were treated with indicated culture medium without penicillin/streptomycin. Cells underwent starvation without FBS medium for 10 to 16 hours before treating with 10ng/ml epidermal growth factor (EGF). EGFR inhibitor Erlotinib and ERK1/2 inhibitor U0126 were dissolved in DMSO to make a 10 mM stock solution and diluted with cell culture medium into indicated

concentration during treatment. 0.1% DMSO was diluted in the same manner as control. Gemcitabine was provided by Prof. Lu LG (Shanghai Jiao Tong University School of Medicine) was dissolved in phosphate-buffered saline to make a 100mM stock solution and diluted with cell culture medium into indicated concentration during treatment.

### 2.2.5 RNA interference (RNAi) of SOX9

Pooled small interfering RNA (siRNA) targeting human and mouse SOX9 were purchased from Dharmacon (human M-021507-00).

Protocol for SOX9 siRNA transfection

Day1: Seeding cells for transfection

Tumor cells were plated at a density of  $1.5 \times 10^5$  cells per well with 2ml corresponding growth medium in a six-well cell culture vessels.

Day2:

For SOX9 siRNA transfection

Step1: Prepare RNA-lipid complexes

- (1) Dilute RNAiMAX reagent in Opti-MEM medium by adding 1.5  $\mu$ l RNAiMAX into 100  $\mu$ l Opti-MEM medium in tube A.
- (2) Dilute siRNA in Opti-MEM medium by adding 20 pmol SOX9 siRNA into 100  $\mu$ l Opti-MEM medium in tube B.
- (3) Add diluted siRNA to diluted RNAiMAX reagent with a ratio of 1 to 1. Then, incubate the mixture for 20 minutes at room temperature.

Step2: Change the culture medium to 500  $\mu$ l Opti-MEM medium per well. Then, add RNA-lipid complexes to cells. 6 hours later, change the Opti-MEM medium to 2 ml cell culture medium. RNA and whole cell protein were extracted 48 hours and 60 hours after transfection for measuring knockdown and overexpression efficiency.

### 2.2.6 Whole cell protein extraction

Wash the cells twice with ice-cold PBS and immediately add 70  $\mu$ l RIPA buffer to per well of 6-well plate and put on ice. Thereafter, scrape the cells to collect lysate and transfer to a 1.5 ml Eppendorf tube. Subsequently, centrifuge at 13000rpm at 4 °C for 5 minutes. Collect the supernatant in a fresh 1.5 ml Eppendorf tube.

### 2.2.7 Cell Subcellular fractionation

Cell subcellular fractionation was performed following the protocol by Huang et al [116]. The following is a modified protocol from Huang et al reported.

#### Protocol of cell subcellular fraction

##### Step1: Extraction of the whole cell protein

Wash the cells twice with ice-cold PBS. Then, immediately add 150  $\mu$ l SF buffer to per well of 6-well plate and put on ice. Thereafter, scrape the cells to collect lysate and transfer to a 1.5 ml Eppendorf tube. Agitate cell lysates at 4 °C for 30 minutes at 50 rpm on a tube roller. Subsequently, centrifuge at 720 g at 4 °C for 5 minutes. Collect the supernatant in a fresh 1.5 ml Eppendorf tube for next step3.

##### Step2: Extract the nuclear fraction

Wash the pellet from step1 with 300 $\mu$ l of SF buffer and disperse the pellet with a pipette. Then, centrifuge the lysate at 720 g at 4°C for 10 minutes. Thereafter, re-suspend the pellet in NL buffer and agitated at 4 °C for 30 minutes at 50 rpm on a tube roller. This is the nuclear fraction including nuclear membranes.

##### Step3: Extract the cytosolic and membrane fraction

Centrifuge the supernatant from step1 at 10.000 x g at 4°C for 10 minutes. Carefully transfer the supernatant to a new 1.5 ml Eppendorf tube. This is the cytosolic and membrane fraction.

### 2.2.8 Protein concentration determination

Protein concentrations were assessed with a Bio-Rad protein assay. After harvesting protein lysates, 20  $\mu$ l Reagent S diluted with Reagent A (1:50) were added into a 96 well plate followed by 2  $\mu$ l of each sample and mixed with 200 $\mu$ l reagent B. The plate was incubated for 10 minutes at room temperature on the shaker. Then, the concentrations of samples were quantified by Infinite M200 at 595nm. A standard curve was produced by quantifying BSA samples of standard concentration (0.125, 0.25, 0.5, 1, 1.5, 2 mg/ml).

### 2.2.9 Immunoblotting

20 $\mu$ g of total cell protein extracts were subjected to 10% or 12% sodium dodecyl sulfate polyacrylamide electrophoresis (SDS-PAGE) gel and transferred to nitrocellulose membranes. 5% BSA in Tris-buffered saline with Tween 20 (TBST) was used to block nonspecific binding. Membranes were probed with primary and

secondary antibodies in TBST according to manufacturer's instructions. HRP-linked anti-mouse, anti-rat and anti-rabbit antibodies were used as secondary antibodies. Alpha-tubulin and GAPDH were used as loading control. Signal was visualized by incubating the blots in Supersignal Ultra (Pierce, Hamburg, Germany).

#### 2.2.10 MTT assay

After knockdown of SOX9 expression, cells were treated with 0.25% trypsin to make single cell suspension and re-plated in a 96-well plate at a density of  $2.0 \times 10^3$  cells per well with 100 $\mu$ l growth medium. 2 days after the cells attachment, cells were incubated with 5mg/ml MTT reagent for 5h. Then, the supernatant was removed carefully and 100 $\mu$ l solvent solution containing 40% of 10% SDS, 40% DMSO and 20% Acetate acid solution (600 $\mu$ l Acetate acid/50mL PBS) was added and incubated overnight for measurement. Absorbance was measured at 570nm with a reference to 630 nm. For proliferation assay, cells were incubated in 96-well plate for 48 hours before incubation with MTT. For gemcitabine IC<sub>50</sub> measurement, cells were incubated for 6 h for attachment. Then, cells were treated with serial concentrations of gemcitabine for 48 hours before incubating with MTT.

#### 2.2.11 Cell cycle analysis

Cells were harvested at 48 hours after siRNA treatment and washed with cold PBS, then fixed with 70% cold ethanol. The cells were re-suspended in solution containing TritonX-100 (0.1%) and 100 $\mu$ g/ml RNase to remove RNA. The samples were stained with propidium iodide (20 $\mu$ g/mL) for 30 minutes in the dark, and then subjected to analysis for DNA content using FACS Calibur (BD Biosciences, Heidelberg, Germany) and data analysis was performed using Flowjo version10 software.

#### 2.2.12 Transwell migration assay

Cell culture inserts with 8 $\mu$ M pore size (Falcon) were used. For tumor cell migration,  $2.0 \times 10^5$  CCA tumor cells were suspended in RPMI 1640 or DMEM medium with 0.5% FBS and plated in the upper chambers. The lower chambers were filled RPMI 1640 or DMEM with 10% FBS. After 16 h, the medium in the inserts were removed and washed with PBS. The inserts were filled with 3.7% formaldehyde for 5 minutes. Subsequently, incubate the inserts in methanol for 30 minutes. The filters were stained with 10% Gimsa (Sigma, St. Louis, MO) for 15 minutes. The inner side was

wiped with cotton swaps. The migrated cells were count under an inversed microscope.

#### 2.2.13 Caspase 3 assay

Caspase 3 assay was performed as previously described [117]. In detail, after wash the cells with ice-cold PBS, immediately add 70  $\mu$ l Caspase 3 lysis buffer to per well of 6-well plate and put on ice. Lysates were collected by cell scraper and put into 1.5ml tube followed by centrifugation at 13000rpm for 10min at 4°C. Supernatant in each tube was collected into a new 1.5ml tube and stored at -20°C until use. Then, 20  $\mu$ l cell extracts were added to 70 $\mu$ l Caspase 3 reaction buffer and 10  $\mu$ l AC-DEVD-AFC caspase 3 fluorimetric substrate (Biomol, Hamburg, Germany) in a white 96-well plate. Then, the plate was incubated for 90 minutes at dark. Subsequently, Caspase 3 activity was detected by fluorometric measurement using Tecan infinite M200 (excitation 400 nm; emission 505 nm). Protein concentrations of the cell extracts were measured by Bio-Rad protein assay as mention in protein concentration determination. The caspase3 activity was normalized with the absorbance intensity dividing the protein concentration and expressed as relative fluorescent units (RFU) per minute per mg protein.

#### 2.2.14 Tumor sphere formation assay

The protocol used for tumor sphere formation culture was as previously described with modification [118]. 12 hours after SOX9 knockdown, cells were washed with PBS and treated with 0.25% trypsin7 EDTA to make single cell suspension. Then, cells were suspended in serum-free DMEM/F12 containing 10% BIT 9500 and 2mM L-glutamine supplied with 10ng/ml human recombinant epidermal growth factor (EGF), 10ng/ml human recombinant basic fibroblast growth factor (FGF-2) and 1% penicillin-streptomycin. Thereafter, culture the cells in non-adherent 12-well plates at a density of  $1 \times 10^4$ /ml pre well. After 10 days incubation, tumorsphere numbers are counted under a Leica phase-contrast microscope using the 20x magnification lens. Tumor spheres bigger than 100  $\mu$ m are considered as positive.

#### 2.2.15 RNA isolation and RNA concentration determination

Total cell RNA was extracted using the InviTrap spin universal RNA mini kit (Stratec, Berlin, Germany), according to the manufacturer's instruction.

Protocol for RNA isolation modified from the *Instruction for the InviTrap® Spin Universal RNA Mini Kit*

### Step1: Cell disruption

Wash the cells twice with ice-cold PBS. Then, immediately add 300µl β-mercaptoethanol-containing lysis solution TR to per well of 6-well plate. Thereafter, scrape the cells to collect lysate and transfer to a 1.5 ml Eppendorf tube and stored at -80°C until use.

### Step2: Binding of genomic DNA to the DNA-Binding Spin Filter

Pipet the lysate resulting from step1 directly onto the DNA-Binding Spin Filter placed in a 2 ml Receiver Tube. Incubate the sample for 1 min and centrifuge at 13.000rpm for 2 minutes. Discard the DNA-Binding Spin Filter.

### Step3: Adjust RNA binding conditions

Add 250µl 70 % ethanol to the RNA containing lysate and mix thoroughly by pipetting up and down.

### Step4: Binding of the total RNA to the RNA-RTA Spin Filter

Pipet the sample from step 3 onto a RNA-RTA Spin Filter and incubate for 1 min and centrifuge at 13.000rpm for 1 minute. Discard the flow-through.

### Step5: 2 times wash of the RNA-RTA Spin Filter

Add 600µl Wash Buffer R1 onto the RNA-RTA Spin Filter and centrifuge for 1 min at 13.000rpm. Discard the flow-through. Then Add 700 µl Wash Buffer R2 onto the RNA-RTA Spin Filter and centrifuge for 1 min at 13.000rpm. Discard the flow-through. Drying of the RNA-RTA Spin Filter membrane to eliminate any trace of ethanol by centrifuging for 4 min at maximum speed.

### Step6: Elution of total RNA

Transfer the RNA-RTA Spin Filter into a RNase-free Elution Tube and pipet 40µl of Elution Buffer R directly onto the membrane of the RNA-RTA Spin Filter. Incubate for 2 min and centrifuge for 1 min at 13.000rpm. Discard the RNA-RTA Spin Filter and place the eluted total RNA immediately on ice.

### Step7: RNA concentration determination

RNA concentration was photometric determined by measuring the RNA solution in a nanocrystalline plate at 260nm with Tecan infinite M200.



### 2.2.16 Quantitative real-time reverse transcription polymerase chain reaction

For first strand cDNA synthesis, reverse transcription of 500ng RNA was performed with random primer (Thermo Scientific) and RevertAid H Minus M-MuLV reverse transcriptase (Thermo Scientific) according to the manufacturer's instructions and subsequently diluted with nuclease-free water (Invitrogen) to 10ng/μl cDNA. For PCR amplification, 10.4μl mixtures contained 5μl (50ng) template cDNA, 5μl SYBR Green (4367659, Life Technologies), and 4μM forward and reverse primer. PCRs were run in triplicate and performed on a StepOnePlus Real-time PCR (Applied Biosystems). PCR amplification cycling conditions comprised 10 min polymerase activation at 95 °C and 40 cycles at 95°C for 15s and 60°C for 1 min. A melting curve analysis was performed for each PCR analysis. Relative quantification of target genes was normalized against the house keeping gene PPIA. The reverse and forward primers used for the current study are listed in Table 15.

Table 15. Primers used for qRT-PCR in this study

Primer	Forward	Reverse
SOX9	AGCGCCCCCACTTTTGCTCTTT	CCGCGGCGAGCACTTAGGAAG
EpCAM	AATCGTCAATGCCAGTGTACTT	TCTCATCGCAGTCAGGATCATAA
ABCB1	AAATTGGCTTGACAAGTTGTATATGG	CACCAGCATCATGAGAGGAAGTC
ABCG2	TCATCAGCCTCGATATTCCATCT	GGCCCGTGGAACATAAGTCTT
ABCC6	TTGGATTCGCCCTCATAGTC	GGTAGCTGGCAAGACAAAGC
PPIA	AGGGTTCCTGCTTTCACAGA	CAGGACCCGTATGCTTTAGG

### 2.2.17 Microarray analyses and Gene set enrichment analysis (GSEA)

Total RNA from cell cultures were isolated as described in RNA isolation. Total RNA (10 μg) from samples was tested for quality using an Agilent 2100 Bioanalyzer Chip, reverse transcribed. Gene expression profiling was performed using arrays of human HuGene-2-0-st-type from Affymetrix. The following protocol was kindly provided by Dr. Carolina De La Torre in Zentrum für Medizinische Forschung of Medical Faculty of Mannheim of Heidelberg University. In detail, biotinylated antisense cDNA was then prepared according to the Affymetrix standard labelling protocol with the GeneChip® WT Plus Reagent Kit and the GeneChip® Hybridization, Wash and Stain

Kit (both from Affymetrix, Santa Clara, USA). Afterwards, the hybridization on the chip was performed on a GeneChip Hybridization oven 640, then dyed in the GeneChip Fluidics Station 450 and thereafter scanned with a GeneChip Scanner 3000. All of the equipment used is from the Affymetrix-Company (Affymetrix, High Wycombe, UK). A Custom CDF Version 21 with ENTREZ based gene definitions was used to annotate the arrays. The Raw fluorescence intensity values were normalized applying quantile normalization and RMA background correction. OneWay-ANOVA was performed to identify differential expressed genes using a commercial software package SAS JMP10 Genomics, version 6, from SAS (SAS Institute, Cary, NC, USA). A false positive rate of  $\alpha=0.05$  with FDR correction was taken as the level of significance.

Integrated analysis of gene expression signatures of CCA patients was performed on a dataset GSE26566 from Andersen JB et al [86], which is a publicly available gene expression dataset from Gene Expression Omnibus (GEO). GSEA was performed using the Broad Institute platform (<http://software.broadinstitute.org>) [119]. Samples were analyzed with weighted, t-test default settings. The GSE26566 dataset included transcriptomes of 104 freshly-frozen tumor tissues and normal biliary epithelial cells from 6 non-tumor patients. Differential expressed genes identified if the fold change was greater than 2 (up or down) in comparison to control group. Gene sets with a false discovery rate (FDR) value  $< 0.25$  after performing 1000 permutations were considered to be significantly enriched.

#### 2.2.18 Statistical analyses

Data were analyzed using the GraphPad Prism built-in tests. Variables were summarized as means  $\pm$  standard deviation (SD) and depicted graphically as means  $\pm$  SD. *P* values were calculated using the chi-square test or calculated using a two-sided Student's *t* test. Kaplan-Meier survival analysis was used to evaluate overall survival rates and disease free survival rate of iCCA patients. *P* values were calculated using the log-rank test.  $P < 0.05$  was considered significant.

### 3 RESULTS

#### 3.1 Clinical significance of SOX9

##### 3.1.1 SOX9 expression in chronic liver disease

Firstly, SOX9 expression was examined in 21 patients with chronic liver disease. Immunohistochemistry analyses reveal that in 17 specimens, SOX9 is expressed in the nuclei of biliary cells, as located in canals of Hering, reactive ductules and bile ducts (**Patients 2, 3 and 4, Figure 6**), whereas 4 patients show negative SOX9 immunoreactivity (**Patient 1, Figure 6**).

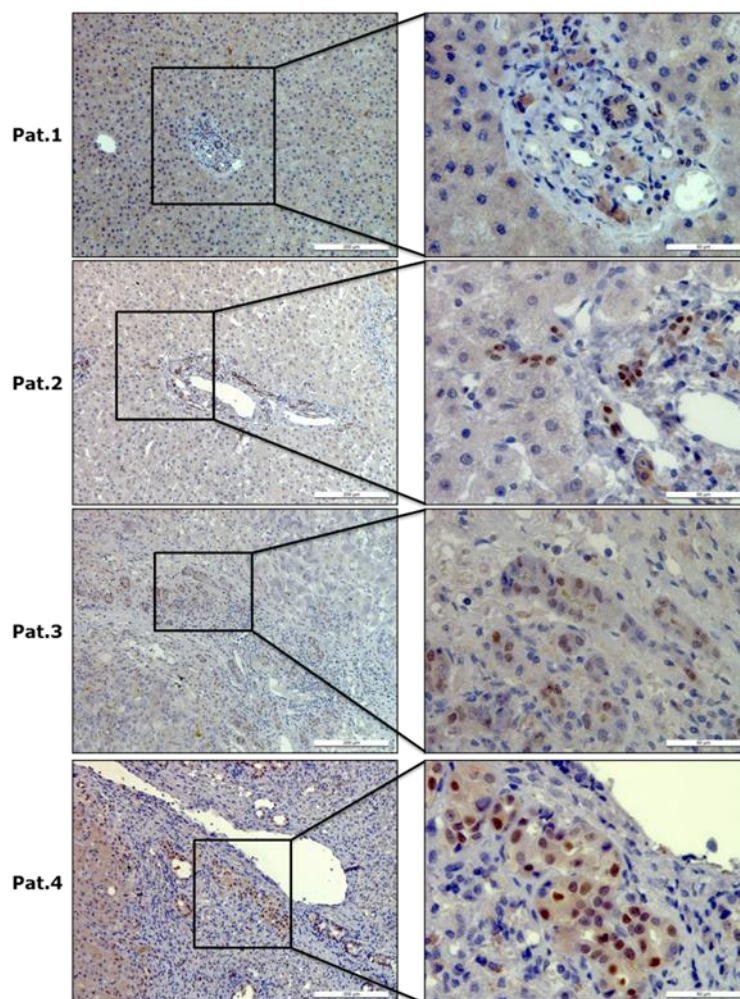


Figure 6. Expression of SOX9 in chronic liver disease (Immunohistochemical staining). Patient 1 (Pat.1) shows negative SOX9 expression in biliary epithelial cells. Patient (Pat.) 2, 3 and 4 show strong expression of SOX9 in the nucleus of the canals of Hering, reactive ductules and bile duct cells.

### 3.1.2 SOX9 expression in iCCA

Next, I examined expression of SOX9 and CK19, another cholangiocyte marker, in paired liver tissue specimens of 69 iCCA patients (tumor surrounding tissue vs. tumor) and 5 eCCA patients by immunohistochemistry. Both, SOX9 and CK19 are markers of cholangiocytes, however localize at different cellular compartments. SOX9 is expressed in the nuclei of cholangiocytes, while CK19 localizes in cytoplasm and membranes. As in chronic liver disease, nuclear immunoreactivity of SOX9 is either positive or negative in the cholangiocytes surrounding CCA tumors (**Figure 7, left panel**). In contrast to such more heterogeneous pattern for SOX9, all cholangiocytes in the CCA tumor surroundings express CK19 (**Figure 7, right panel**).

In iCCA tumor tissue, 27% patients highly express SOX9, while 37% patients express high levels of CK19. Taking into account intensity of immunoreactivity, four different patterns of SOX9 and CK19 expression are defined in iCCA cancer cells, that is SOX9<sup>high</sup>CK19<sup>high</sup>, SOX9<sup>high</sup>CK19<sup>low</sup>, SOX9<sup>low</sup>CK19<sup>high</sup> and SOX9<sup>low</sup>CK19<sup>low</sup> (**Figure 8**). Statistically, expression of SOX9 and CK19 in iCCA tumor cells are positively associated ( $P < 0.05$ , **Table 16**). From 5 eCCA patients, 4 highly expressed SOX9 (**Figure 9**). In all examined tissue specimens, neither SOX9 nor CK19 are detected in hepatocytes.

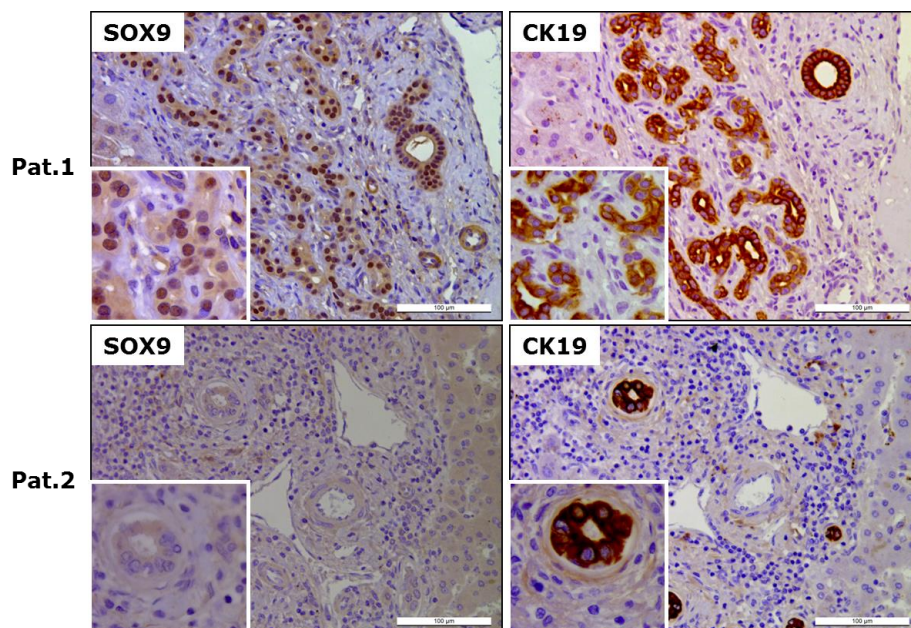


Figure 7. Expressions of SOX9 and CK19 in CCA tumor surrounding tissue (Immunohistochemical staining).



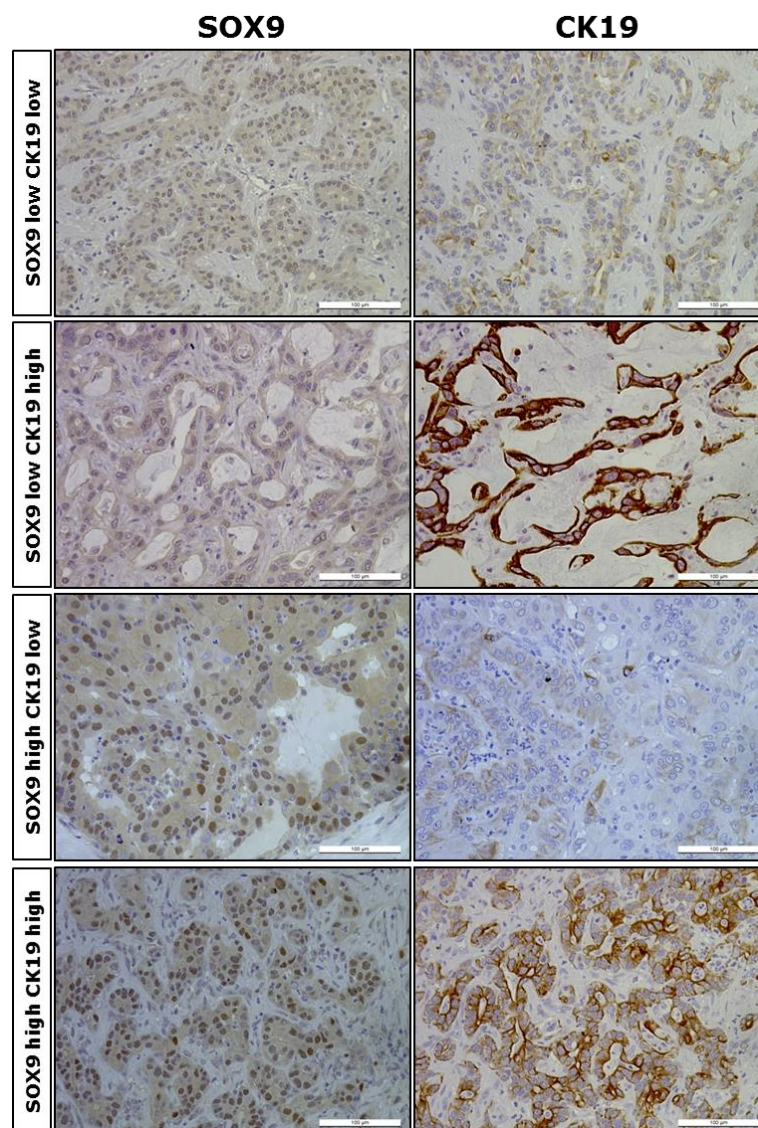


Figure 8. Expression patterns of SOX9 and CK19 in iCCA tumor tissue (Immunohistochemical staining). According to the immunoreaction intensity for SOX9 and CK19, four expression patterns of SOX9 and CK19 were defined: SOX9<sup>high</sup>CK19<sup>high</sup>, SOX9<sup>high</sup>CK19<sup>low</sup>, SOX9<sup>low</sup>CK19<sup>high</sup> and SOX9<sup>low</sup>CK19<sup>low</sup>.

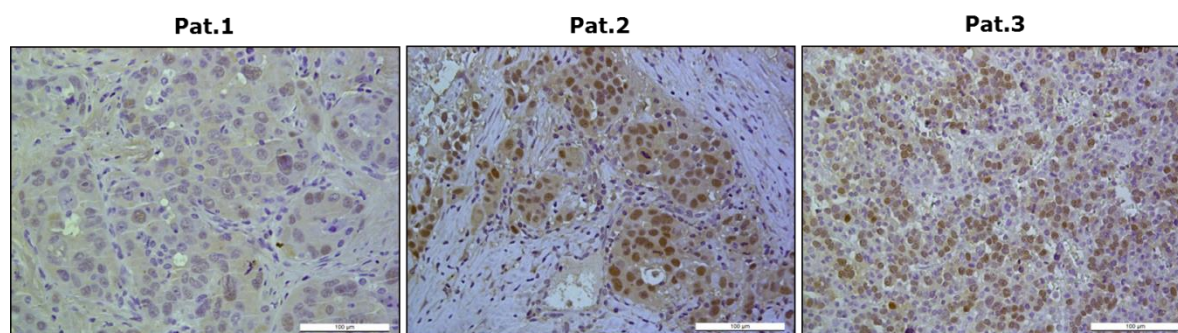


Figure 9. Expression of SOX9 in eCCA (Immunohistochemical staining). Patient 1 (Pat.1) is negative for SOX9 expression. Patients 2 and 3 show strong SOX9 staining in the nuclei of tumor cells.

Table 16. Correlation of SOX9 and CK19 expression in iCCA

CK19 expression	SOX9 expression		No. of patients	P value
	high	low		
high	15	11	26	0.033
low	35	8	43	

### 3.1.3 CCA patients with high SOX9 expression have poor clinical outcome

Then, I analyzed the relationship between SOX9 or CK19 expression and the clinical outcome for the patients, including clinical parameters and patients' survival time. **Table 17** shows that SOX9 expression is not associated with the indicated clinical parameters, whereas CK19 expression is associated with lymph node involvement and the AJCC stage of iCCA (**Table 18**). Kaplan-Meier analysis and log-rank test showed that patients with high SOX9 expression had shorter overall survival (OS) and disease free survival (DFS) rates than those with low SOX9 expression ( **$P < 0.01$  and  $P < 0.05$ , Figure 10A and B**). There is no significant association between CK19 expression and the OS of the patients ( **$P > 0.05$ , Figure 10C**). Patients with CK19 high expression show shorter DFS rate in comparison to those with CK19 low expression, although this is without a statistical difference ( **$P = 0.0575$ , Figure 10D**). Median OS and DFS times of the patients in correlation to SOX9 and CK19 expression are presented in **Tables 19 and 20**. The results reveal that patients with high SOX9 expression display shorter median OS time (22 months) than those with high CK19 expression (26 months), whereas both presented with the same median DFS time (9 months).

In the presented study, 9 iCCA patients received chemotherapy. SOX9 and CK19 expression, treatment approaches and clinical outcome of these patients are presented in **Table 21**. Kaplan-Meier analysis and log-rank test show that SOX9 high expression patients, who received chemotherapy, had shorter OS rates in comparison to those with low SOX9 expression ( **$P=0.0171$ , Figure 11**). There is no significant difference in OS rates between CK19 high and low expression patients ( **$P=0.6815$ , Figure 12**). Median OS times of the two groups of patients, who received

chemotherapy, are 22 and 62 months, respectively (**Table 22**). These results suggest that patients with low SOX9 expression are more sensitive to chemotherapy.

Table 17. Patient characteristics and tumor parameters in relation to SOX9 expression in iCCA

Clinicopathological parameters	SOX9 expression		No. of the patients per group	P value
	low expression (n=50)	high expression (n=19)		
Age(year)	64.08±9.24	60.42±10.29	69	0.194
<60	14	8	22	0.261
≥60	36	11	47	
Gender				0.296
Male	33	15	48	
Female	17	4	21	
Tumor extension				0.447
T1	19	9	28	
T2	19	6	25	
T3	12	2	14	
Lymph node involvement				0.219
Yes	12	2	14	
No	36	16	52	
Metastasis				0.079
Yes	7	0	7	
No	39	18	57	
Differentiation grade				0.634
G1	5	1	6	
G2	18	9	27	
G3	10	3	13	
Vascular invasion				0.247
Yes	6	4	10	
No	41	12	53	
Satellite nodules				0.502
Yes	16	4	20	
No	31	12	43	
Cirrhosis				0.318
Yes	11	6	17	
No	34	10	44	
AJCC classification				0.135
I+II	28	13	41	
II+III	22	4	26	

## RESULTS

Table 18. Patient characteristics and tumor parameters in relation to CK19 expression in iCCA

Clinicopathological parameters	CK19 expression		No. of the patients per group	P value
	low expression (n=43)	high expression (n=26)		
Age(year)	64.77±9.17	60.27±9.84	69	0.060
<60	11	11	22	0.149
≥60	32	15	47	
Gender				0.260
Male	32	16	48	
Female	11	10	21	
Tumor extension				0.394
T1	20	8	28	
T2	16	9	25	
T3	7	7	14	
Lymph node involvement				<b>0.022</b>
Yes	5	9	14	
No	36	16	52	
Metastasis				0.695
Yes	5	2	7	
No	34	23	57	
Differentiation grade				0.088
G1	6	0	6	
G2	14	13	27	
G3	7	6	13	
Vascular invasion				0.722
Yes	7	3	10	
No	34	19	53	
Satellite nodules				0.799
Yes	16	4	20	
No	31	12	43	
Cirrhosis				0.929
Yes	11	6	17	
No	29	15	44	
AJCC classification				<b>0.014</b>
I+II	31	10	41	
II+III	12	14	26	



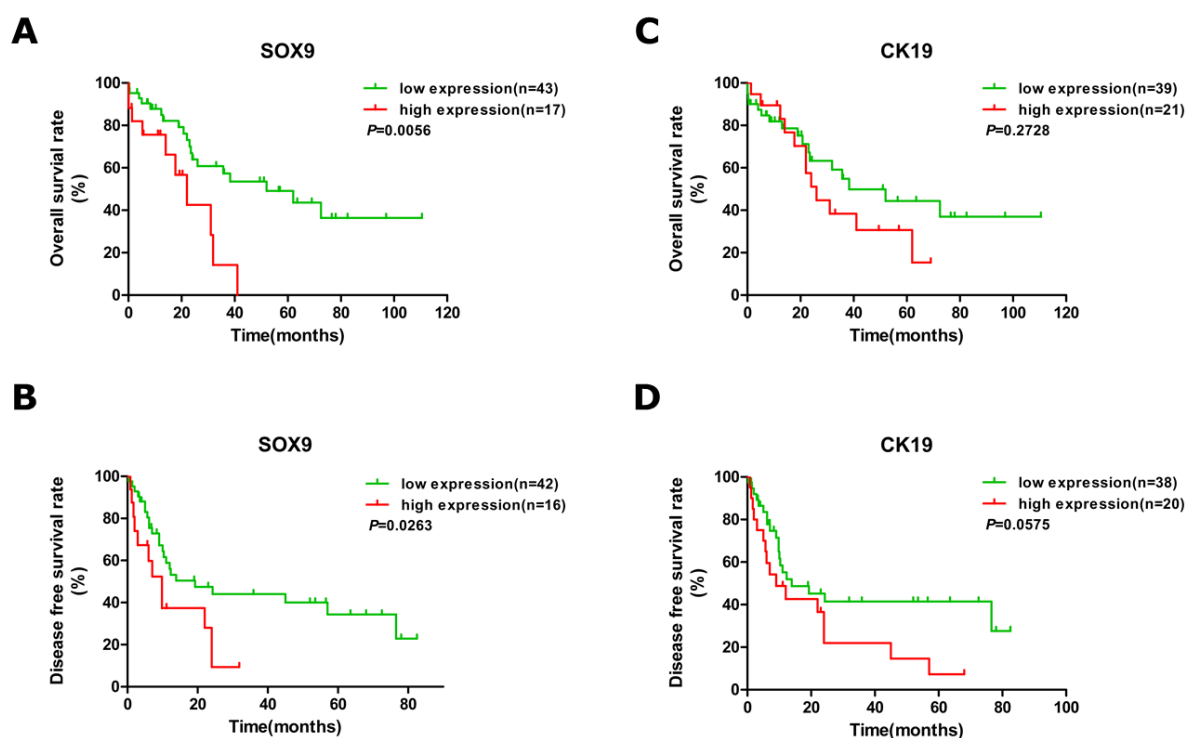


Figure 10. Kaplan-Meier survival curves of iCCA patients in relation to SOX9 and CK19 expression.

Table 19. Median overall survival time of iCCA patients in relation to SOX9 and CK19 expression

Staining and expression		Median survival time (months)		
		Overall survival	HR (95% CI)	P
SOX9	Low	52.0	0.2362 (0.085 to 0.656)	0.0056
	High	22.0		
CK19	Low	38.3	0.6425 (0.291 to 1.417)	0.2728
	High	26.0		

## RESULTS

Table 20. Median disease free survival time of iCCA patients in relation to SOX9 and CK19 expression

Staining and expression		Median survival time (months)		
		Disease free survival	HR (95% CI)	<i>P</i>
<b>SOX9</b>	Low	19.3	0.3820(0.163 to 0.893)	<b>0.0263</b>
	High	9		
<b>CK19</b>	Low	13.9	0.4968(0.241 to 1.023)	0.0575
	High	9		

Table 21. SOX9 and CK19 expression and clinical outcome of iCCA patients receiving chemotherapy

SOX9 IHC intensity	CK19 IHC intensity	Death or survival (1=survival, 0=death)	Survival time (months)	Treatment
low	low	0	23	Gemcitabine plus XELOX
low	strong	0	62	Gemcitabine plus Cisplatin plus XELOX
low	strong	1	33	Gemcitabine
low	low	1	36	Palliative chemotherapy
low	strong	1	57	Cisplatin plus Gemcitabine
low	low	1	51	Palliative chemotherapy
strong	strong	0	14	Erlotinib
strong	strong	0	22	Gemcitabine plus Cisplatin
strong	strong	0	41	Palliative chemotherapy

XELOX: Capecitabine plus Oxaliplatin.

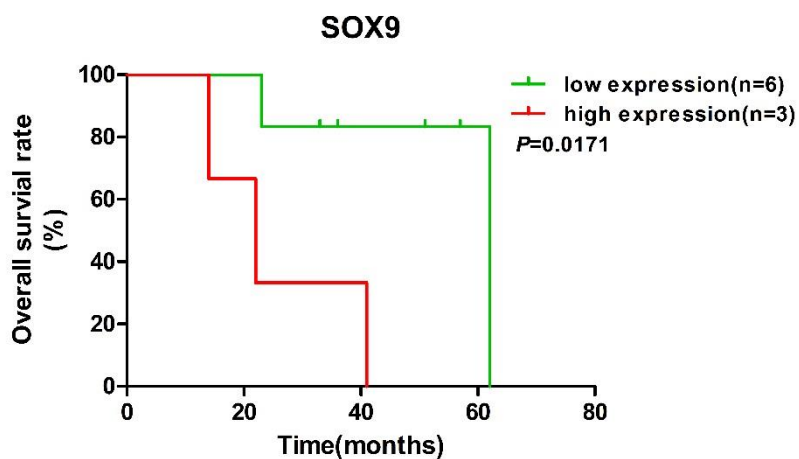


Figure 11. Kaplan-Meier survival curve of iCCA patients having received chemotherapy in relation to SOX9 expression.

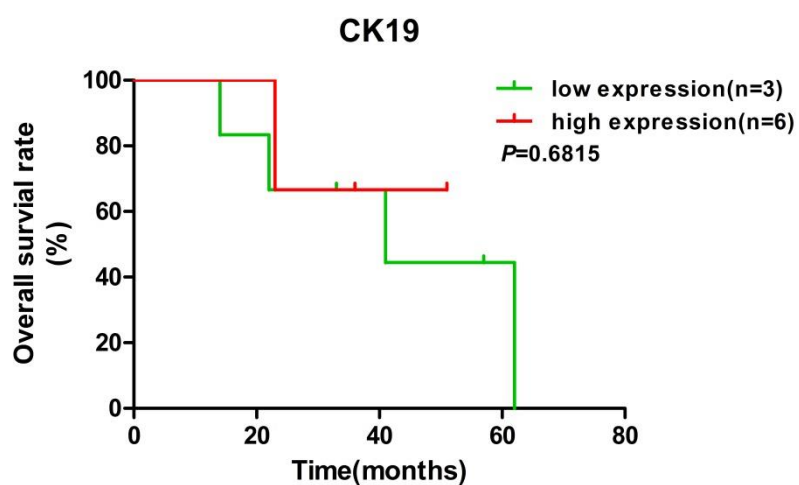


Figure 12. Kaplan-Meier survival curve of iCCA patients having received chemotherapy in relation to CK19 expression.

Table 22. Median overall survival times of patients having received chemotherapy

SOX9 expression		Median survival time	HR (95% CI)	P
SOX9	Low	62.0	0.06 (0.006 to 0.605)	0.0171
	High	22.0		

### 3.1.4 Integrated analysis of CCA patients gene expression signatures

To comprehensively elucidate the role of SOX9 in CCA patients, several approaches were set up. First, an integrated analysis of gene expression signatures was performed with the CCA patient dataset GSE26566, which is publicly available from Gene Expression Omnibus (GEO) that included transcriptomes of 104 freshly-frozen CCA tumor tissues and “normal” primary biliary epithelial cells isolated from 6 non-tumor patients. SOX9 is significantly highly expressed in CCA tumor cells as compared to normal biliary epithelial cells (**Figure 13A and B**). We next categorized the 104 CCA patients into SOX9 high (n=66) and SOX9 (n=38) low expression groups, based on SOX9 mRNA expression levels being above or below 2 fold of the average SOX9 expression in normal NBEC (**Figure 13B**).

Subsequently, I performed GSEA to define the CCA related Kyoto Encyclopedia of Genes and Genomes (KEGG) pathways related to SOX9 expression **Tables 23 and 24 ( $P<0.05$  and  $FDR<0.25$ )**. The most significantly enriched pathways in CCA with high SOX9 expression are *DNA damage repair*, more specifically *homologous recombination and mismatch repair*, *DNA replication*, *base excision repair*, *nucleotide excision repair* and *cell cycle* (**Figure 13C**). SOX9 high expression tumors also presented with upregulated *epithelial junction* genes, such as *adherens*, *tight junction* and *actin cytoskeleton*. Additionally, genes associated with Notch, Wnt and mTOR signalings are enriched in the SOX9 high expression patients group. Patients with low SOX9 expression displayed gene signatures associated with *drug metabolism pathways*, including *cytochromes P450* as well as other *drug metabolism enzymes* (**Figure 13D**). In summary, the results imply that SOX9 expression in CCA is associated with DNA damage repair, the formation of tight junction and drug metabolism.

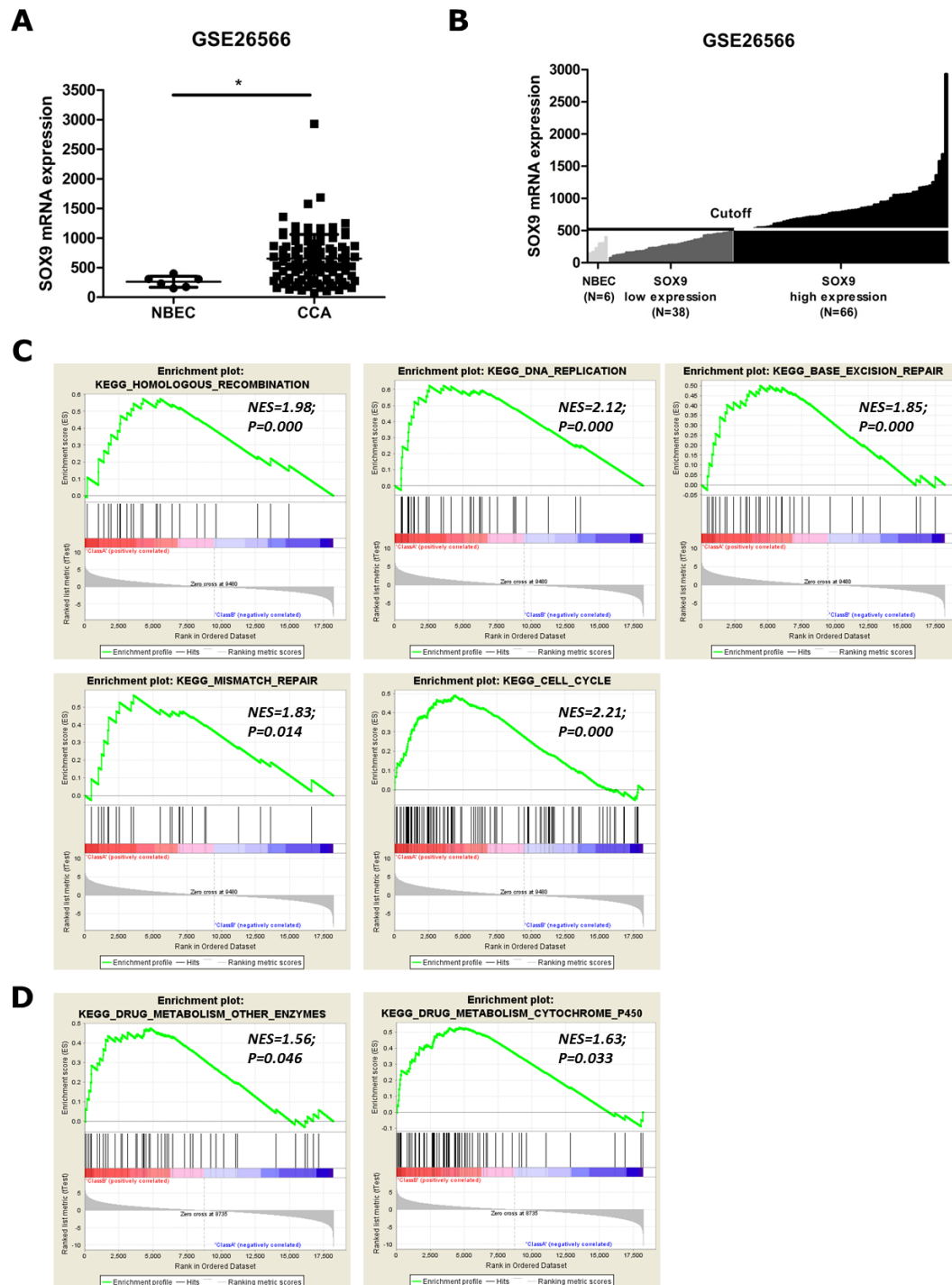


Figure 13. Integrated analyses of CCA patients gene expression signatures related to SOX9 expression. **A.** Expression of SOX9 is higher in CCA tumor tissues as compared to normal biliary epithelial cells (NBEC). **B.** CCA patients were categorized into SOX9 high (Class A) and SOX9 low (Class B) expression groups according to the SOX9 mRNA expression in CCA. The cutoff value for categorizing the patients was set as 2 fold of average mRNA expression of SOX9 in NBECs. **C.** GSEA showing enrichment of gene signatures associated with, among others, *homologous recombination*, *mismatch repair*, *DNA replication*, *base excision repair* and *cell cycle* in CCA patients with high SOX9 expression. **D.** Significantly enriched gene signatures in SOX9 low CCA patients comprise especially drug metabolism enzymes. NES: normalized enrichment score. FDR: false discovery rate.

## RESULTS

Table 23. GSEA of KEGG pathway ranked by a positive correlation with SOX9 expression in CCA patients ( $P < 0.05$ ,  $FDR < 0.25$ )

Name	NES	NOM p-val	FDR q-val
<b>CELL_CYCLE</b>	2.21	0.000	0.000
<b>NOTCH_SIGNALING_PATHWAY</b>	2.18	0.000	0.000
RIBOSOME	2.15	0.000	0.000
<b>DNA_REPLICATION</b>	2.12	0.000	0.000
SPLICEOSOME	2.07	0.000	0.000
VASOPRESSIN_REGULATED_WATER_REABSORPTION	2.02	0.000	0.001
<b>HOMOLOGOUS_RECOMBINATION</b>	1.98	0.000	0.001
ALDOSTERONE_REGULATED_SODIUM_REABSORPTION	1.95	0.000	0.001
VIBRIO_CHOLERAE_INFECTION	1.94	0.000	0.002
GLYCOSYLPHOSPHATIDYLINOSITOL_GPI_ANCHOR_BIOSYNTHESIS	1.88	0.000	0.002
PYRIMIDINE_METABOLISM	1.87	0.000	0.002
<b>BASE_EXCISION_REPAIR</b>	1.85	0.000	0.003
<b>MISMATCH_REPAIR</b>	1.83	0.014	0.003
OOCYTE_MEIOSIS	1.77	0.000	0.006
AMINOACYL_TRNA_BIOSYNTHESIS	1.66	0.000	0.025
ENDOCYTOSIS	1.61	0.000	0.040
<b>TIGHT_JUNCTION</b>	1.58	0.000	0.052
RNA_POLYMERASE	1.57	0.006	0.051
PHOSPHATIDYLINOSITOL_SIGNALING_SYSTEM	1.56	0.000	0.053
GLYCOSPHINGOLIPID_BIOSYNTHESIS_LACTO_AND_NEOLACTO_SERIES	1.55	0.007	0.057
<b>NUCLEOTIDE_EXCISION_REPAIR</b>	1.55	0.010	0.055
PURINE_METABOLISM	1.50	0.007	0.088
<b>ADHERENS_JUNCTION</b>	1.45	0.011	0.123
PROGESTERONE_MEDIATED_OOCYTE_MATURATION	1.44	0.004	0.127
CARDIAC_MUSCLE_CONTRACTION	1.44	0.030	0.123
PATHOGENIC_ESCHERICHIA_COLI_INFECTION	1.44	0.039	0.122
<b>MTOR_SIGNALING_PATHWAY</b>	1.44	0.033	0.119
ERBB_SIGNALING_PATHWAY	1.41	0.018	0.143
<b>REGULATION_OF_ACTIN_CYTOSKELETON</b>	1.40	0.007	0.152
UBIQUITIN_MEDIATED_PROTEOLYSIS	1.38	0.011	0.158
FC_GAMMA_R_MEDIATED_PHAGOCYTOSIS	1.38	0.000	0.154
RENAL_CELL_CARCINOMA	1.35	0.021	0.187
<b>WNT_SIGNALING_PATHWAY</b>	1.30	0.049	0.240

## RESULTS

Table 24. GSEA of KEGG pathways ranked by negative correlation with SOX9 expression in CCA patients ( $P < 0.05$ , FDR  $< 0.25$ )

Name	NES	NOM p-val	FDR q-val
<b>PPAR_SIGNALING_PATHWAY</b>	1.92	0.003	0.041
LINOLEIC_ACID_METABOLISM	1.86	0.003	0.046
RETINOL_METABOLISM	1.74	0.014	0.120
FATTY_ACID_METABOLISM	1.73	0.001	0.108
COMPLEMENT_AND_COAGULATION_CASCADES	1.68	0.007	0.141
ALANINE_ASPARTATE_AND_GLUTAMATE_METABOLISM	1.67	0.021	0.138
TRYPTOPHAN_METABOLISM	1.67	0.006	0.125
<b>PRIMARY_BILE_ACID_BIOSYNTHESIS</b>	1.66	0.003	0.120
STEROID_HORMONE_BIOSYNTHESIS	1.64	0.038	0.124
PEROXISOME	1.64	0.019	0.115
<b>DRUG_METABOLISM_CYTOCHROME_P450</b>	1.63	0.033	0.106
PENTOSE_AND_GLUCURONATE_INTERCONVERSIONS	1.62	0.027	0.109
GLYCINE_SERINE_AND_THREONINE_METABOLISM	1.62	0.008	0.102
VALINE_LEUCINE_AND_ISOLEUCINE_DEGRADATION	1.60	0.011	0.116
<b>METABOLISM_OF_XENOBIOTICS_BY_CYTOCHROME_P450</b>	1.56	0.046	0.150
PROPANOATE_METABOLISM	1.56	0.012	0.144
ASCORBATE_AND_ALDARATE_METABOLISM	1.55	0.014	0.146
<b>DRUG_METABOLISM_OTHER_ENZYMES</b>	1.51	0.047	0.187
PRION_DISEASES	1.50	0.031	0.189
STARCH_AND_SUCROSE_METABOLISM	1.50	0.033	0.179
BETA_ALANINE_METABOLISM	1.49	0.032	0.185
BUTANOATE_METABOLISM	1.49	0.047	0.178
TYROSINE_METABOLISM	1.46	0.038	0.213

### 3.2 Investigating SOX9 function in CCA tumorigenesis and chemotherapy *in vitro*

#### 3.2.1 SOX9 is highly expressed in CCA cell lines

SOX9 and CK19 protein expression were examined in CCA cell lines CC-SW-1, HuCCT-1, HCCC-9810, EGI-1 and TFK-1, as well as in the normal biliary epithelial cell line MMNK-1 using immunoblotting. Both SOX9 and CK19 is highly expressed in CCA cells in comparison to MMNK-1 (**Figure 14**).

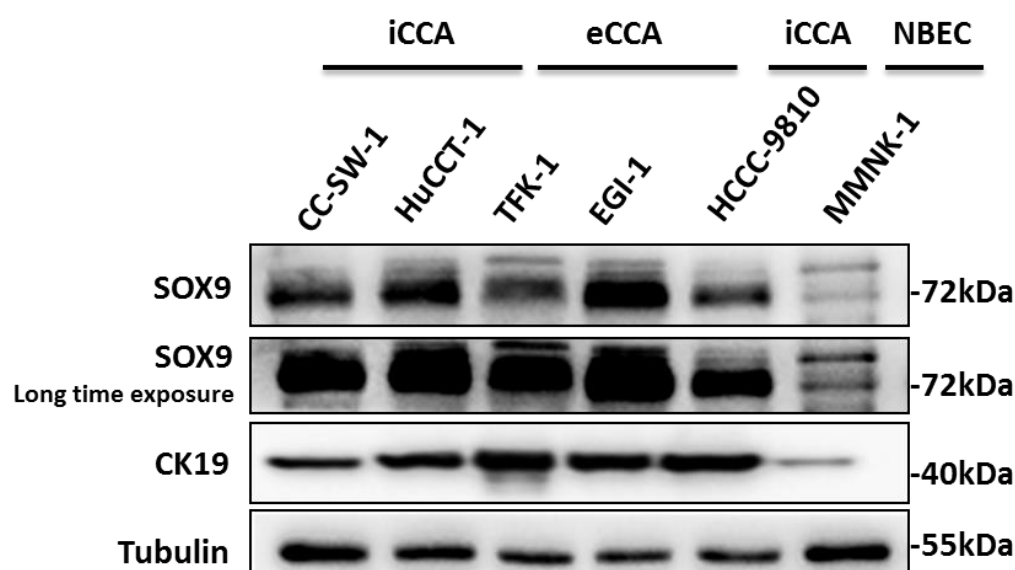


Figure 14. Expression of SOX9 and CK19 in CCA cell lines and normal biliary epithelia cell line MMNK-1 (immunoblot, Tubulin was used as loading control).

#### 3.2.2 Comparative microarray analysis of parental and SOX9 depleted CC-SW-1 cells

In a second approach to position SOX9 in the cellular fate of CCA tumors, small interfering RNAs were used to knock down SOX9 expression in the above CC-SW-1 cells. SOX9 mRNA depletion was confirmed by immunoblot showing a significantly reduced signal after treating the cells with SOX9 siRNA for 48 hours (**Figure 15**). In this stage, I purified the mRNA from knock down and control cells and a microarray analysis was performed to evaluate the respective gene expression signatures. **Figure 16A** shows 146 upregulated and 222 downregulated genes (Fold change > 2) upon SOX9 depletion. GSEA revealed that upregulated genes (that is suppressed from SOX9 in parental cells) were enriched in KEGG pathways ( $P < 0.05$  and  $FDR < 0.25$ ) relating to p53, MAPK signaling, complement and coagulation cascades (**Figure 16B**). Downregulated genes (that is under the control of SOX9 in parental



cells) enriched in KEGG pathway are related to cytochrome P450 related metabolism of xenobiotics and drugs, mTOR signaling pathway ( $P<0.05$  and  $FDR<0.25$ ). In detail, genes dedicated for drug metabolism comprise UGT1A6, UGT1A9, ALDH1A3, GSTA2, GSTA4, AKR1C3 and MAOB, and related to adenosine triphosphate (ATP)–binding cassette (ABC) transporters include ABCB1 and ABCC4 (**Figure 17A**). Upregulated genes that integrate into the p53 pathway are FAS, SFN and PMAIP1 (**Figure 17A**). In addition, SOX9 inhibition decreases expression of genes related to the actin cytoskeleton, including PIK3R, PDGFD, FGFR2 and FGFR4. Moreover, SOX9 silencing dysregulated genes related to cell adhesion, including upregulation of CLDN1, CDH4, NEGR1, JUN, ITGA2, LAMB3 and LAMC2, whereas downregulation of CDH1, HLA-DMA, NLGN1, CADM1 and EGR1 (**Figure 17B**). Taken together, microarray analysis implied that SOX9 in CCA cells has impacts on cellular fate related to drug metabolism, survival and cell adhesion.

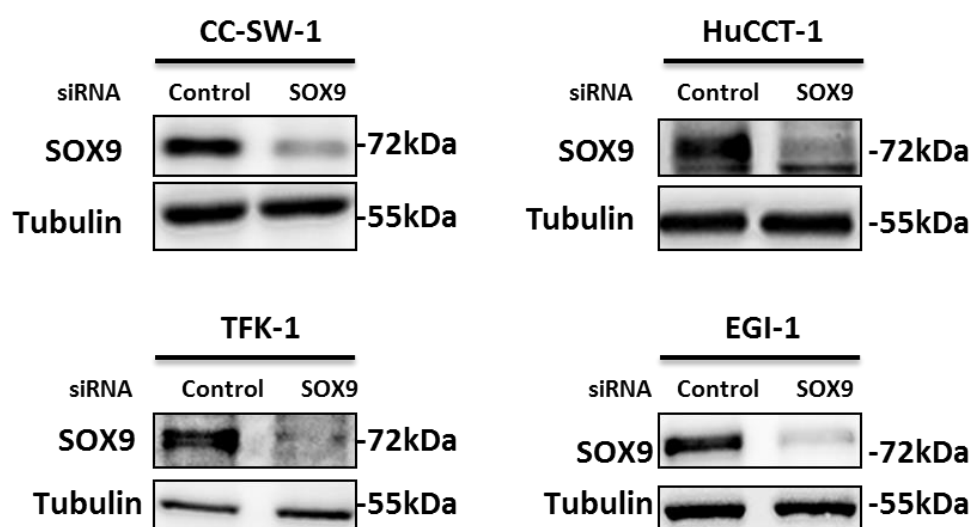


Figure 15. SOX9 expression in CCA cells with or without SOX9 siRNA treatment for 48 hours (immunoblot, Tubulin was used as loading control).

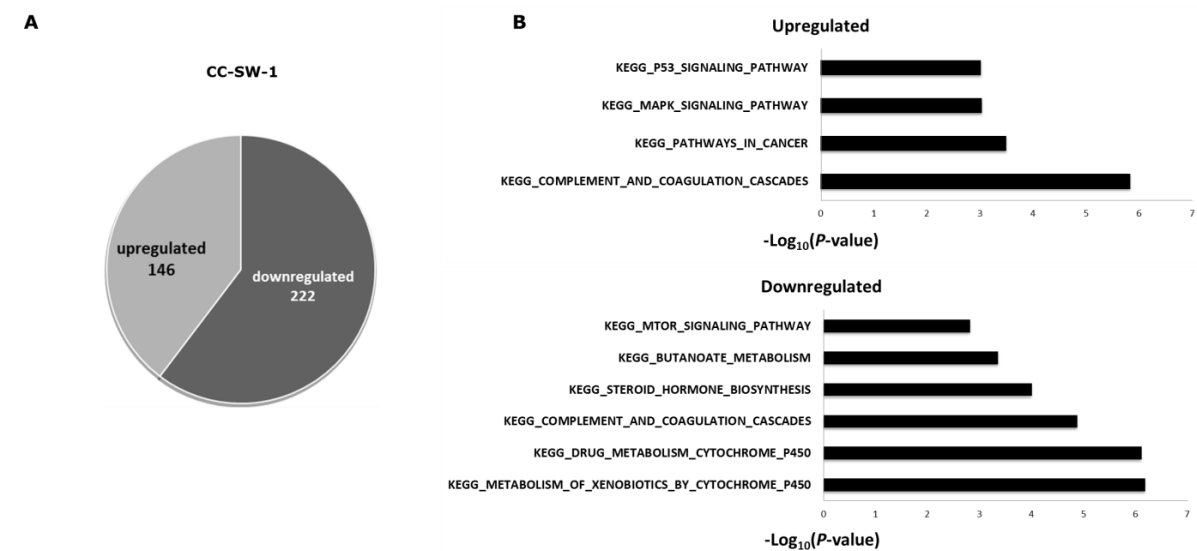


Figure 16. Comparative microarray analysis of CC-SW-1 cells with SOX9 knockdown as compared to control cells. **A.** Pie chart shows gene expression changes of more than 2 fold. **B.** Bar plots for enriched KEGG pathways of the top 146 upregulated and 222 downregulated genes ( $P<0.05$  and  $FDR<0.25$ ).

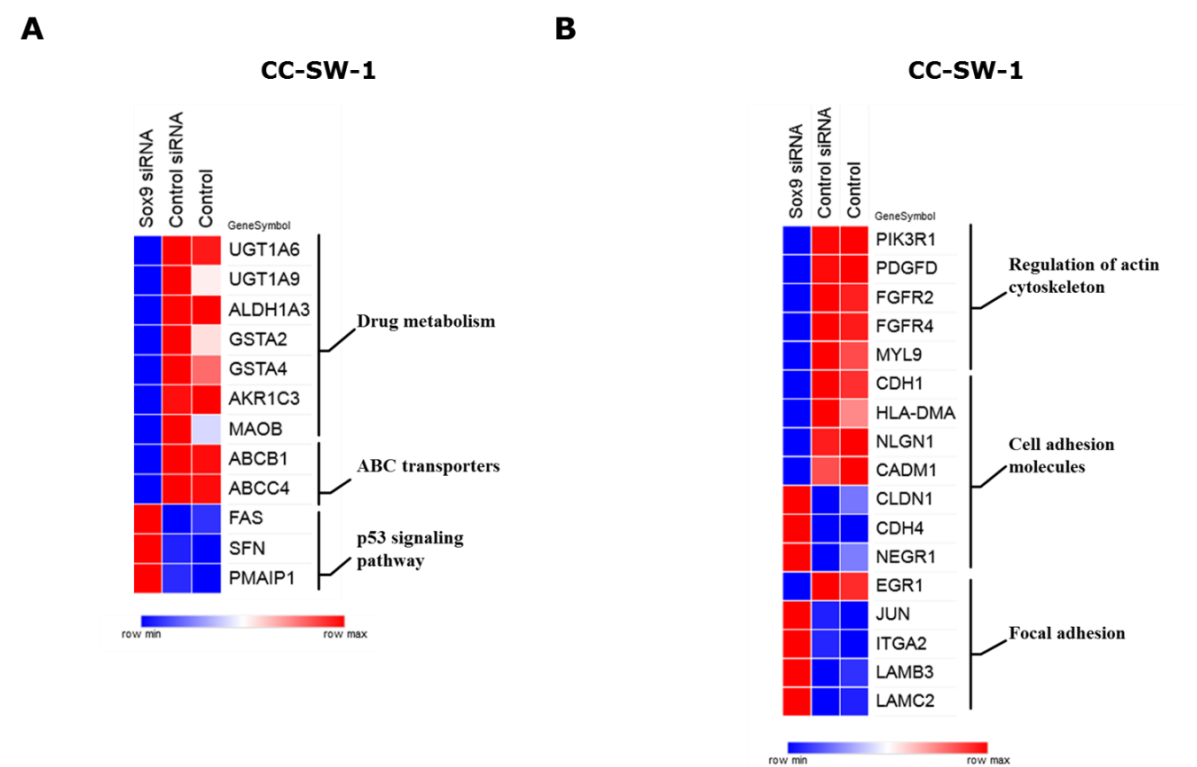


Figure 17. Heatmap illustration of the gene expression analyses in CC-SW-1 CCA cells with or without SOX9 siRNA treatment. **A, B.** Heatmap graphs showing Sox9 dependent genes relating to pathways as indicated. ABC, adenosine triphosphate (ATP)–binds cassette.

### 3.2.3 Depleting SOX9 suppresses CCA cell survival

Then, I investigated the function of SOX9 on CCA cell survival. The MTT assay shows that knockdown of SOX9 expression inhibits cell viability of CCA cells (**Figure 18**). Then, cell cycle analyses reveal that SOX9 knockdown significantly decreases the proportion of cells in G1 phase, whereas cell numbers in G2/M phase are increased in both CC-SW-1 and EGI-1 cells (**Figure 19**). Immunoblots further show that depleting SOX9 reduces the expression of cyclin-dependent kinase inhibitors p27 and p16, whereas p21 expression is induced in CC-SW-1 cells (**Figure 20**). EGI-1 cells, in contrast to CC-SW-1 cells, show the opposite result regarding p21 (**Figure 20**). Importantly, SOX9 inhibition induced cell apoptosis in both CC-SW-1 and EGI-1 cells (**Figure 21**). Disruption of SOX9 had no effect on the expression of anti-apoptotic proteins Bcl-xL and Bcl-2, cell cycle regulatory proteins Cyclin D1 and p53 in the two CCA cell lines, indicating that the observed pro-proliferative SOX9 effect does not involve these components of the cell cycle/apoptosis machinery (**Figure 22**).

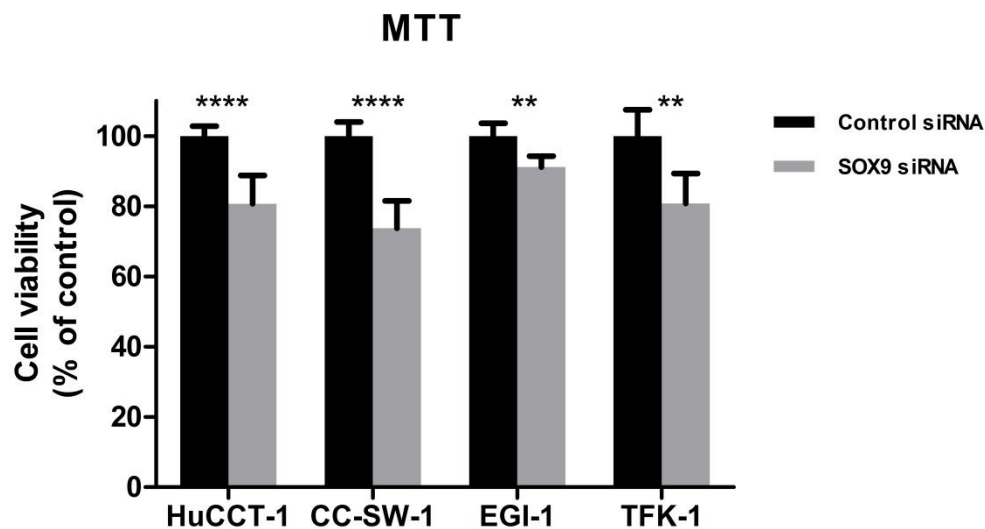


Figure 18. Cell viability measured by MTT assay in CCA cells with or without SOX9 knockdown. \*\*:  $P < 0.01$ , \*\*\*\* :  $< 0.0001$ .

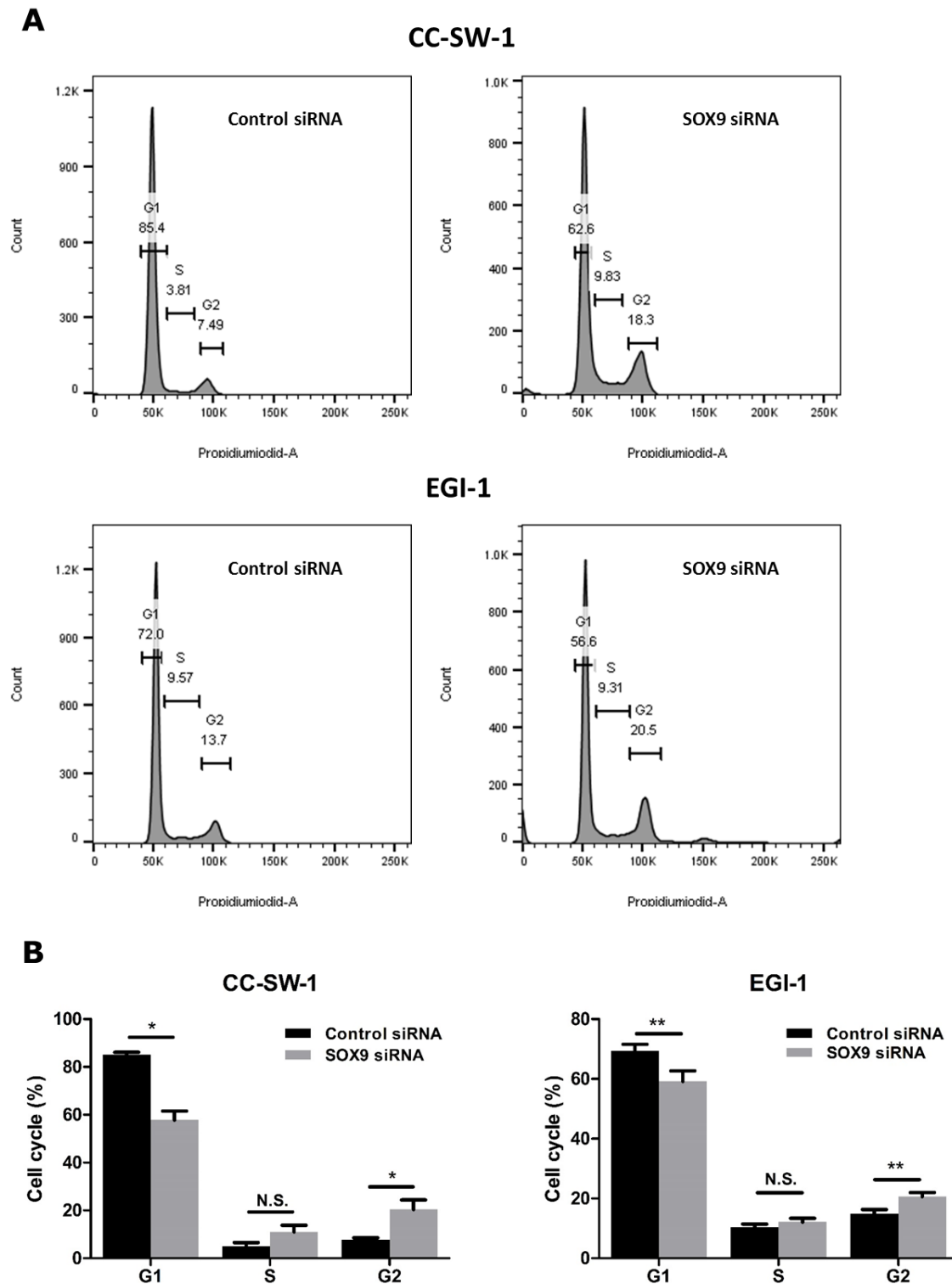


Figure 19. SOX9 and cell cycle progression in CC-SW-1 and EGI-1 cells. **A.** Comparative cell cycle analyses of CC-SW-1 and EGI-1 CCC cell lines treated with control or SOX9 targeting siRNA. **B.** Respective quantification of CC-SW-1 and EGI-1 cells in the different cell cycle phases upon control or SOX9 siRNA treatment. The results are presented as mean  $\pm$  SD. \*:  $P < 0.05$ . \*\*:  $P < 0.01$ .

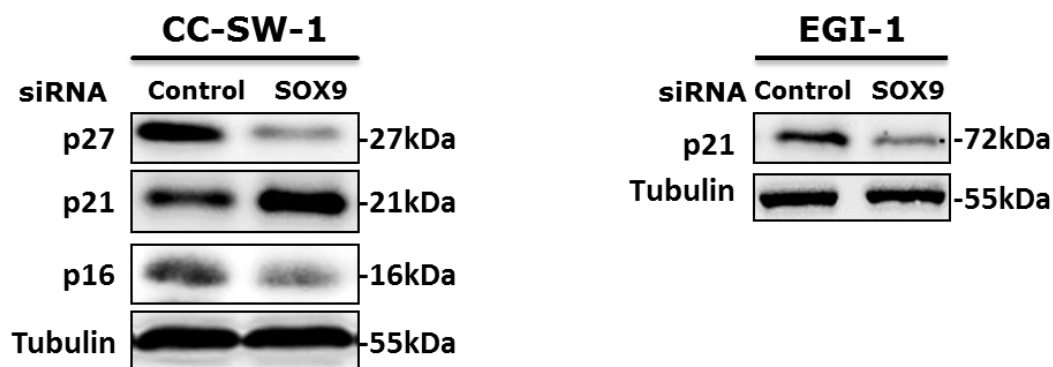


Figure 20. SOX9 and expression of cyclin-dependent kinase inhibitors in CC-SW-1 and EGI-1 cells (immunoblot assay, Tubulin was used as loading control).

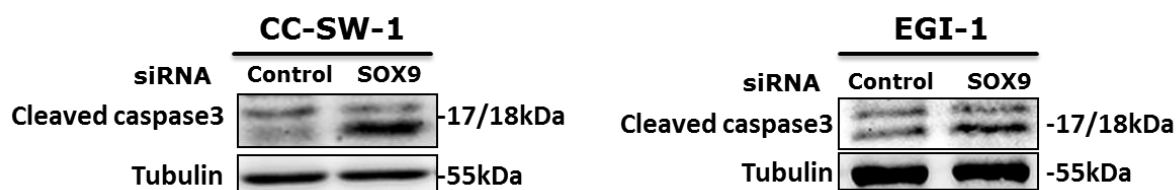


Figure 21. SOX9 and expression of cleaved caspase 3 in CC-SW-1 and EGI-1 cells (immunoblot assay, Tubulin was used as loading control).

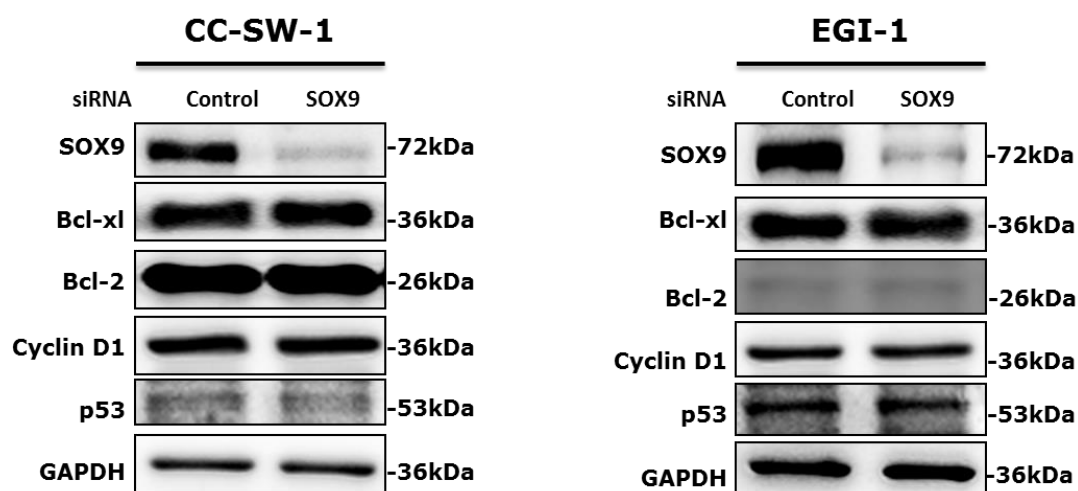


Figure 22. SOX9 and expression of anti-apoptotic proteins Bcl-xL and Bcl-2, cell cycle regulatory proteins Cyclin D1 and p53 in CC-SW-1 and EGI-1 cells (immunoblot assay, GAPDH was used as loading control).

### 3.2.4 SOX9 is required for cell migration

Next, I assessed the role of SOX9 on CCA cell migration. Transwell assays show that SOX9 knockdown significantly inhibits cell migration in CC-SW-1 and HuCCT-1 cells (**Figure 23**). To further investigate whether the role of SOX9 on cell migration involves EMT, I examined epithelial and mesenchymal cell marker expression in CCA cells as a function of SOX9 presence or depletion. SOX9 knockdown at least does not change expression of cell adhesion marker E-Cadherin and mesenchymal cell markers N-Cadherin and Vimentin (**Figure 24**). Moreover, immunoblot assays and immunofluorescence staining show that SOX9 reduction has no effect on  $\beta$ -Catenin nuclear translocation in the tested CCA cells (**Figures 25 and 26**). These results suggest that the impact of SOX9 on CCA migration is not EMT-dependent.

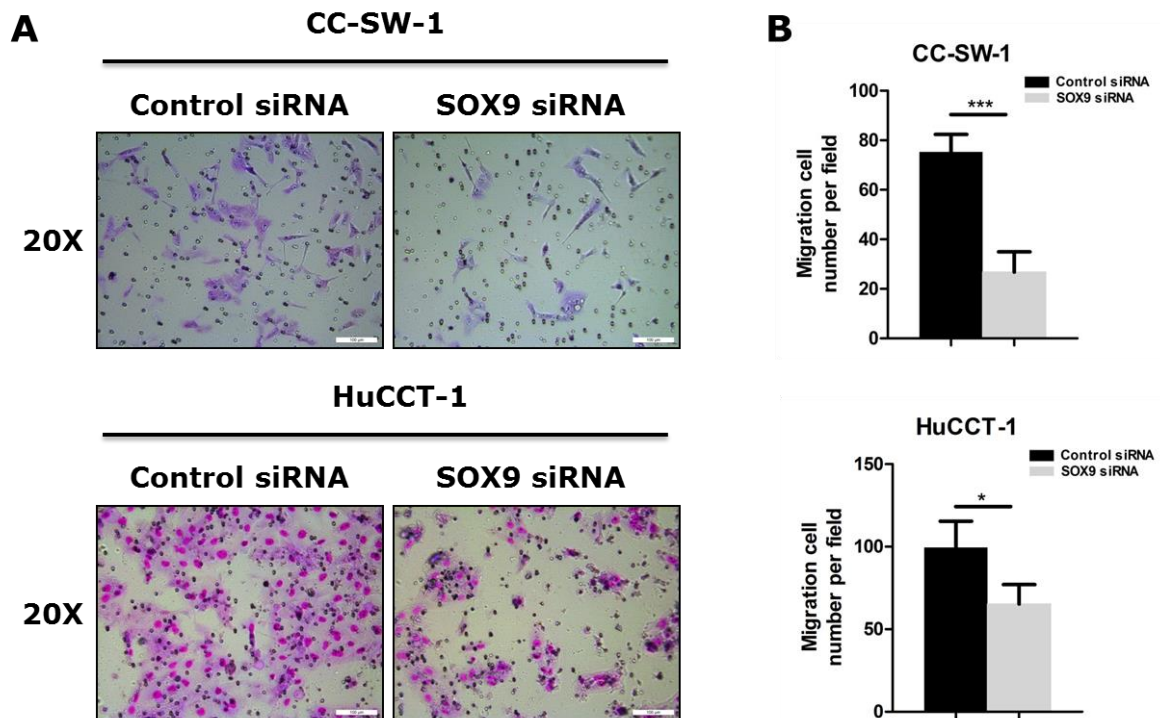


Figure 23. SOX9 and CCA cell migration, as measured by transwell assays. **A**. Transwell assays were performed in CC-SW-1 and HuCCT-1 cells transfected with control or SOX9 siRNA as indicated. **B**. Quantification of cell migration (red cell number) in CC-SW-1 and HuCCT-1 treated with control or SOX9 siRNAs. Results are presented as mean  $\pm$  SD. \*:  $P < 0.05$ . \*\*\*:  $P < 0.001$ .

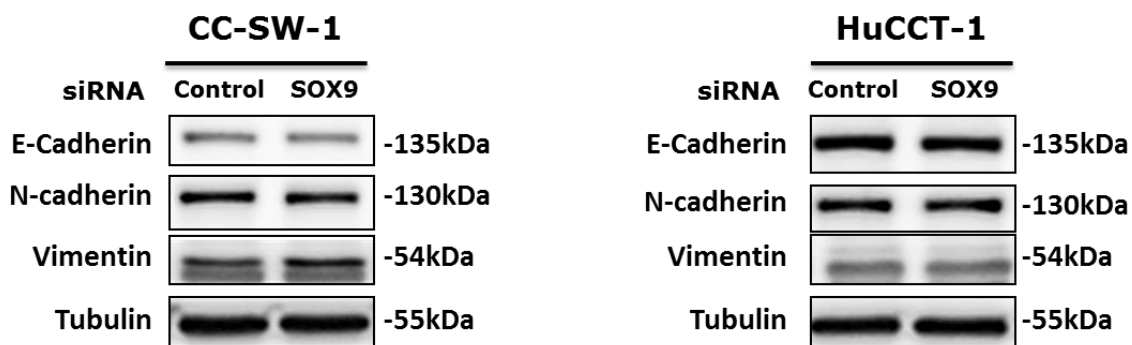


Figure 24. SOX9 and expression of epithelial cell marker E-Cadherin or mesenchymal cell markers N-Cadherin and Vimentin (immunoblot assay).

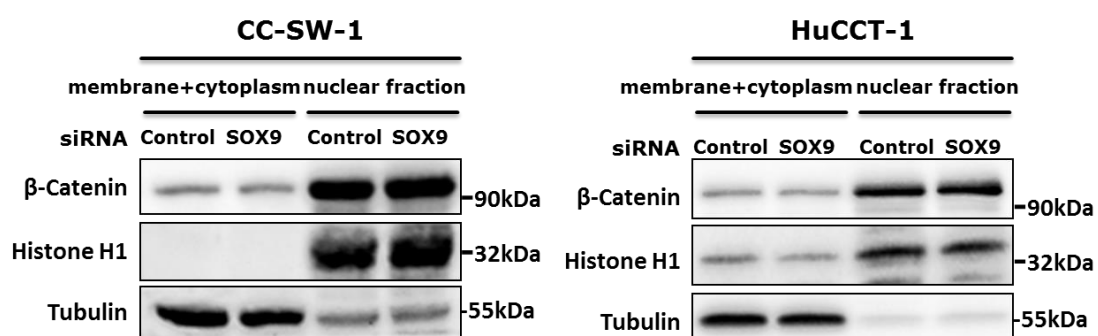


Figure 25. SOX9 and subcellular localization of β-Catenin in CC-SW-1 and HuCCT-1 cells (immunoblot assay upon nuclear/cytoplasmic fractionation).

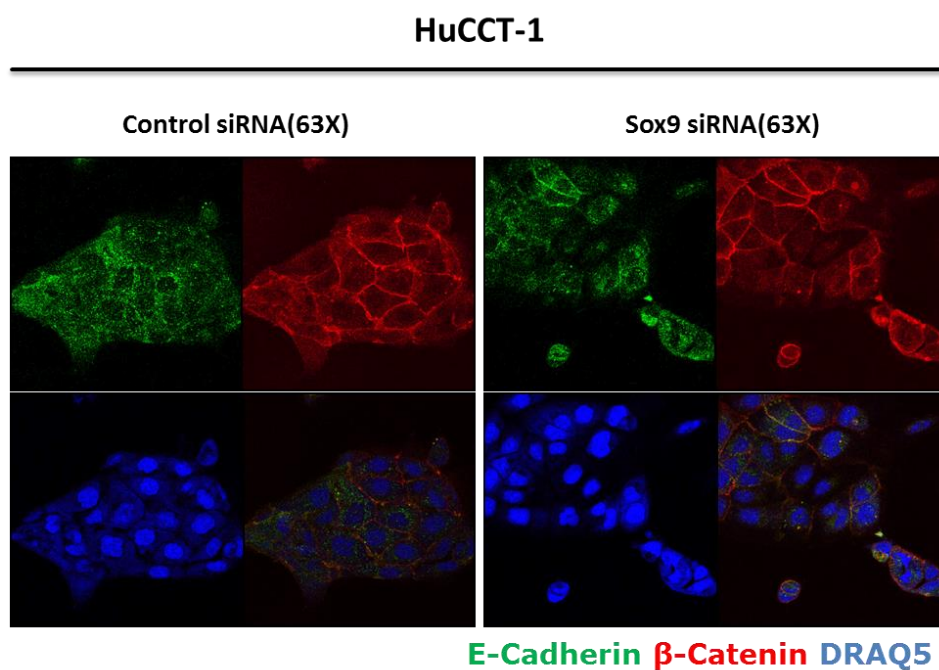


Figure 26. Expression of E-Cadherin and β-Catenin in HuCCT-1 cells treated with control or SOX9 siRNA (immunofluorescence).

### 3.2.5 SOX9 is required for CCA cell stemness

In HCC, SOX9 is recognized as a CSC marker, participating in CSC self-renewal, transdifferentiation and tumorigenicity. To investigate whether SOX9 is also related to cancer stemness of CCA cells, I performed tumor sphere formation assays, a widely used method to evaluate self-renewal and differentiation of CSC *in vitro* [120]. In CC-SW-1 cells, SOX9 knockdown significantly inhibits tumor sphere formation capacity **(Figure 27)**. Moreover, silencing SOX9 expression reduces expression of EpCAM at mRNA and protein levels **(Figure 28)**. EpCAM has been known as a marker for maintaining CSC-features in HCC.

CSC-derived tumors display an impressive capacity to resist to chemotherapy, which is at least partially due to high level adenosine triphosphate (ATP)–binding cassette (ABC) transporter expression [121]. In CCA cells, immunoblot assays show that SOX9 knockdown downregulates expression of multidrug resistance protein 4 (MRP4), also known as ATP-binding cassette sub-family C member 4 (ABCC4), which belongs to the ABCC family of multidrug resistant genes **(Figure 29A)**. In consistent with microarray data **(Figure 17A)**, where CC-SW-1 cells with SOX9 knockdown have decreased ATP-binding cassette (ABC) transporters ABCB1 and ABCC4, real-time PCR displays that SOX9 depletion reduces expression of multidrug resistance genes ABCB1, as well as other genes including ABCG2 and ABCC6 **(Figure 29B)**. The results implied that SOX9 may be critical to maintain the stem cell features of CCA.



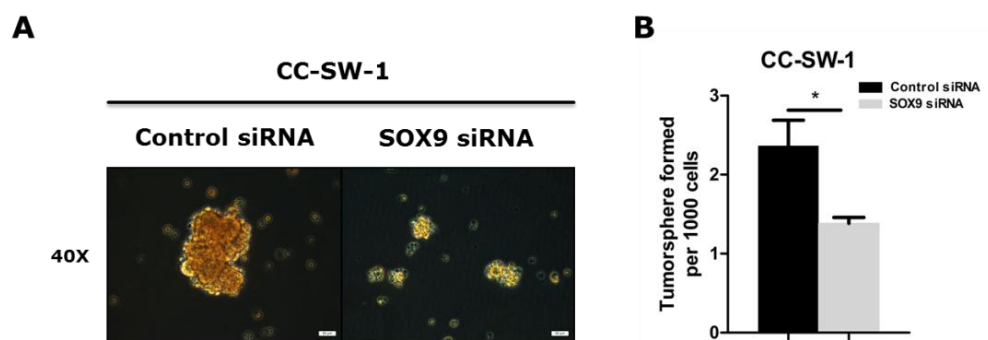


Figure 27. SOX9 and CC-SW-1 tumor sphere formation. **A.** Representative picture of CC-SW-1 cells tumor sphere formation upon treatment with SOX9 or control siRNA. **B.** Quantification of tumor sphere formation (Tumor spheres above 100  $\mu$ m are considered as positive) upon treatment with SOX9 or control siRNA. \*:  $P < 0.05$ .

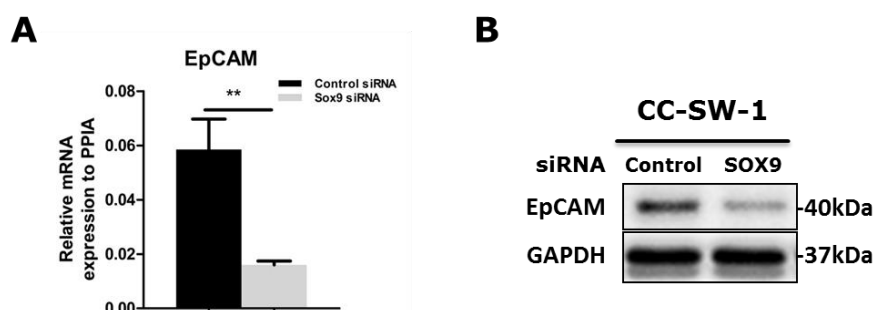


Figure 28. SOX9 and CCA transdifferentiation. **A.** Real-Time PCR showing that SOX9 knockdown inhibits EpCAM expression at RNA level. **B.** Immunoblot showing that SOX9 knockdown decreases EpCAM expression at the protein level. GAPDH was used as loading control.

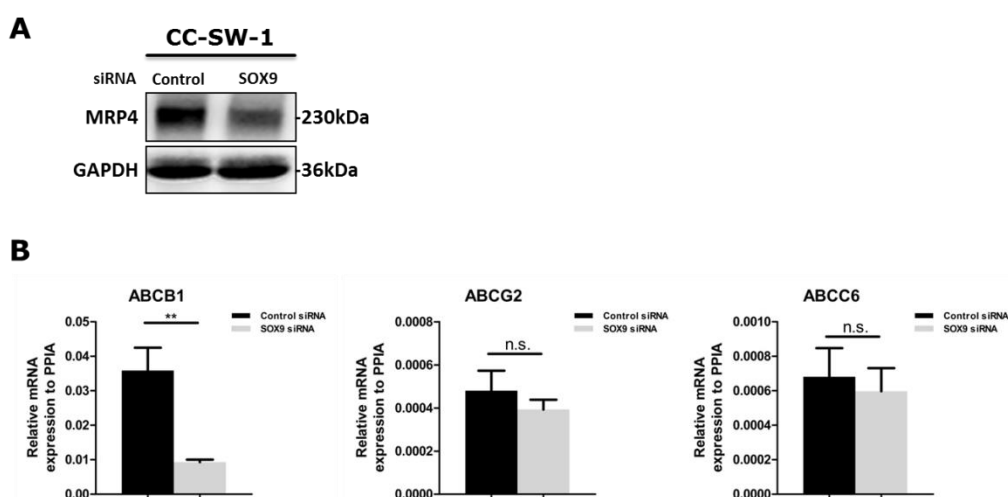


Figure 29. SOX9 and multidrug resistance gene expression. **A.** Immunoblot showing that SOX9 knockdown decreases expression of multidrug resistance-associated protein 4 (MRP4). GAPDH was used as loading control. **B.** Real-Time PCR showing that SOX9 knockdown downregulates expression of multidrug resistance genes ABCB1, ABCG2 and ABCC6.

### 3.2.6 SOX9 inhibition sensitizes CCA cells to gemcitabine

To investigate SOX9 in CCA chemotherapy, I treated CCA cells with gemcitabine, an analog of deoxycytidine widely used for treatment of multiple cancers, including CCA. Interestingly, immunoblots revealed that SOX9 expression is increased upon gemcitabine treatment, both in CC-SW-1 and EGI-1 cells (**Figure 30**). Next, I treated CC-SW-1 and EGI-1 cells with gemcitabine for 24 hours upon control or SOX9 siRNA transfection and comparatively measured survival using MTT assays. Depletion of SOX9 shows significantly reduced IC50 values (**Figure 31**), which is in CC-SW-1 cells, gemcitabine/SOX9 siRNA =  $2.0 \pm 0.23\text{nM}$  vs control =  $7.1 \pm 0.15\text{nM}$ , and in EGI-1, gemcitabine/SOX9 siRNA =  $46.3 \pm 21.9\text{nM}$  vs control =  $380.3 \pm 249.1\text{nM}$ . These results demonstrate that upregulated SOX9 expression protects CCA cells to gemcitabine induced cell apoptosis. In addition, immunoblots reveal that combination treatment downregulated multidrug resistance-associated protein 4 expression in CC-SW-1 cells, and inhibited the activation of Checkpoint kinase 1 (Chk1) both in CC-SW-1 and EGI-1 cells (**Figure 32**). Finally, immunoblots and Caspase 3 assays confirm that gemcitabine induces significant cell death in CC-SW-1 and EGI-1 cells upon SOX9 knockdown as compared to control cells (**Figure 33**).

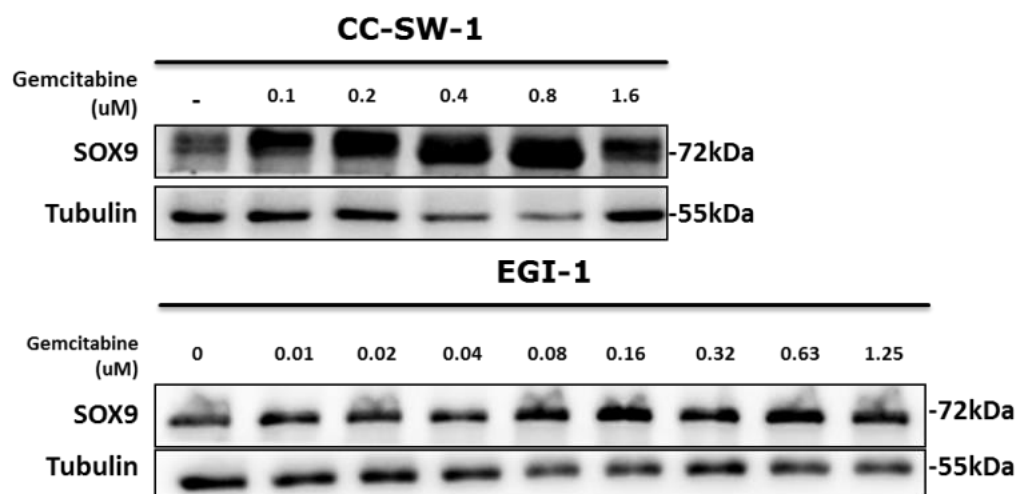


Figure 30. SOX9 expression in CC-SW-1 and EGI-1 cells treated with indicated concentration of gemcitabine (immunoblot, Tubulin was used as loading control).

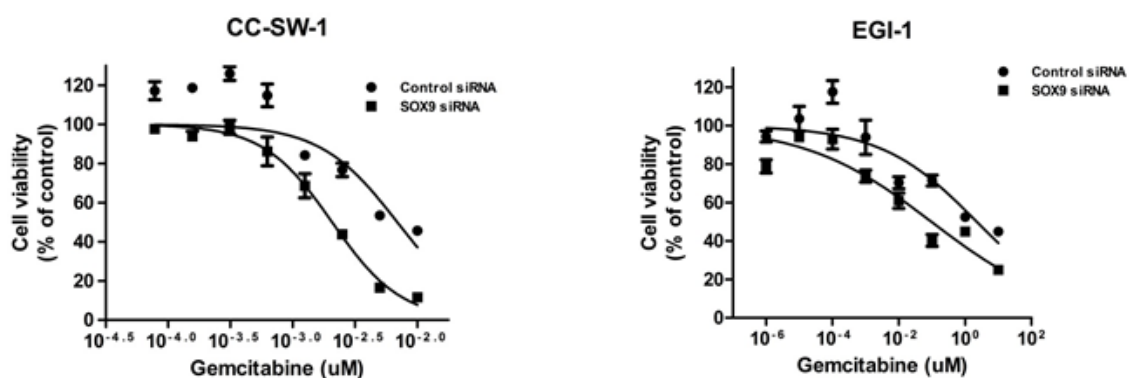


Figure 31. IC<sub>50</sub> evaluation of gemcitabine using MTT method in CC-SW-1 and EGI-1 cells treated with or without SOX9 siRNA for 24 hours.

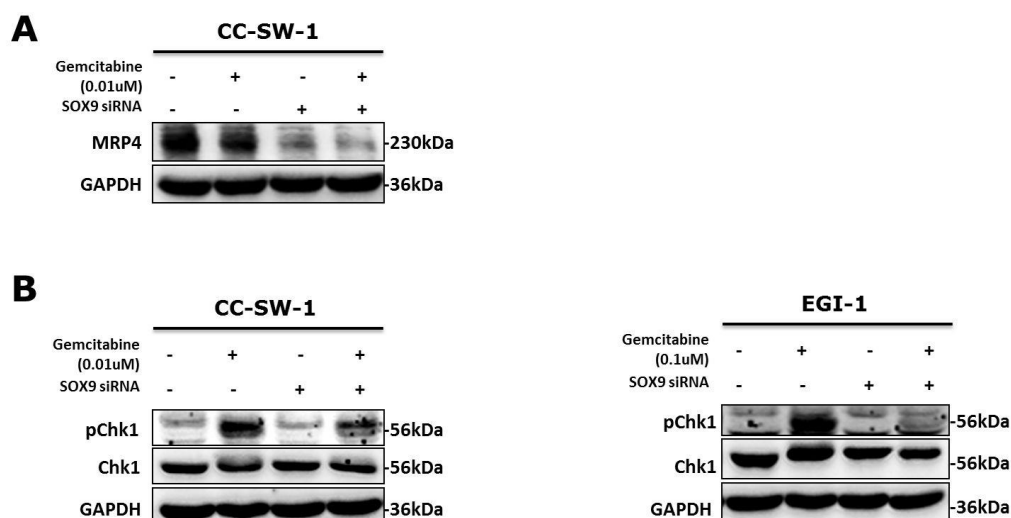


Figure 32. SOX9 regulates expression of MRP4 and phosphorylation Chk1 in CCA cells. **A.** Immunoblot of MRP4 expression in CC-SW-1 cells with the indicated treatments. **B.** Immunoblot showing expression respective phosphorylation of Checkpoint kinase 1 (Chk1) in CC-SW-1 and EGI-1 cells. GAPDH was used as loading control.

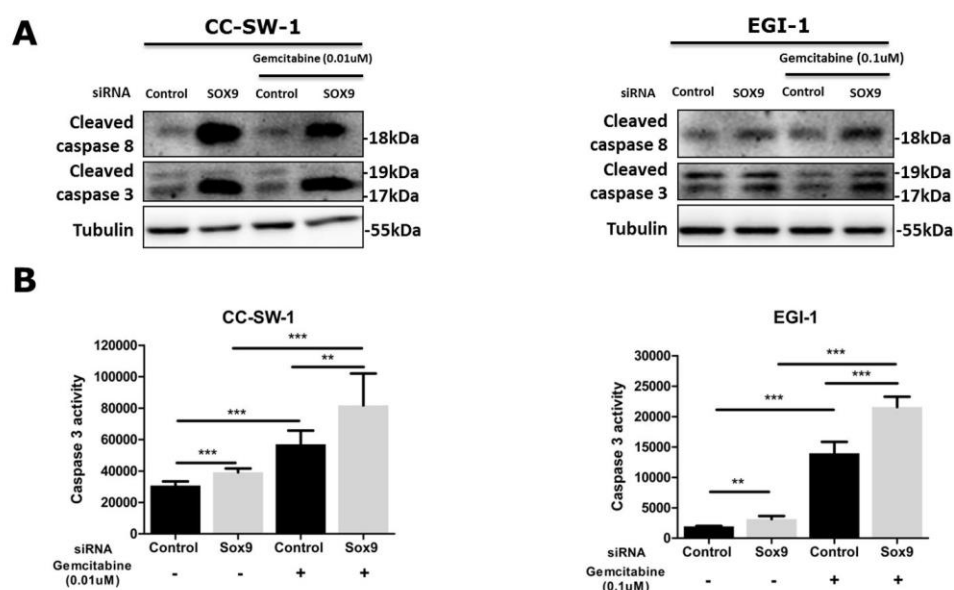


Figure 33. SOX9 and gemcitabine mediated CCA cell apoptosis. **A.** Immunoblot showing Cleaved caspase 3 and 8 expression in CC-SW-1 and EGI-1 cells with the indicated treatments. Tubulin was used as loading control. **B.** Caspase 3 assay as performed in CC-SW-1 and EGI-1 cells with the indicated treatments.

### 3.2.7 SOX9 is downstream of EGFR/ERK1/2 signaling

EGF/EGFR signaling was described as key to govern migration and invasion of CCA cells via an EMT process [81]. I have shown above that SOX9 facilitates cell migration of CCA cells. To assess a potential relationship between SOX9 and EGF/EGFR signaling, I treated CCA cells with EGF (10ng/ml) for 24 hours, and observed that the cells became scattered with appearance of membrane protrusions (**Figure 34A**). Immunoblots revealed that EGF treatment decreases expression of epithelial marker E-Cadherin, whereas expression of the mesenchymal marker Vimentin increases (**Figure 34B**), supporting a role of EGF/EGFR signaling to induce EMT in CCA cells. Of note, SOX9 expression is also upregulated upon EGF treatment and this is inhibited, when the cells are treated with EGFR inhibitor Erlotinib or ERK1/2 inhibitor U0126 (**Figure 35**). These results indicate that EGFR/ERK1/2 signaling upregulates SOX9 expression in CCA cells. Then, I investigated if SOX9 participates in EGF/EGFR-mediated CCA cell migration. Therefore, I performed transwell assays with CCA cells treated with EGF and control or in SOX9 siRNA. SOX9 knockdown significantly inhibits EGF-induced CCA cell migration (**Figure 36A**). However, immunoblots show that SOX9 depletion has no effect on EMT marker expression, regardless of EGF treated or not (**Figure 36B**). These results suggest that SOX9 is a downstream effector of EGFR/ERK1/2 signaling pathway and is directly involved in CCA cell motility, whereas EMT occurs independent and in parallel to Sox9 expression induction.

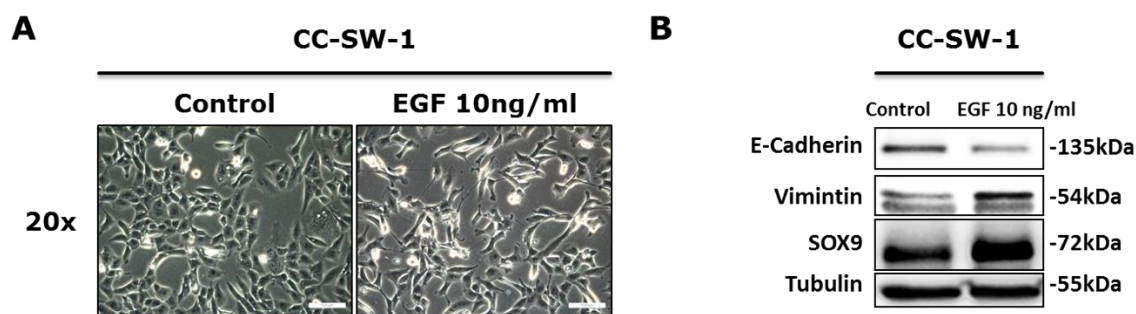


Figure 34. EGF and CCA cells. **A.** Representative phase-contrast images of CC-SW-1 treated with 10ng/ml EGF for 24 hours and controls. **B.** Immunoblot of EGF impact on expression of SOX9, E-Cadherin and Vimentin. Tubulin was used as loading control.

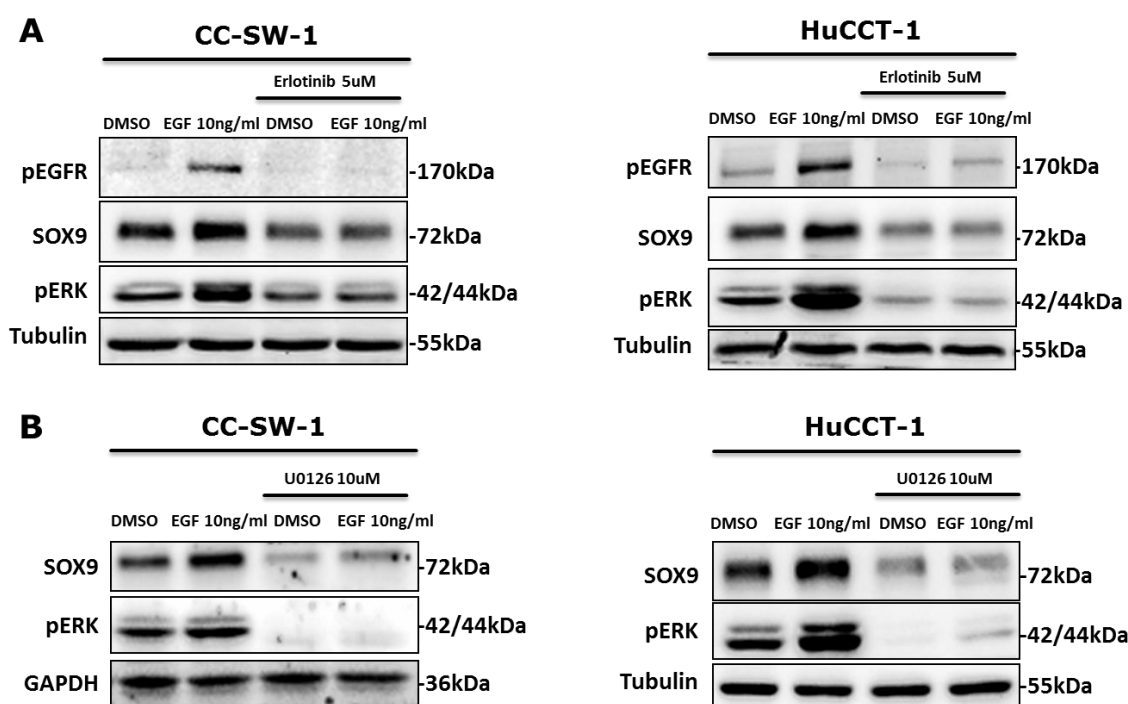


Figure 35. EGFR/ERK1/2 signaling and SOX9 expression. **A.** Immunoblot for SOX9 in CC-SW-1 and HuCCCT-1 cells treated with EGF for 24h. Erlotinib is an EGFR inhibitor. **B.** ERK1/2 pathway and SOX9 expression in CC-SW-1 and HuCCCT-1 cells. U0126 is an ERK1/2 inhibitor. Tubulin and GAPDH were used as loading control.

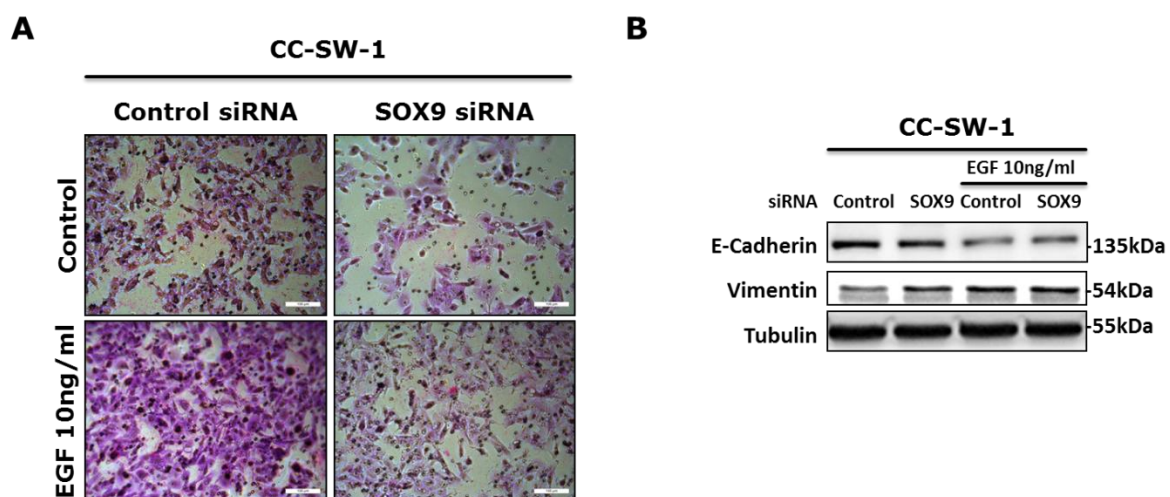


Figure 36. SOX9 and EGFR/ERK1/2 signaling induced cell migration. **A.** Representative images of transwell assays in CC-SW-1 cells treated with EGF (10ng/ml for 24hours) and control or SOX9 siRNA. **B.** Immunoblot showing that knockdown of SOX9 does not affect expression of E-Cadherin and Vimentin with and without EGF treatment. Tubulin was used as loading control.

## 4 DISCUSSION

The major findings of the study are: (1) SOX9 is a more sensitive marker for the prognosis of iCCA in comparison to CK19; (2) SOX9 determines the CCA cell response to chemotherapy; (3) SOX9 is critical for CCA cell survival, migration, self-renewal and differentiation.

### 4.1 SOX9 is a prognostic marker for iCCA

CK19 and SOX9 are classical markers for cholangiocytes. CK19 contributes to the differentiation of iCCA from metastatic adenocarcinoma and is associated with the histological differentiation of iCCA. Shimonishi et al. demonstrated that moderate and extensive expression of CK19 was associated with well-differentiated iCCA, whereas decreased expression of the protein is associated with the poorly differentiated cancer [122]. However, Demarez et al. reported that CK19 expression in iCCA patients does not correlate with the iCCA histological differentiation grade [123]. In the iCCA patients of the present study, CK19 expression is associated with the tumor differentiation grade. Moreover, CK19 expression correlates with AJCC classification of iCCA.

In the current cohort of iCCA patients, SOX9 expression is correlated with CK19 expression, it does not associate with any analyzed clinical parameters, including cirrhosis, vascular invasion and AJCC classification. Of note, survival analysis revealed that patients with high SOX9 expression present with the shortest OS and DFS times in comparison to patients with high CK19 expression or low SOX9 expression. These results indicate that currently measured clinical parameters in clinical practice are not capable of evaluating any potential effects of SOX9 on CCA progression. Despite this fact, SOX9 expression is more sensitive to predict the clinical outcome of iCCA patients in comparison to CK19.

### 4.2 SOX9 determines the response of CCA cells to chemotherapy

To clarify the potential role of SOX9 in CCA, I investigated SOX9 expression and the clinical outcome of 9 CCA patients who received chemotherapy. Survival analysis showed that patients with SOX9 low expression had significantly longer OS time than those with high SOX9 expression after chemotherapy, indicating that SOX9 expression in cancer cells may determine the survival time of CCA patients who



received chemotherapy and therewith suggesting a critical role of SOX9 in chemoresistance of CCA cells.

Besides the clinical findings, several additional lines of evidence supported the link between SOX9 expression and multidrug resistance. The integrative analysis of gene expression signatures in 104 CCA patients showed that SOX9 expression is positively correlated with DNA repair pathways including homologous recombination and mismatch repair, DNA replication, base excision repair, as well as nucleotide excision repair. It has been demonstrated that the ability of cancer cells to repair therapeutically induced DNA damage facilitates cancer cell survival and impacts therapeutic efficacy [124]. Hence, targeting DNA repair pathways has been proposed as a strategy for the development of anti-cancer agents to consequently increase sensitivity to chemotherapeutics. To date, inhibitors of DNA damage repair pathways have entered several clinical trials, either as a monotherapy or in combination with chemotherapeutics [124, 125]. In addition, SOX9 expression is positively correlated with Wnt and Notch signaling pathways, both demonstrated to account for chemoresistance of cancer cells to gemcitabine through inactivating the apoptosis pathway, increasing the expression of drug efflux pumps or activating CSCs formation [114]. Thus, my data suggests that SOX9 integrates in DNA repair pathways, Wnt and Notch signaling in the context of chemoresistance for CCA patients.

Microarray analyses from cultured CCA cells reveal that the expression of genes related to multidrug resistance genes, including ABCB1 and ABCC4, are positively regulated by SOX9. Treatment of CCA cells with gemcitabine, a widely used chemotherapeutic agent in cancer, induces SOX9 expression, which further confirms the relationship between SOX9 expression and chemoresistance. IC<sub>50</sub> decreases significantly and apoptosis rate is higher in gemcitabine treated CCA cells upon SOX9 knockdown. Moreover, expression of proteins critical for multidrug resistance, DNA stability and DNA repair, very interestingly MRP4 and pChk1, are blunted with SOX9 expression depletion. Chk1 functions as regulator of the G2/M checkpoint and is crucial for replication fork stability, replication origin firing and homologous recombination, particularly in cells which are facing genotoxic stress [126]. In gemcitabine-treated cancer cells, Chk1 inhibition rapidly results in cell death due to destabilization of the DNA replication apparatus [127]. Therefore, targeting Chk1 has

become a strategy for improving chemotherapy and several inhibitors of Chk1 have entered clinical trials either as stand-alone agents or in combination with radiotherapy or chemotherapy [128]. The present study now suggests SOX9 as a critical component for Chk1 phosphorylation, although the underlying mechanism requires further investigation. Taken together, my data demonstrates that SOX9 inhibition sensitizes CCA cells to chemotherapeutics by inducing cell apoptosis, suppressing the efflux of chemotherapeutic drugs and reducing tumor cell DNA repair ability upon chemotherapeutic agents induced DNA damage. Therefore, SOX9 expression levels have potential to predict chemoresistance and efficacy of chemotherapy in CCA patients.

### 4.3 SOX9 as oncogene in CCA

In 2000, Hanahan D and Weinberg RA proposed six hallmarks of cancer as follows: (1) sustaining proliferative signaling, (2) evading growth suppressors, (3) resisting cell death, (4) enabling replicative immortality, (5) inducing angiogenesis, and (6) activating invasion and metastasis [129]. In 2011, four additional cancer hallmarks were added to the list, which are (7) genome instability and mutation, (8) tumor-promoting inflammation, (9) reprogramming energy metabolism and (10) evading immune destruction [130]. These cancer cells hallmarks are acquired during the multi-step process of cancer development. In the present study, in the context of the above features, I investigated the role of SOX9 in survival, migration and cancer stem cell features in CCA cells.

#### 4.3.1 Survival

Previous studies assessed the role of SOX9 in cancer cell survival. SOX9 knockdown in lung adenocarcinoma CL1-5 cells decreased the cell fraction in G1 phase and increased that in G2/M phase, which consequently resulted in cell proliferation inhibition [24]. The altered cell cycle distribution induced by SOX9 depletion was attributed to increased p21 and decreased CDK4 expression. In contrast to these data, SOX9 overexpression in melanoma cells inhibited cell proliferation due to increased p21 expression and cell cycle arrest in G1 phase [25]. Consistent with the former report, my results show that SOX9 knockdown results in a similar cell cycle distribution in both CC-SW-1 and EGI-1 cells, although p21 expression is increased in CC-SW-1 and decreased in EGI-1 as compared to the parental cells. Furthermore,

cell apoptosis was significantly induced by SOX9 knockdown in both CCA cell lines. As an explanation for these contradicting data, we and others previously described p21 as protein with context dependent functions that sometimes present with opposite outcome [131, 132]. For instance, in mice with severe liver injury p21 deletion led to continuous hepatocyte proliferation but also facilitated rapid tumor development, whereas in p21-deficient mice with moderate injury liver regeneration and hepatocarcinogenesis were impaired [131]. As a negative regulator of cell cycle, p21 is involved in cell apoptosis and cell cycle distribution. Thereby, high p21 expression in the cytoplasm facilitates apoptosis, while its accumulation in nucleus is related to cell cycle arrest [133]. Taken together, the opposing results revealed the function of SOX9 on p21 expression is cancer cell dependent. In addition, whether SOX9 inhibition-induced cell cycle alteration and apoptosis is p21 dependent needs further investigation.

SOX9 inhibition-induced cell apoptosis might be associated with p53-related signaling. The notion was supported by a microarray analysis showing upregulation of p53 signaling pathway-related genes in CC-SW-1 cells with SOX9 knockdown, e.g. FAS, SFN and PMAIP1, all of which are essential mediators of cell apoptosis [134-136]. p53, as a tumor suppressor, can be activated by DNA damage, hypoxia and aberrant oncogene expression [137, 138]. Activated p53 functions to integrate multiple stress signals into a series of diverse anti-proliferative responses by activating and decreasing number of genes involved in cell death, senescence, or cell cycle arrest [138]. In the current study, although SOX9 knockdown in CCA cells has no effects on the p53 expression, SOX9 inhibition significantly increases cleaved caspase 3 and 8 expression and subsequently induces cell apoptosis. Hence, whether SOX9 inhibition induced cell apoptosis is p53 pathway dependent needs further investigation. Nevertheless, these facts provide evidence that dysregulation of SOX9 expression is associated with cell cycle progression and consequently affects the proliferation and survival of CCA cells.

### 4.3.2 Migration

EMT is a biologic process that allows a polarized epithelial cell to acquire a mesenchymal fate [139]. Cancer cells through EMT process acquire cell-biological traits associated with high-grade malignancy, including resistance to apoptosis, motility and invasiveness [140]. In the present study, I present *in vitro* evidence that

SOX9 is necessary for efficient cancer cell migration in CCA tumor cells. In short, starting with an examination of the “usual suspects” of EMT, SOX9 knockdown significantly inhibits cell migration while has no effects on the expression of epithelia cell marker and mesenchymal marker in CCA cells. On one hand, migration of these cells is significantly blunted upon SOX9 knockdown. Looking at microarray data, SOX9 expression is associated with genes related to regulation of actin cytoskeleton, cell-cell contacts and focal adhesion. Interestingly in this context, I further found out that SOX9 expression is regulated by the EGF/EGFR/ERK1/2 pathway and required for cell migration induced by EGF stimulation of CCA cells. These results are consistent with Ling’s report describing the contribution of the EGFR/ERK1/2/SOX9 pathway to malignant transformation of stressed urothelial cells, as well as migration and invasion of urothelial cancer cells [141]. On the other hand, in CCA, SOX9 inhibition is not involved in the route of EGF induced expression of EMT markers. In summary, my data reveal that *in vitro*, SOX9 expression is regulated by the EGF/EGFR/1/2 pathway and is an essential component of EGF-induced CCA cell migration.

#### 4.3.3 Cancer stem cell features

CSCs are highly tumorigenic, metastatic, chemo- and radiation therapy resistant, and able to divide symmetrically and asymmetrically to orchestrate tumor mass and account for tumor relapse [142]. As a marker of cholangiocytes, SOX9 is expressed in HPCs but not in hepatocytes. In HCC, cancer cells that express SOX9 are thought as CSC-derived, since a role of SOX9 in maintaining CSCs properties in HCC is known. For example, SOX9 is required for acquiring stemness and chemoresistance of HCC cells [46]. Further, SOX9 is essential for symmetric cell division and self-renewal of CSCs in HCC [47]. So far, it is unclear whether SOX9 expression in CCA is related with the CSC fate. In the present study, I show that SOX9 depletion inhibits tumor sphere formation of CCA cells, suggesting its participation in self-renewal. Of note, SOX9 silencing decreases EpCAM expression. In normal liver, EpCAM is a differentiation marker of cholangiocytes and hepatocytes lack its expression [143]. In HCC, EpCAM expression is essential for maintaining CSC features [144]. In CCA, EpCAM was reported as a poor prognostic marker and subsequently dedicated as a marker for CSCs [145]. This link between SOX9 and EpCAM provides the first evidence that SOX9 may play a role in CCA related CSC generation. In addition, CSCs are more resistant to chemotherapeutic agents than differentiated tumor cells,

due to increased expression of ATP-binding cassette transporters [121]. *In vitro*, SOX9 inhibition disrupted the expression of several multidrug resistance genes and consequently sensitized CCA cells to gemcitabine. Taken together, these facts illustrated that SOX9 might be an essential regulator for maintaining CSC-features of CCA.

#### 4.4 Regulation of SOX9 expression

Gene expression profiling of publicly available CCA patient data sets revealed that SOX9 expression is associated with the Notch pathway. In liver, Notch is critical for activation, proliferation and differentiation of hepatoblasts/HPCs [96, 98]. SOX9 is a well described target gene of the Notch pathway. Aberrant activity of Notch related signaling is involved in tumorigenesis of CCA [65]. These facts implied SOX9 might be involved in Notch pathway during the carcinogenesis of CCA. As discussed above, I revealed that EGF/EGFR/ERK1/2 participate in the regulation of SOX9 expression in CCA cells. A relationship between EGFR/ERK1/2 and Notch pathways exists in the context of cholangiocyte differentiation [146]. However, the network of EGFR/ERK1/2, Notch and SOX9 in CCA has not been delineated yet. Maybe we can learn something from HCC. There, SOX9 regulates the Notch pathway via inhibition of Numb, a Notch signaling antagonist, which results in maintenance of CSCs-features [47]. Also this aspect contains substance for future studies.

## 5 SUMMARY

SOX9 is a critical transcription factor for liver embryogenesis, homeostasis and HCC development. However, the oncogenic role of SOX9 has not been investigated in CCA. As CCA is a devastating malignancy with limited treatment options, elucidation of its underlying mechanisms and identification of new molecular markers of tumorigenesis and progression of CCA is necessary for improving diagnosis and prognosis of this cancer type. This study aims at investigating the effects and underlying mechanisms of SOX9 in tumorigenesis and chemotherapy of CCA.

In this thesis, I examined SOX9 expression in CCA patients, including intrahepatic CCA (iCCA) and extrahepatic CCA (eCCA), by immunohistochemistry. Association of SOX9 expression and clinical outcome was evaluated. A SOX9 gene signature and its biological functions were investigated in CCA cell lines. My results reveal that SOX9 expression is significantly associated with overall survival of iCCA patients, with high SOX9 expression presenting with a shorter survival time, as compared to patients with low SOX9. Impressively, in the investigated patient cohort, CCA patients with low SOX9 levels have 62 months of median survival time following chemotherapy, whereas median survival time is only 22 months for patients with high SOX9 expression. *In vitro*, gemcitabine treatment induces SOX9 expression in CCA cells. When SOX9 is knocked down by small interfering RNA (siRNA), gemcitabine-induced cell death is markedly increased. Molecularly, SOX9 silencing inhibits gemcitabine-induced phosphorylation of checkpoint kinase 1 (CHEK1), a key cell cycle check point regulator that coordinates the DNA damage response and expression of multidrug resistance genes. Microarray analyses show that SOX9 knockdown in CCA cells alters the gene signature with respect to adenosine triphosphate-binding cassette (ABC) transporters, drug metabolism enzymes and p53 signaling. Moreover, I demonstrate that SOX9 expression is required for survival, migration and stemness of CCA cells. Finally, I found out that EGFR/ERK signaling is important in regulating SOX9 expression in CCA cells.

In conclusion, my thesis has revealed that (1) SOX9 is critical for CCA cell survival, migration and CSCs-features, (2) governs the response of CCA cells to chemotherapy through regulating activation of CHEK1 and multidrug resistance

genes. (3) My data also provides a strong rational for a clinical study to confirm SOX9 as a biomarker to predict which CCA patients are eligible for efficient chemotherapy.

## 6 REFERENCES

1. Wagner, T., et al., *Autosomal sex reversal and campomelic dysplasia are caused by mutations in and around the SRY-related gene SOX9*. Cell, 1994. **79**(6): p. 1111-20.
2. Foster, J.W., et al., *Campomelic dysplasia and autosomal sex reversal caused by mutations in an SRY-related gene*. Nature, 1994. **372**(6506): p. 525-30.
3. Baker, M., *Cancer stem cells tracked*. Nature, 2012. **488**(7409): p. 13-4.
4. Barker, N., et al., *Crypt stem cells as the cells-of-origin of intestinal cancer*. Nature, 2009. **457**(7229): p. 608-11.
5. Chen, J., et al., *A restricted cell population propagates glioblastoma growth after chemotherapy*. Nature, 2012. **488**(7412): p. 522-6.
6. Driessens, G., et al., *Defining the mode of tumour growth by clonal analysis*. Nature, 2012. **488**(7412): p. 527-30.
7. Schepers, A.G., et al., *Lineage tracing reveals Lgr5+ stem cell activity in mouse intestinal adenomas*. Science, 2012. **337**(6095): p. 730-5.
8. Kawaguchi, Y., *Sox9 and programming of liver and pancreatic progenitors*. J Clin Invest, 2013. **123**(5): p. 1881-6.
9. Jo, A., et al., *The versatile functions of Sox9 in development, stem cells, and human diseases*. Genes Dis, 2014. **1**(2): p. 149-161.
10. Cotsarelis, G., *Gene expression profiling gets to the root of human hair follicle stem cells*. J Clin Invest, 2006. **116**(1): p. 19-22.
11. Furuyama, K., et al., *Continuous cell supply from a Sox9-expressing progenitor zone in adult liver, exocrine pancreas and intestine*. Nat Genet, 2011. **43**(1): p. 34-41.
12. Passeron, T., et al., *SOX9 is a key player in ultraviolet B-induced melanocyte differentiation and pigmentation*. Proc Natl Acad Sci U S A, 2007. **104**(35): p. 13984-9.
13. Scott, C.E., et al., *SOX9 induces and maintains neural stem cells*. Nat Neurosci, 2010. **13**(10): p. 1181-9.
14. Pritchett, J., et al., *Understanding the role of SOX9 in acquired diseases: lessons from development*. Trends Mol Med, 2011. **17**(3): p. 166-74.
15. Peten, E.P., et al., *The contribution of increased collagen synthesis to human glomerulosclerosis: a quantitative analysis of alpha 2IV collagen mRNA expression by competitive polymerase chain reaction*. J Exp Med, 1992. **176**(6): p. 1571-6.
16. Airik, R., et al., *Hydrourteronephrosis due to loss of Sox9-regulated smooth muscle cell differentiation of the ureteric mesenchyme*. Hum Mol Genet, 2010. **19**(24): p. 4918-29.
17. Bennett, M.R., et al., *Laser capture microdissection-microarray analysis of focal segmental glomerulosclerosis glomeruli*. Nephron Exp Nephrol, 2007. **107**(1): p. e30-40.



18. Pritchett, J., et al., *Osteopontin is a novel downstream target of SOX9 with diagnostic implications for progression of liver fibrosis in humans*. Hepatology, 2012. **56**(3): p. 1108-16.
19. Sumi, E., et al., *SRY-related HMG box 9 regulates the expression of Col4a2 through transactivating its enhancer element in mesangial cells*. Am J Pathol, 2007. **170**(6): p. 1854-64.
20. Xia, S., et al., *Clinical implication of Sox9 and activated Akt expression in pancreatic ductal adenocarcinoma*. Med Oncol, 2015. **32**(1): p. 358.
21. Zhou, C.H., et al., *Clinical significance of SOX9 in human non-small cell lung cancer progression and overall patient survival*. J Exp Clin Cancer Res, 2012. **31**: p. 18.
22. Kopp, J.L., et al., *Identification of Sox9-dependent acinar-to-ductal reprogramming as the principal mechanism for initiation of pancreatic ductal adenocarcinoma*. Cancer Cell, 2012. **22**(6): p. 737-50.
23. Vidal, V.P., N. Ortonne, and A. Schedl, *SOX9 expression is a general marker of basal cell carcinoma and adnexal-related neoplasms*. J Cutan Pathol, 2008. **35**(4): p. 373-9.
24. Jiang, S.S., et al., *Upregulation of SOX9 in lung adenocarcinoma and its involvement in the regulation of cell growth and tumorigenicity*. Clin Cancer Res, 2010. **16**(17): p. 4363-73.
25. Passeron, T., et al., *Upregulation of SOX9 inhibits the growth of human and mouse melanomas and restores their sensitivity to retinoic acid*. J Clin Invest, 2009. **119**(4): p. 954-63.
26. Matheu, A., et al., *Oncogenicity of the developmental transcription factor Sox9*. Cancer Res, 2012. **72**(5): p. 1301-15.
27. Antoniou, A., et al., *Intrahepatic bile ducts develop according to a new mode of tubulogenesis regulated by the transcription factor SOX9*. Gastroenterology, 2009. **136**(7): p. 2325-33.
28. Carpentier, R., et al., *Embryonic ductal plate cells give rise to cholangiocytes, periportal hepatocytes, and adult liver progenitor cells*. Gastroenterology, 2011. **141**(4): p. 1432-8, 1438 e1-4.
29. Rowe, C., et al., *Proteome-wide analyses of human hepatocytes during differentiation and dedifferentiation*. Hepatology, 2013. **58**(2): p. 799-809.
30. Poncy, A., et al., *Transcription factors SOX4 and SOX9 cooperatively control development of bile ducts*. Dev Biol, 2015. **404**(2): p. 136-48.
31. Raynaud, P., et al., *A classification of ductal plate malformations based on distinct pathogenic mechanisms of biliary dysmorphogenesis*. Hepatology, 2011. **53**(6): p. 1959-66.
32. Vestentoft, P.S., et al., *Three-dimensional reconstructions of intrahepatic bile duct tubulogenesis in human liver*. BMC Dev Biol, 2011. **11**: p. 56.
33. Carpino, G., et al., *Biliary tree stem/progenitor cells in glands of extrahepatic and intrahepatic bile ducts: an anatomical in situ study yielding evidence of maturational lineages*. J Anat, 2012. **220**(2): p. 186-99.
34. Jors, S., et al., *Lineage fate of ductular reactions in liver injury and carcinogenesis*. J Clin Invest, 2015. **125**(6): p. 2445-57.

35. Cardinale, V., et al., *Multipotent stem/progenitor cells in human biliary tree give rise to hepatocytes, cholangiocytes, and pancreatic islets*. Hepatology, 2011. **54**(6): p. 2159-72.
36. Dorrell, C., et al., *Prospective isolation of a bipotential clonogenic liver progenitor cell in adult mice*. Genes Dev, 2011. **25**(11): p. 1193-203.
37. Tarlow, B.D., M.J. Finegold, and M. Grompe, *Clonal tracing of Sox9+ liver progenitors in mouse oval cell injury*. Hepatology, 2014. **60**(1): p. 278-89.
38. Yanger, K., et al., *Adult hepatocytes are generated by self-duplication rather than stem cell differentiation*. Cell Stem Cell, 2014. **15**(3): p. 340-9.
39. Malato, Y., et al., *Fate tracing of mature hepatocytes in mouse liver homeostasis and regeneration*. J Clin Invest, 2011. **121**(12): p. 4850-60.
40. Lu, W.Y., et al., *Hepatic progenitor cells of biliary origin with liver repopulation capacity*. Nat Cell Biol, 2015. **17**(8): p. 971-83.
41. Friedman, S.L., *Mechanisms of hepatic fibrogenesis*. Gastroenterology, 2008. **134**(6): p. 1655-69.
42. Hanley, K.P., et al., *Ectopic SOX9 mediates extracellular matrix deposition characteristic of organ fibrosis*. J Biol Chem, 2008. **283**(20): p. 14063-71.
43. Omenetti, A., et al., *Hedgehog signaling regulates epithelial-mesenchymal transition during biliary fibrosis in rodents and humans*. J Clin Invest, 2008. **118**(10): p. 3331-42.
44. Guo, X., et al., *Expression features of SOX9 associate with tumor progression and poor prognosis of hepatocellular carcinoma*. Diagn Pathol, 2012. **7**: p. 44.
45. Matsushima, H., et al., *Sox9 expression in carcinogenesis and its clinical significance in intrahepatic cholangiocarcinoma*. Dig Liver Dis, 2015. **47**(12): p. 1067-75.
46. Leung, C.O., et al., *Sox9 confers stemness properties in hepatocellular carcinoma through Frizzled-7 mediated Wnt/beta-catenin signaling*. Oncotarget, 2016. **7**(20): p. 29371-86.
47. Liu, C., et al., *Sox9 regulates self-renewal and tumorigenicity by promoting symmetrical cell division of cancer stem cells in hepatocellular carcinoma*. Hepatology, 2016. **64**(1): p. 117-29.
48. de Groen, P.C., et al., *Biliary tract cancers*. N Engl J Med, 1999. **341**(18): p. 1368-78.
49. Welzel, T.M., et al., *Impact of classification of hilar cholangiocarcinomas (Klatskin tumors) on the incidence of intra- and extrahepatic cholangiocarcinoma in the United States*. J Natl Cancer Inst, 2006. **98**(12): p. 873-5.
50. Rizvi, S. and G.J. Gores, *Pathogenesis, diagnosis, and management of cholangiocarcinoma*. Gastroenterology, 2013. **145**(6): p. 1215-29.
51. Farley, D.R., A.L. Weaver, and D.M. Nagorney, *"Natural history" of unresected cholangiocarcinoma: patient outcome after noncurative intervention*. Mayo Clin Proc, 1995. **70**(5): p. 425-9.
52. Banales, J.M., et al., *Expert consensus document: Cholangiocarcinoma: current knowledge and future perspectives consensus statement from the*

- European Network for the Study of Cholangiocarcinoma (ENS-CCA). Nat Rev Gastroenterol Hepatol, 2016. 13(5): p. 261-80.*
53. Razumilava, N. and G.J. Gores, *Cholangiocarcinoma. Lancet, 2014. 383(9935): p. 2168-79.*
54. Komuta, M., et al., *Histological diversity in cholangiocellular carcinoma reflects the different cholangiocyte phenotypes. Hepatology, 2012. 55(6): p. 1876-88.*
55. Tyson, G.L. and H.B. El-Serag, *Risk factors for cholangiocarcinoma. Hepatology, 2011. 54(1): p. 173-84.*
56. Fausto, N., *Liver regeneration and repair: hepatocytes, progenitor cells, and stem cells. Hepatology, 2004. 39(6): p. 1477-87.*
57. Guest, R.V., et al., *Cell lineage tracing reveals a biliary origin of intrahepatic cholangiocarcinoma. Cancer Res, 2014. 74(4): p. 1005-10.*
58. Komuta, M., et al., *Clinicopathological study on cholangiolocellular carcinoma suggesting hepatic progenitor cell origin. Hepatology, 2008. 47(5): p. 1544-56.*
59. Zhang, F., et al., *Combined hepatocellular cholangiocarcinoma originating from hepatic progenitor cells: immunohistochemical and double-fluorescence immunostaining evidence. Histopathology, 2008. 52(2): p. 224-32.*
60. Goodman, Z.D., et al., *Combined hepatocellular-cholangiocarcinoma. A histologic and immunohistochemical study. Cancer, 1985. 55(1): p. 124-35.*
61. Roskams, T., *Liver stem cells and their implication in hepatocellular and cholangiocarcinoma. Oncogene, 2006. 25(27): p. 3818-22.*
62. Cardinale, V., et al., *Mucin-producing cholangiocarcinoma might derive from biliary tree stem/progenitor cells located in peribiliary glands. Hepatology, 2012. 55(6): p. 2041-2.*
63. Terasaki, S., et al., *Involvement of peribiliary glands in primary sclerosing cholangitis: a histopathologic study. Intern Med, 1997. 36(11): p. 766-70.*
64. Cardinale, V., et al., *Multiple cells of origin in cholangiocarcinoma underlie biological, epidemiological and clinical heterogeneity. World J Gastrointest Oncol, 2012. 4(5): p. 94-102.*
65. Sekiya, S. and A. Suzuki, *Intrahepatic cholangiocarcinoma can arise from Notch-mediated conversion of hepatocytes. J Clin Invest, 2012. 122(11): p. 3914-8.*
66. Fan, B., et al., *Cholangiocarcinomas can originate from hepatocytes in mice. J Clin Invest, 2012. 122(8): p. 2911-5.*
67. Borger, D.R., et al., *Frequent mutation of isocitrate dehydrogenase (IDH)1 and IDH2 in cholangiocarcinoma identified through broad-based tumor genotyping. Oncologist, 2012. 17(1): p. 72-9.*
68. Wang, P., et al., *Mutations in isocitrate dehydrogenase 1 and 2 occur frequently in intrahepatic cholangiocarcinomas and share hypermethylation targets with glioblastomas. Oncogene, 2013. 32(25): p. 3091-100.*
69. Turcan, S., et al., *IDH1 mutation is sufficient to establish the glioma hypermethylator phenotype. Nature, 2012. 483(7390): p. 479-83.*
70. Saha, S.K., et al., *Mutant IDH inhibits HNF-4alpha to block hepatocyte differentiation and promote biliary cancer. Nature, 2014. 513(7516): p. 110-4.*

71. Borad, M.J., et al., *Integrated genomic characterization reveals novel, therapeutically relevant drug targets in FGFR and EGFR pathways in sporadic intrahepatic cholangiocarcinoma*. PLoS Genet, 2014. **10**(2): p. e1004135.
72. Zheng, Z., et al., *Anchored multiplex PCR for targeted next-generation sequencing*. Nat Med, 2014. **20**(12): p. 1479-84.
73. Arai, Y., et al., *Fibroblast growth factor receptor 2 tyrosine kinase fusions define a unique molecular subtype of cholangiocarcinoma*. Hepatology, 2014. **59**(4): p. 1427-34.
74. Wu, Y.M., et al., *Identification of targetable FGFR gene fusions in diverse cancers*. Cancer Discov, 2013. **3**(6): p. 636-47.
75. Ross, J.S., et al., *New routes to targeted therapy of intrahepatic cholangiocarcinomas revealed by next-generation sequencing*. Oncologist, 2014. **19**(3): p. 235-42.
76. Harder, J., et al., *EGFR and HER2 expression in advanced biliary tract cancer*. World J Gastroenterol, 2009. **15**(36): p. 4511-7.
77. Yoshikawa, D., et al., *Clinicopathological and prognostic significance of EGFR, VEGF, and HER2 expression in cholangiocarcinoma*. Br J Cancer, 2008. **98**(2): p. 418-25.
78. Gwak, G.Y., et al., *Detection of response-predicting mutations in the kinase domain of the epidermal growth factor receptor gene in cholangiocarcinomas*. J Cancer Res Clin Oncol, 2005. **131**(10): p. 649-52.
79. Nakazawa, K., et al., *Amplification and overexpression of c-erbB-2, epidermal growth factor receptor, and c-met in biliary tract cancers*. J Pathol, 2005. **206**(3): p. 356-65.
80. Miyamoto, M., et al., *Prognostic significance of overexpression of c-Met oncoprotein in cholangiocarcinoma*. Br J Cancer, 2011. **105**(1): p. 131-8.
81. Claperon, A., et al., *EGF/EGFR axis contributes to the progression of cholangiocarcinoma through the induction of an epithelial-mesenchymal transition*. J Hepatol, 2014. **61**(2): p. 325-32.
82. Leelawat, K., et al., *Involvement of c-Met/hepatocyte growth factor pathway in cholangiocarcinoma cell invasion and its therapeutic inhibition with small interfering RNA specific for c-Met*. J Surg Res, 2006. **136**(1): p. 78-84.
83. Sia, D., et al., *Integrative molecular analysis of intrahepatic cholangiocarcinoma reveals 2 classes that have different outcomes*. Gastroenterology, 2013. **144**(4): p. 829-40.
84. Park, J., et al., *Inhibition of interleukin 6-mediated mitogen-activated protein kinase activation attenuates growth of a cholangiocarcinoma cell line*. Hepatology, 1999. **30**(5): p. 1128-33.
85. Goydos, J.S., et al., *Marked elevation of serum interleukin-6 in patients with cholangiocarcinoma: validation of utility as a clinical marker*. Ann Surg, 1998. **227**(3): p. 398-404.
86. Andersen, J.B., et al., *Genomic and genetic characterization of cholangiocarcinoma identifies therapeutic targets for tyrosine kinase inhibitors*. Gastroenterology, 2012. **142**(4): p. 1021-1031 e15.

87. Kobayashi, S., et al., *Interleukin-6 contributes to Mcl-1 up-regulation and TRAIL resistance via an Akt-signaling pathway in cholangiocarcinoma cells*. Gastroenterology, 2005. **128**(7): p. 2054-65.
88. Chen, Y., et al., *TGF-beta1 expression is associated with invasion and metastasis of intrahepatic cholangiocarcinoma*. Biol Res, 2015. **48**: p. 26.
89. Lu, J.P., et al., *In situ detection of TGF betas, TGF beta receptor II mRNA and telomerase activity in rat cholangiocarcinogenesis*. World J Gastroenterol, 2003. **9**(3): p. 590-4.
90. Araki, K., et al., *E/N-cadherin switch mediates cancer progression via TGF-beta-induced epithelial-to-mesenchymal transition in extrahepatic cholangiocarcinoma*. Br J Cancer, 2011. **105**(12): p. 1885-93.
91. Jaiswal, M., et al., *Nitric oxide-mediated inhibition of DNA repair potentiates oxidative DNA damage in cholangiocytes*. Gastroenterology, 2001. **120**(1): p. 190-9.
92. Jaiswal, M., et al., *Inflammatory cytokines induce DNA damage and inhibit DNA repair in cholangiocarcinoma cells by a nitric oxide-dependent mechanism*. Cancer Res, 2000. **60**(1): p. 184-90.
93. Artavanis-Tsakonas, S., M.D. Rand, and R.J. Lake, *Notch signaling: cell fate control and signal integration in development*. Science, 1999. **284**(5415): p. 770-6.
94. D'Souza, B., L. Meloty-Kapella, and G. Weinmaster, *Canonical and non-canonical Notch ligands*. Curr Top Dev Biol, 2010. **92**: p. 73-129.
95. Zong, Y., et al., *Notch signaling controls liver development by regulating biliary differentiation*. Development, 2009. **136**(10): p. 1727-39.
96. Geisler, F. and M. Strazzabosco, *Emerging roles of Notch signaling in liver disease*. Hepatology, 2015. **61**(1): p. 382-92.
97. Wu, W.R., et al., *Clinicopathological significance of aberrant Notch receptors in intrahepatic cholangiocarcinoma*. Int J Clin Exp Pathol, 2014. **7**(6): p. 3272-9.
98. Huntzicker, E.G., et al., *Differential effects of targeting Notch receptors in a mouse model of liver cancer*. Hepatology, 2015. **61**(3): p. 942-52.
99. Zhou, Q., et al., *The roles of Notch1 expression in the migration of intrahepatic cholangiocarcinoma*. BMC Cancer, 2013. **13**: p. 244.
100. Boulter, L., et al., *WNT signaling drives cholangiocarcinoma growth and can be pharmacologically inhibited*. J Clin Invest, 2015. **125**(3): p. 1269-85.
101. El Khatib, M., et al., *Inhibition of hedgehog signaling attenuates carcinogenesis in vitro and increases necrosis of cholangiocellular carcinoma*. Hepatology, 2013. **57**(3): p. 1035-45.
102. Fingas, C.D., et al., *Myofibroblast-derived PDGF-BB promotes Hedgehog survival signaling in cholangiocarcinoma cells*. Hepatology, 2011. **54**(6): p. 2076-88.
103. Sia, D., et al., *Intrahepatic cholangiocarcinoma: pathogenesis and rationale for molecular therapies*. Oncogene, 2013. **32**(41): p. 4861-70.
104. Rizvi, S. and G.J. Gores, *Emerging molecular therapeutic targets for cholangiocarcinoma*. J Hepatol, 2017.

105. DeOliveira, M.L., et al., *Cholangiocarcinoma: thirty-one-year experience with 564 patients at a single institution*. Ann Surg, 2007. **245**(5): p. 755-62.
106. Bridgewater, J., et al., *Guidelines for the diagnosis and management of intrahepatic cholangiocarcinoma*. J Hepatol, 2014. **60**(6): p. 1268-89.
107. Valle, J., et al., *Cisplatin plus gemcitabine versus gemcitabine for biliary tract cancer*. N Engl J Med, 2010. **362**(14): p. 1273-81.
108. Sia, D., et al., *Massive parallel sequencing uncovers actionable FGFR2-PPHLN1 fusion and ARAF mutations in intrahepatic cholangiocarcinoma*. Nat Commun, 2015. **6**: p. 6087.
109. Moeini, A., et al., *Molecular Pathogenesis and Targeted Therapies for Intrahepatic Cholangiocarcinoma*. Clin Cancer Res, 2016. **22**(2): p. 291-300.
110. Anderson, C.D., et al., *Diagnosis and treatment of cholangiocarcinoma*. Oncologist, 2004. **9**(1): p. 43-57.
111. Shimizu, Y., et al., *Two new human cholangiocarcinoma cell lines and their cytogenetics and responses to growth factors, hormones, cytokines or immunologic effector cells*. Int J Cancer, 1992. **52**(2): p. 252-60.
112. Miyagiwa, M., et al., *A new human cholangiocellular carcinoma cell line (HuCC-T1) producing carbohydrate antigen 19/9 in serum-free medium*. In Vitro Cell Dev Biol, 1989. **25**(6): p. 503-10.
113. Saijyo, S., et al., *Establishment of a new extrahepatic bile duct carcinoma cell line, TFK-1*. Tohoku J Exp Med, 1995. **177**(1): p. 61-71.
114. Jia, Y. and J. Xie, *Promising molecular mechanisms responsible for gemcitabine resistance in cancer*. Genes & Diseases, 2015. **2**(4): p. 299-306.
115. Strick-Marchand, H. and M.C. Weiss, *Inducible differentiation and morphogenesis of bipotential liver cell lines from wild-type mouse embryos*. Hepatology, 2002. **36**(4 Pt 1): p. 794-804.
116. Huang, Z., et al., *Tumor suppressor Alpha B-crystallin (CRYAB) associates with the cadherin/catenin adherens junction and impairs NPC progression-associated properties*. Oncogene, 2012. **31**(32): p. 3709-20.
117. Meyer, C., et al., *Caveolin-1 abrogates TGF-beta mediated hepatocyte apoptosis*. Cell Death Dis, 2013. **4**: p. e466.
118. Johnson, S., H. Chen, and P.K. Lo, *In vitro Tumorsphere Formation Assays*. Bio Protoc, 2013. **3**(3).
119. Subramanian, A., et al., *Gene set enrichment analysis: a knowledge-based approach for interpreting genome-wide expression profiles*. Proc Natl Acad Sci U S A, 2005. **102**(43): p. 15545-50.
120. Pastrana, E., V. Silva-Vargas, and F. Doetsch, *Eyes wide open: a critical review of sphere-formation as an assay for stem cells*. Cell Stem Cell, 2011. **8**(5): p. 486-98.
121. Jordan, C.T., M.L. Guzman, and M. Noble, *Cancer stem cells*. N Engl J Med, 2006. **355**(12): p. 1253-61.
122. Shimonishi, T., K. Miyazaki, and Y. Nakanuma, *Cytokeratin profile relates to histological subtypes and intrahepatic location of intrahepatic cholangiocarcinoma and primary sites of metastatic adenocarcinoma of liver*. Histopathology, 2000. **37**(1): p. 55-63.

123. Demarez, C., et al., *Expression of Molecular Differentiation Markers Does Not Correlate with Histological Differentiation Grade in Intrahepatic Cholangiocarcinoma*. PLoS One, 2016. **11**(6): p. e0157140.
124. Gavande, N.S., et al., *DNA repair targeted therapy: The past or future of cancer treatment?* Pharmacol Ther, 2016. **160**: p. 65-83.
125. Helleday, T., et al., *DNA repair pathways as targets for cancer therapy*. Nat Rev Cancer, 2008. **8**(3): p. 193-204.
126. Petermann, E., M. Woodcock, and T. Helleday, *Chk1 promotes replication fork progression by controlling replication initiation*. Proc Natl Acad Sci U S A, 2010. **107**(37): p. 16090-5.
127. Koh, S.B., et al., *CHK1 Inhibition Synergizes with Gemcitabine Initially by Destabilizing the DNA Replication Apparatus*. Cancer Res, 2015. **75**(17): p. 3583-95.
128. Manic, G., et al., *Trial Watch: Targeting ATM-CHK2 and ATR-CHK1 pathways for anticancer therapy*. Mol Cell Oncol, 2015. **2**(4): p. e1012976.
129. Hanahan, D. and R.A. Weinberg, *The hallmarks of cancer*. Cell, 2000. **100**(1): p. 57-70.
130. Hanahan, D. and R.A. Weinberg, *Hallmarks of cancer: the next generation*. Cell, 2011. **144**(5): p. 646-74.
131. Buitrago-Molina, L.E., et al., *The degree of liver injury determines the role of p21 in liver regeneration and hepatocarcinogenesis in mice*. Hepatology, 2013. **58**(3): p. 1143-52.
132. Marhenke, S., et al., *p21 promotes sustained liver regeneration and hepatocarcinogenesis in chronic cholestatic liver injury*. Gut, 2014. **63**(9): p. 1501-12.
133. Asada, M., et al., *Apoptosis inhibitory activity of cytoplasmic p21(Cip1/WAF1) in monocytic differentiation*. EMBO J, 1999. **18**(5): p. 1223-34.
134. Bennett, M., et al., *Cell surface trafficking of Fas: a rapid mechanism of p53-mediated apoptosis*. Science, 1998. **282**(5387): p. 290-3.
135. Hermeking, H., et al., *14-3-3sigma is a p53-regulated inhibitor of G2/M progression*. Mol Cell, 1997. **1**(1): p. 3-11.
136. Sullivan, K.D., et al., *The p53 circuit board*. Biochim Biophys Acta, 2012. **1825**(2): p. 229-44.
137. Brooks, C.L. and W. Gu, *New insights into p53 activation*. Cell Res, 2010. **20**(6): p. 614-21.
138. Fridman, J.S. and S.W. Lowe, *Control of apoptosis by p53*. Oncogene, 2003. **22**(56): p. 9030-40.
139. Kalluri, R. and R.A. Weinberg, *The basics of epithelial-mesenchymal transition*. J Clin Invest, 2009. **119**(6): p. 1420-8.
140. Guo, W., et al., *Slug and Sox9 cooperatively determine the mammary stem cell state*. Cell, 2012. **148**(5): p. 1015-28.
141. Ling, S., et al., *An EGFR-ERK-SOX9 signaling cascade links urothelial development and regeneration to cancer*. Cancer Res, 2011. **71**(11): p. 3812-21.

142. Yamashita, T. and X.W. Wang, *Cancer stem cells in the development of liver cancer*. J Clin Invest, 2013. **123**(5): p. 1911-8.
143. Zhang, L., et al., *The stem cell niche of human livers: symmetry between development and regeneration*. Hepatology, 2008. **48**(5): p. 1598-607.
144. Yamashita, T., et al., *EpCAM-positive hepatocellular carcinoma cells are tumor-initiating cells with stem/progenitor cell features*. Gastroenterology, 2009. **136**(3): p. 1012-24.
145. Sulpice, L., et al., *Epithelial cell adhesion molecule is a prognosis marker for intrahepatic cholangiocarcinoma*. J Surg Res, 2014. **192**(1): p. 117-23.
146. Kitade, M., et al., *Specific fate decisions in adult hepatic progenitor cells driven by MET and EGFR signaling*. Genes Dev, 2013. **27**(15): p. 1706-17.



## 7 LISTS OF FIGURES AND TABLES

### 7.1 List of figures

- Figure 1. Worldwide incidence of cholangiocarcinoma.
- Figure 2. Potential cells of origin in intrahepatic cholangiocarcinoma (iCCA)
- Figure 3. Summary of key molecular alterations involved in iCCA carcinogenesis
- Figure 4. A semi-quantitative scoring system for evaluation of SOX9 expression in intrahepatic cholangiocarcinoma.
- Figure 5. CK19 expression in iCCA.
- Figure 6. Expression of SOX9 in chronic liver disease.
- Figure 7. Expressions of SOX9 and CK19 in CCA tumor surrounding tissue.
- Figure 8. Expression patterns of SOX9 and CK19 in iCCA tumor tissue.
- Figure 9. Expression of SOX9 in eCCA.
- Figure 10. Kaplan-Meier survival curves of iCCA patients in relation to SOX9 and CK19 expression.
- Figure 11. Kaplan-Meier survival curve of iCCA patients having received chemotherapy in relation to SOX9 expression.
- Figure 12. Kaplan-Meier survival curve of iCCA patients having received chemotherapy in relation to CK19 expression.
- Figure 13. Integrated analyses of CCA patients gene expression signatures related to SOX9 expression.
- Figure 14. Expression of SOX9 and CK19 in CCA cell lines and normal biliary epithelia cell line MMNK-1.
- Figure 15. SOX9 expression in CCA cells with or without SOX9 siRNA treatment for 48 hours.
- Figure 16. Comparative microarray analysis of CC-SW-1 cells with SOX9 knockdown as compared to control cells.
- Figure 17. Heatmap illustration of the gene expression analyses in CC-SW-1 CCA cells with or without SOX9 siRNA treatment.
- Figure 18. Cell viability measured by MTT assay in CCA cells with or without SOX9 knockdown.
- Figure 19. SOX9 and cell cycle progression in CC-SW-1 and EGI-1 cells.

Figure 20. SOX9 and expression of cyclin-dependent kinase inhibitors in CC-SW-1 and EGI-1 cells (immunoblot assay).

Figure 21. SOX9 and expression of cleaved caspase 3 in CC-SW-1 and EGI-1 cells (immunoblot assay).

Figure 22. SOX9 and expression of anti-apoptotic proteins Bcl-xL and Bcl-2, cell cycle regulatory proteins Cyclin D1 and p53 in CC-SW-1 and EGI-1 cells (immunoblot assay).

Figure 23. SOX9 and CCA cell migration, as measured by transwell assays.

Figure 24. SOX9 and expression of epithelial cell marker E-Cadherin or mesenchymal cell markers N-Cadherin and Vimentin (immunoblot assay).

Figure 25. SOX9 and subcellular localization of  $\beta$ -Catenin in CC-SW-1 and HuCCT-1 cells (immunoblot assay upon nuclear/cytoplasmic fractionation).

Figure 26. Expression of E-Cadherin and  $\beta$ -Catenin in HuCCT-1 cells treated with control or SOX9 siRNA (immunofluorescence).

Figure 27. SOX9 and CC-SW-1 tumor sphere formation.

Figure 28. SOX9 and CCA transdifferentiation.

Figure 29. SOX9 and multidrug resistance gene expression.

Figure 30. SOX9 expression in CC-SW-1 and EGI-1 cells treated with indicated concentration of gemcitabine (immunoblot).

Figure 31. IC<sub>50</sub> evaluation of gemcitabine using MTT method in CC-SW-1 and EGI-1 cells treated with or without SOX9 siRNA for 24 hours.

Figure 32. SOX9 regulates expression of MRP4 and phosphorylation Chk1 in CCA cells.

Figure 33. SOX9 and gemcitabine mediated CCA cell apoptosis.

Figure 34. EGF and CCA cells.

Figure 35. EGFR/ERK1/2 signaling and SOX9 expression.

Figure 36. SOX9 and EGFR/ERK1/2 signaling induced cell migration.

## 7.2 List of tables

Table 1. SOX9 expression in embryonic and adult liver

Table 2. Established risk factors and corresponding geographic distribution for cholangiocarcinoma

Table 3. Possible risk factors for cholangiocarcinoma

Table 4. Molecular pathogenesis of CCA

Table 5. Clinicopathological features of the validating set iCCA

Table 6. Chemicals and reagents

Table 7. Primary antibodies used for immunoblotting

Table 8. Primary antibodies used for immunohistochemistry

Table 9. Primary antibodies used for immunofluorescence

Table 10. Secondary antibodies

Table 11. Buffer

Table 12. Cell culture materials

Table 13. Apparatus and Software

Table 14. Cell lines and cell culture medium used in the study

Table 15. Primers used for qRT-PCR in this study

Table 16. Correlation of SOX9 and CK19 expression in iCCA

Table 17. Patient characteristics and tumor parameters in relation to SOX9 expression in iCCA

Table 18. Patient characteristics and tumor parameters in relation to CK19 expression in iCCA

Table 19. Median overall survival time of iCCA patients in relation to SOX9 and CK19 expression

Table 20. Median disease free survival time of iCCA patients in relation to SOX9 and CK19 expression

Table 21. SOX9 and CK19 expression and clinical outcome of iCCA patients receiving chemotherapy

Table 22. Median overall survival times of patients having received chemotherapy

Table 23. GSEA of KEGG pathway ranked by a positive correlation with SOX9 expression in CCA patients ( $P < 0.05$ ,  $FDR < 0.25$ )

Table 24. GSEA of KEGG pathways ranked by negative correlation with SOX9 expression in CCA patients ( $P < 0.05$ ,  $FDR < 0.25$ )

## 8 CURRICULUM VITAE

### Personal information

Name: Xiaodong Yuan  
Date of birth: Feb. 1st, 1985  
Nationality: Chinese.  
Marital state: Happily married  
Email: docyuan@162.com  
Address: Dammstrasse 10a, 68169, Mannheim

### Education

Oct. 2013-present      Ph.D. student (Dr.sc.hum.)  
Ruprecht-Karls-University Heidelberg

Ph.D. project: SOX9 in the development and chemotherapy of cholangiocarcinoma

Sep. 2012 – Sep. 2013      M.Sc. Medical Physics  
Ruprecht-Karls-University Heidelberg

Thesis: Radioimmunotherapy with Anti-CD66 Antibody: The Antigen Quantity Evaluation of Organs of Interest Using a Physiologically Based Pharmacokinetic Model

Aug. 2009 - July 2012      Master of Medicine  
Peking University Shenzhen Hospital

Thesis: Investigating the expression features of T memory lymphocytes surface markers: CD45RO, CD62L and CCR7 in Hepatocellular carcinoma (HCC) patients

Sep. 2005 - July 2009      Bachelor of Medicine  
Anhui Medical University

### Scholarship

Ph.D. scholarship from China Scholarship Council

### Publications

- Weng H-L, CAI X, **Yuan X**, et al. Two sides of one coin: massive hepatic necrosis and progenitor cell-mediated regeneration in acute liver failure.

*Frontiers in Physiology*

- F Teng, J Dzieran, **X Yuan**, et al. Hepatocyte-specific Smad7 deletion accelerates DEN-induced HCC via activation of STAT3 signaling in mice. *Oncogenesis*
- Cai XB, Zhang WX, Zhang RL, **Yuan X**, et al. Safety and efficacy of a novel plastic stent coated with stone-dissolving agents for the treatment of biliary stones in a porcine model. *Endoscopy*.

**Conference presentations and published abstracts**

- ***GASL Poster presentation:***

Lack of Polarity in liver progenitor cell-derived hepatocytes determines poor clinical outcome of acute-on-chronic liver failure. Yuan, X. et al. *Z Gastroenterol* 2016; 54(12): 1343-1404

- ***ESAL Poster presentation:***

**April 2017 (Amsterdam, Young Investigator Bursary)**

Formation of bile canaliculi in liver progenitor cell-derived hepatocytes determines clinical outcome of acute-on-chronic liver failure. Yuan, X. et al. *Journal of Hepatology* (ILC 2017 abstract book-No. FRI-417), Volume 66, Issue 1, S337 - S338

**June 2017 (Oslo, Full Young Investigator Bursary)**

SOX9 is a crucial transcription factor in the development of intrahepatic cholangiocarcinoma. OSLO 2017 – ebook. P05-07.

- ***33rd Ernst Klenk Symposium in Molecular Medicine in Cologne***

Transcription factor complex TRIM33-Smad2/3 is crucial for progenitor cell-mediated liver regeneration in liver cirrhosis. Yuan, X. et al. *Poster Abstracts book D-10*. 2017

### 9 ACKNOWLEDGEMENT

Firstly, I would like to express my sincere appreciation to my mentor Professor Dr. Steven Dooley. I will never forget the days when he helped me to revise my PhD project proposal 4 years ago. I am extremely grateful that he provided me with the opportunity of my scientific research in liver disease. I benefit a lot from his professional knowledge and friendly guidance during my whole PhD project.

I would like to thank Dr. Honglei Weng for the continuous support in my Ph.D research and thesis. His invaluable comments and suggestions encourage me to complete my PhD thesis and are very useful for my career.

Thanks to the members of the Sektion *Molecular Hepatology*. I appreciate that I met Bedair, Zeribe, Teng, Simeng, Anne and Tatjana in my 4 years PhD training. They were always helpful. Without them, I would not have finished my project.

I would like to thank Professor Cédric Coulouarn and Dr. Jun Li for providing me with precious tissue samples.

Especially, the Chinese Scholarship Council is gratefully acknowledged for financing my whole project in Germany.

Last but not the least, I would like to thank my family: my parents and my brother and sisters for supporting me throughout my life. In particular, my thanks come to my wife, Yun, who has been there for me at all times. I sincerely appreciate her assistance in my PhD study.

I appreciate... and want to say thanks.